Generation and analyses of mouse models for USP18 and USP15 via gene targeting

Dissertation zur Erlangung des akademischen Grades des
Doktors der Naturwissenschaften (Dr. rer. nat.)

eingereicht im Fachbereich Biologie, Chemie, Pharmazie
der Freien Universität Berlin

vorgelegt von

Dipl.-Biol. Ronny Hannß

aus Berlin

im Juli 2012

Diese Arbeit entstand zwischen Februar 2007 und August 2008 unter der Leitung von Dr. Klaus-Peter Knobeloch am Leibniz-Institut für molekulare Pharmakologie Berlin (FMP) und zwischen September 2008 und Juni 2012 unter der Leitung von Prof. Dr. Wolfgang Dubiel an der Charité Berlin.

1. Gutachter: Prof. Dr. Wolfgang Dubiel
Abteilung Molekularbiologie
Klinik für Allgemein- Viszeral-, Gefäß- und Thoraxchirurgie
Charité – Universitätsmedizin Berlin

2. Gutachter: Prof. Dr. Rupert Mutzel
Institut für Biologie
Fachbereich Biologie, Chemie, Pharmazie
Freie Universität Berlin

Disputation am 12.10.2012

Como siempre: lo urgente no deja tiempo para lo más importante
Mafalda, QUINO

Contents

Zusammenfassung ix

Summary xi

1. Introduction 1
- 1.1. Ubiquitin and ubiquitin-like proteins . . . 2
- 1.2. Processing, conjugation and deconjugation . . . 4
- 1.3. Regulation mediated by Ub- and UbL-deconjugating enzymes . . . 5
- 1.4. The ubiquitin-like modifier ISG15 . . . 8
- 1.5. Function of ISG15 . . . 9
- 1.6. USP18 function in vitro and in vivo . . . 12
  - 1.6.1. USP18 as an isopeptidase for ISG15 . . . 12
  - 1.6.2. USP18 in IFN signaling . . . 12
- 1.7. USP15 function . . . 14
  - 1.7.1. USP15 is a Ub-specific isopeptidase . . . 14
  - 1.7.2. USP15 is implicated in diverse cellular processes . . . 15
  - 1.7.3. USP15 in cell signaling . . . 16
- 1.8. Manipulation of the mouse genome . . . 18
  - 1.8.1. Gene knockouts in mice . . . 19
  - 1.8.2. Introducing subtle mutations into the mouse genome . . . 23
  - 1.8.3. Procedure and general principles for gene targeting in mice . . . 23
- 1.9. Aim of this study . . . 24

2. Materials and methods 25
- 2.1. Materials . . . 25
  - 2.1.1. Centrifuges . . . 25
  - 2.1.2. Reagents and chemicals . . . 25
  - 2.1.3. Buffers and solutions . . . 27
  - 2.1.4. Protein and DNA markers . . . 31
  - 2.1.5. Vectors . . . 31
  - 2.1.6. Primary antibodies . . . 31
  - 2.1.7. Secondary antibodies . . . 32
  - 2.1.8. Cytokines . . . 32
  - 2.1.9. Kits . . . 32
  - 2.1.10. Equipment and devices . . . 33
  - 2.1.11. Enzymes . . . 34

2.1.12. Expendable materials 34
2.1.13. Filters and membranes 35
2.1.14. Media and supplements for eukaryotic cells 35
2.1.15. Media and supplements for bacteria 37
2.1.16. Bacteria 37
2.1.17. Eukaryotic cells 37
2.1.18. Animals 37
2.1.19. Mouse genomic library 38
2.1.20. Software 38
2.1.21. DNA primers 38
2.1.22. Colony hybridization probes 40
2.1.23. Southern blot probes 40
2.2. DNA and RNA methods 41
2.2.1. DNA isolation from eukaryotic cells and mouse tail biopsies . 41
2.2.2. Phenol chloroform extraction 41
2.2.3. DNA precipitation using isopropanol 41
2.2.4. DNA agarose gel electrophoresis 42
2.2.5. Isolation of DNA from agarose gels 42
2.2.6. Photometric determination of DNA/RNA concentration and purity 42
2.2.7. Determination of DNA concentration by agarose gel electrophoresis 43
2.2.8. Estimation of DNA concentration by dot quantification 43
2.2.9. Isolation of genomic DNA from ES cells 43
2.2.10. Preparation of plasmid DNA from small bacterial cultures . . 44
2.2.11. Preparation of plasmid DNA from large bacterial cultures . . 44
2.2.12. Digestion of DNA with restriction enzymes 44
2.2.13. Blunting DNA with 5′protruding termini 44
2.2.14. Dephosphorylation of DNA 5′termini 45
2.2.15. Ligation of DNA fragments 45
2.2.16. Annealing of DNA oligomeres 45
2.2.17. Site directed mutagenesis 46
2.2.18. Isolation of RNA from mammalian cells 46
2.2.19. Synthesis of cDNA 46
2.2.20. Generation of competent bacteria 47
2.2.21. Transformation of competent *E. coli* by heat shock 47
2.2.22. Polymerase chain reaction (PCR) 48
2.2.23. Genotyping of *Usp15* mutants by PCR 48
2.2.24. Purification of DNA fragments and PCR products 49
2.2.25. Southern blotting 49
2.2.26. Northern blotting 50
2.2.27. Preparation of radiolabeled probes by single labeling 50
2.2.28. Preparation of radiolabeled probes by double labeling 51
2.2.29. Colony hybridization 52

2.2.30. Stripping and reprobing of colony hybridizations and Southern blots . . . 53
2.2.31. Generation of sheared and denatured salmon sperm ssDNA . . 53
2.3. Protein methods . . . 53
2.3.1. Preparation of protein extracts . . . 53
2.3.2. SDS polyacrylamide gel electrophoresis (SDS-PAGE) . . . 54
2.3.3. Western blotting . . . 55
2.4. Cell culture methods . . . 56
2.4.1. Preparation of mouse embryonic fibroblasts . . . 56
2.4.2. Preparation of mouse adult fibroblasts . . . 56
2.4.3. Stimulation of MAFs with TNF-α or TGF-β . . . 57
2.4.4. Cryopreservation of mammalian cells . . . 57
2.4.5. Cell culture methods for ES cells . . . 58
2.4.6. Preparation of ES cells for blastocyst injection . . . 60
2.5. Bioinformatical methods . . . 60
2.5.1. Primer design . . . 60
2.5.2. Design of probes for Southern blotting . . . 60
2.5.3. Alignments . . . 61

3. Results **62**
3.1. Generation of mice expressing catalytically inactive USP18 . . . 62
3.1.1. Targeting strategy . . . 62
3.1.2. Construction of *Usp18*^{C61A} targeting vector . . . 64
3.1.3. Manipulation and identification of mutated ES cells . . . 66
3.1.4. Generation of chimeric mice and identification of germline transmission . . . 67
3.2. Generation of conditional *Usp15* knockout mice . . . 69
3.2.1. Targeting strategy . . . 69
3.2.2. Generation of a targeting vector . . . 71
3.2.3. Manipulation and identification of mutated ES cells . . . 73
3.2.4. Generation of chimeric mice and identification of germline transmission . . . 74
3.2.5. Deletion of the neomycin resistance gene . . . 75
3.2.6. Deletion of *Usp15* using Cre deleter mice . . . 76
3.2.7. Design of PCRs for genotyping . . . 77
3.2.8. Cre-mediated deletion of *Usp15* results in a null allele . . . 78
3.2.9. *Usp15*$^{-/-}$ mice are viable . . . 79
3.2.10. Analyses of MAFs . . . 81
3.2.11. Loss of USP15 does not reduce protein steady state levels of the endogenous RING box protein RBX1 . . . 82
3.2.12. IκBα degradation and reaccumulation is not altered in *Usp15* deficient MAFs . . . 83
3.2.13. TGF-β induced SMAD2 phosphorylation is not altered in *Usp15*$^{-/-}$ MAFs . . . 84

3.2.14. USP15 does not influence protein steady state levels of neither CSN5 nor CSN8 84

4. Discussion **86**
4.1. USP18 86
4.1.1. Generation of mice expressing catalytically inactive USP18 . . 86
4.1.2. *Usp18*$^{C61A/C61A}$ mice as a tool to dissect enzymatic functions in vivo 88
4.2. USP15 90
4.2.1. Generation of mice carrying a conditional *Usp15* allele 90
4.2.2. *Usp15* deficient mice are viable 91
4.2.3. *Usp15* deficient mice lack transcript and protein 91
4.2.4. USP15 does not reduce the endogenous protein steady state levels of the CRL component RBX1 92
4.2.5. Reexamination of TNF-α signaling 93
4.2.6. Reexamination of TGF-β signaling 94
4.2.7. USP15 has most likely no influence on CSN stability 95
4.2.8. Outlook 96

References **98**

A. Appendix **111**
A.1. List of abbreviations 112
A.2. Acknowledgment 116
A.3. Declaration 118
A.4. Publications, talks and posters 119

List of Figures

1.1. Ub- and UbL-conjugation cascade 3
1.2. Induction of ISG15 and its function 9
1.3. Scheme of homologous recombination. 20
1.4. Sequence features of loxP and FRT sites. 21
1.5. Possible recombinations mediated by Cre/loxP or FLP/FRT. 22

3.1. Alignment of USP15 and USP18 with other USPs 63
3.2. Genomic structure of *Usp18* 64
3.3. Targeting strategy for *Usp18*^{C61A} knockin 65
3.4. Successful mutation of *Usp18* in ES cells 67
3.5. Detection of germline transmission and FLP-mediated deletion for the mutated *Usp18* allele 69
3.6. Genomic structure of *Usp15* and exon seven to nine 71
3.7. Targeting strategy for *Usp15* 72
3.8. Successful manipulation of the *Usp15* gene locus 74
3.9. Established PCR to detect germline transmission 76
3.10. Detection of germline transmission for *Usp15* 76
3.11. Verification of Cre- and FLP-mediated deletion by Southern blotting 77
3.12. Strategy for genotyping by PCR 79
3.13. Established PCRs for genotyping 80
3.14. Transcript and protein expression in the liver of *Usp15* knockout animals 80
3.15. Picture of *Usp15* knockout mouse 81
3.16. Generation of MAFs from littermates 82
3.17. Protein levels of RBX1 is not altered in *Usp15* knockout MAFs . . . 83
3.18. IκBα degradation is not altered in *Usp15* knockout MAFs 83
3.19. *Usp15* deficient MAFs respond normally to TGF-β1 84
3.20. Loss of USP15 does not influence CSN5 or CSN8 steady state levels . 85

4.1. Model for USP15 function in vivo 96

Zusammenfassung

Ubiquitin (Ub) und Ubiquitin-ähnliche Proteine (UbLs) dienen als posttranslationelle Modifikatoren von Proteinen und beeinflussen eine Fülle von zellulären Funktionen. Deubiquitinierungsenzyme (DUBs) wirken der Modifikation mit Ub/UbL durch dessen Abspaltung bzw. Dekonjugation entgegen. Inzwischen wird klar, dass der Prozess der Dekonjugation ein genau regulierter Vorgang von großer physiologischer Bedeutung ist. Da Proteasen als pharmakologisch intervenierbar gelten und DUBs mit pathologischen Anomalien und Krebs in Verbindung gebracht wurden, sind sie attraktiv für die Entwicklung solcher Inhibitoren. Leider ist die physiologische Relevanz und Funktion vieler DUBs in vivo nicht bekannt, da entsprechende Mausmodelle nicht zur Verfügung stehen. In dieser Arbeit wurden zwei Mausmodelle für DUBs mittels gezielter Mutagenese von embryonalen Stammzellen hergestellt: ein knockin Mausmodell in welchem USP18 durch eine enzymatisch inaktive Variante ersetzt wurde und ein konditioneller knockout von USP15, welcher eine zeitliche oder räumliche Deletion dieses Genes erlaubt.

USP18 ist die Hauptisopeptidase, die der Proteinmodifikation durch ISG15 (ISGylierung) entgegenwirkt. Die ISGylierung ist eine der Haupteffektoren des Interferonsystems und daher wichtig bei der Bekämpfung von Pathogenen in höheren Eukaryoten. *Usp18* defiziente Mäuse zeigen starke Gehirnanomalien, überreagieren auf Interferonstimulation, sterben frühzeitig, sind resistenter gegenüber bestimmten Infektionen und zeigen eine vermehrte ISGylierung nach Interferonstimulation. Anfänglich wurde der Verlust der Dekonjugation von ISG15 als Ursache dieser phänotypischen Veränderungen angenommen. Da sich jedoch *Isg15* defiziente Mäuse normal entwickeln und *Isg15*/*Usp18* Doppel-Knockout-Mäuse phänotypisch nicht von *Usp18* defizienten Tieren zu unterscheiden sind stellt sich die Frage, welche phänotypische Veränderung der Proteasefunktion zuzuschreiben und welche davon unabhängig ist. Experimente deuteten bereits auch auf eine Protease-unabhängige Funktion von USP18 hin. Daher wurde ein neues Mausmodell mittels gezielter Mutagenese von embryonalen Stammzellen hergestellt, welchem die Proteasefunktion des

endogenen USP18 fehlt. Darüber hinaus dient dieses Mausmodell als ein wertvolles Werkzeug, um die physiologische Konsequenz einer selektiven Inhibition der enzymatischen Funktion von USP18 zu untersuchen.

Es wurde berichtet, dass USP15 den NFκB und TGF-β Signalweg beeinflusst und deutet daher auf eine Rolle von USP15 in Immunität und Entwicklung hin. Darüber hinaus ließen in vitro Experimente auf eine Stabilisierung von RBX1, eine Komponente von fast allen Cullin Ub E3 RING Ligasen, durch USP15 schließen. USP15 bindet außerdem an das CSN, ein Proteinkomplex welcher diese Ligasen reguliert. Um die Rolle von USP15 in vivo zu analysieren, wurde ein konditionelles *Usp15* Knockout-Mausmodell mittels gezielter Mutagenese von embryonalen Stammzellen, geplant und hergestellt. *Usp15* defiziente Mäuse sind lebensfähig, werden nach mendelscher Verteilung geboren und sind Wachstumsverzögert. Um zuvor gemachte Beobachtungen im physiologischen Kontext zu bewerten wurde der TGF-β and NFκB Signalweg untersucht. Diese Analysen wurden an Fibroblasten durchgeführt, welche aus USP15 defizienten bzw. Wildtyp-Mäusen hergestellt wurden. Im Gegensatz zu publizierten Beobachtungen führte der Verlust von USP15 zu keiner Veränderung der SMAD2 Phosphorylierung nach TGF-β Stimulation, weder in dessen Kinetik noch Intensität. Gleichermaßen verhielt es sich, entgegen eines Berichtes, mit der Reakkumulation von IκBα nach TNF-α Stimulation, da ebenfalls keine Veränderung in USP15 defizienten Zellen festzustellen war. Desweiteren führte der Verlust von USP15 zu keiner Reduktion von endogenem RBX1. Folglich spielt USP15 zumindest in Fibroblasten für den TGF-β, TNF-α Signalweg und die Stabilität von RBX1, unter den angewandeten experimentellen Bedingungen, keine Rolle. Zudem waren in USP15 defizienten Zellen die Proteinmengen der CSN Untereinheiten CSN5 und CSN8 unverändert. Der generierte konditionelle Mausstamm stellt ein wertvolles und vielseitiges Werkzeug zur Untersuchung der physiologischen Rolle von USP15 dar. Durch den konditionellen Charakter lässt sich USP15 in spezifischen Zelltypen (z. B. $CD4^+$) oder induzierbar in adulten Tieren mittels der Verwendung von Mx-cre Transgenen deletieren.

Summary

Ubiquitin (Ub) and ubiquitin-like proteins (UbLs) are posttranslational protein modifiers which affect a pleiotropy of cellular functions. Deubiquitinating enzymes (DUBs) counteract these modifications and it is emerging that the deconjugation of Ub and UbLs also is a highly regulated process of great physiological importance. Moreover, as being proteases which belong to the group of proven 'drugable' molecules DUBs are attractive for pharmacological intervention and have been linked to pathological abnormalities and cancer. However, the physiological relevance and in vivo functions of individual DUBs are poorly defined as mouse models are only available for a limited number of these Ub/UbL deconjugating enzymes at this time. In this study, two mouse models were generated via gene targeting in embryonic stem cells: a knockin mouse model in which USP18 is replaced by an enzymatically inactive variant and a conditional knockout of *Usp15* which allows the deletion of USP15 in a temporal and spatial manner.

USP18 is the main isopeptidase counteracting ISG15 modification of target proteins (ISGylation). The ISG15 modification system is one of the major interferon effector systems and an important player in higher eukaryotes against pathogens. *Usp18* knockout animals display severe brain injury, are hyperresponsive to IFN stimulation, die prematurely, were reported to be more resistant against certain infections, and have a higher ISGylation levels after interferon stimulation. Primarily loss of ISG15 deconjugation was alluded to be the main cause for these phenotypical alterations. However, *Isg15* knockout mice develop normally. Interestingly, *Isg15 Usp18* double knockout mice do not differ from *Usp18* knockout mice and also a protease independent function of USP18 was described raising the question which alteration can be ascribed to protease or nonprotease functions of USP18. Thus, severe brain injury and hyperresponsiveness to IFN is not connected to ISG15. To clearly discriminate isopeptidase dependent from isopeptidase independent function, a novel mouse strain was generated by gene targting in which the endogenous USP18 lacks protease function. Additionally, this knockin mouse model serves as a valu-

able model to mimick the physiological consequences of selective USP18 protease inhibition.

Based on cell culture experiments USP15 has been reported to affect NFκB and TGF-α signaling suggesting an important role of USP15 in immunity and development. Moreover, in vitro experiments alluded USP15 to stabilize RBX1, a component of nearly all cullin Ub E3 ligases recruiting the E2 enzyme for Ub conjugation. USP15 associates with the CSN, a protein complex which regulates the activity of these ligases. To gain insight into the role of USP15 within the context of the whole organism a conditional knockout mouse strain was planned and generated via gene targeting in embryonic stem cells. Knockout animals were born at expected mendelian ratio and were growth retarded. To challenge previous observations and to relate them in a physiological context, TGF-β and NFκB signaling was monitored in fibroblasts generated from USP15 deficient and wildtype mice. In contrast to previous reports, lack of USP15 did alter neither kinetics nor intensity of TGF-β induced SMAD2 phosphorylation. Likewise, there was no inhibition of TNF-α induced IκBα reaccumulation in fibroblasts as has been reported from *USP15* knockdown experiments. Furthermore, RBX1 levels were not altered in *Usp15* knockout fibroblasts. Hence, at least in fibroblasts USP15 is not essential for TGF-β, TNF-α signaling, and RBX1 stability under the experimental conditions employed. Moreover, loss of USP15 did not change protein levels of the CSN subunits CSN5 or CSN8. The generated conditional mouse strain provides a valuable tool to investigate the physiological role of USP15 in a temporal and spatial manner. The generated conditional *Usp15* gene knockout gives the opportunity to analyze USP15 function either in specific cell types (e.g., $CD4^+$) or to induce deletion of *Usp15* in adult animals using an Mx1-cre deleter strain.

1. Introduction

Ubiquitin (Ub) is a highly conserved protein that regulates miscellaneous processes in eukaryotic cells [111]. Its function is in general carried out through covalent attachment to target proteins via an isopeptide bond. This posttranslational modification causes change of function [136], localization [38] or stability of its targets [51]. There is a multitude of structurally related proteins, so-called Ub-like proteins (UbLs), e. g., interferon stimulated gene 15 (ISG15), that function as posttranslational protein modifiers in a similar manner [54]. The conjugation of Ub and UbL proteins to their targets is catalyzed by a set of enzymes usually including a three step enzymatic cascade (E1, E2 and E3) [16]. An additional level of regulation is achieved by isopeptidases that counteract target conjugation [77]. The importance of these isopeptidases was underestimated for a long time and is now emerging. Unfortunately, animal models for most isopeptidases against Ub or UbLs are still missing hampering the analysis of their physiological role. This work focuses on two of these deconjugating enzymes, namely USP15 and USP18 specific for ubiquitin and ISG15, respectively. Genetic approaches were performed in this study to enlighten their function in vivo. This chapter gives an introduction to the state-of-the-art of Ub, UbLs (focusing on ISG15) and the role of USP15 and USP18. Furthermore, it gives an introduction to the technique of gene targeting in mice.

1.1. Ubiquitin and ubiquitin-like proteins

Ub is a 76 amino acid (8 kDa) modifier that can be attached to substrate proteins by isopeptide bond formation on the ϵ-amino group of a lysine (K, Lys) residue on the substrate [51]. The discovery of its function in labeling proteins for ATP-dependent proteasomal degradation [51] was awarded with the Nobel prize in 2004 jointly to Aaron Ciechanover, Avram Hershko, and Irwin Rose for »the discovery of Ub-mediated protein degradation«. Since then, ubiquitination has been shown to be crucial for various cellular processes, e. g., endocytosis and cell signaling [111]. Unlike other posttranslational modifications (e. g., phosphorylation and acetylation), Ub can form chains by ligation of a Ub to another Ub already linked to the substrate [75]. Additionally, substrate proteins can either be modified with only one Ub (monoubiquitination) or with many single Ubs on different Lys on the substrate (multi-monoubiquitination). Ub itself contains seven Lys residues that can be used for chain formation including methionine at position one (M1) [25, 166]. The chain types are called M1, K6, K11, K27, K29, K33, K48, and K63 depending on which residue on another Ub it is bound. Beside homogeneous chain formation, Ub chains can also be heterologeous or branched [59]. All forms of chain linkages exist in eukaryotic cells [77]. This fact gives tremendous complexity, thus, it is not surprising that Ub is involved in almost every cellular process. Analogous to other posttranslational modication there exist receptors that recognize Ub modifications via Ub binding domains (UBD) [58]. Approximately 20 families of UBDs exist that recognize different Ub signals and decode it [58], extremely broadening the physiological function of this postranslational modification. The best studied Ub chain linkage types on proteins are K48 and K63. It is has been shown that K6, K11, K27, K29, K33 and K48 linked chains can target the modified proteins for degradation by a multiprotein complex called the 26 S proteasome [25, 180]. The 26 S proteasome consits of two major subcomplexes: the 20 S cylindric core particle (CP) governing the proteolytic activity [131] and the 19 S regulatory particle (RP) [35]. The 19 S regulatory particle itself consists of a lid and a base [35]. In general polyubiquitinated proteins are handed over to the proteasome by adaptor proteins [44] or directly bind to receptors in the RP [35]. ATPases within the RP unfold and translocate it into the CP [35]. The unfolded substrate is cleaved to small peptides [42]. Ub itself as a signal for proteasomal degradation is recycled by proteasome-associated deubiquitinating enzymes (USP14, UCHL5 and POH1) [35] which explains Ub's half-life

of several days within the cell [76]. K63-linked polyUb chains participate in DNA repair, cell signaling, regulate receptor endocytosis and endosomal sorting [174] and do not target proteins for degradation [75].

UbLs, which are similar to Ub in terms of molecular structure and mode of conjugation [54], are attached to target proteins by isopeptide bond formation using an enzymatic cascade analogous to Ub [54]. Interestingly, in contrast to Ub which is well established in protein degradation, most UbLs do not target proteins for proteasomal degradation suggesting other functions [127]. However, modification of a substrate with a UbL can also protect proteasomal degradation by opposing or competing with Ub conjugation [97]. Some examples for UbLs are neuronal precursor expressed developmentally down regulated 8 (NEDD8) [154], ISG15 [73], small ubiquitin-related modifier (SUMO) [39] and human leukocyte antigen F adjacent transcript 10 (FAT10) [127]. NEDD8 is mainly attached to cullins, the scaffolds of cullin Ub really interesting new gene (RING) ligases, affecting their activity [139]. ISG15 is well established to play a crucial role in antiviral defense, although the mechanism is not completely understood [73].

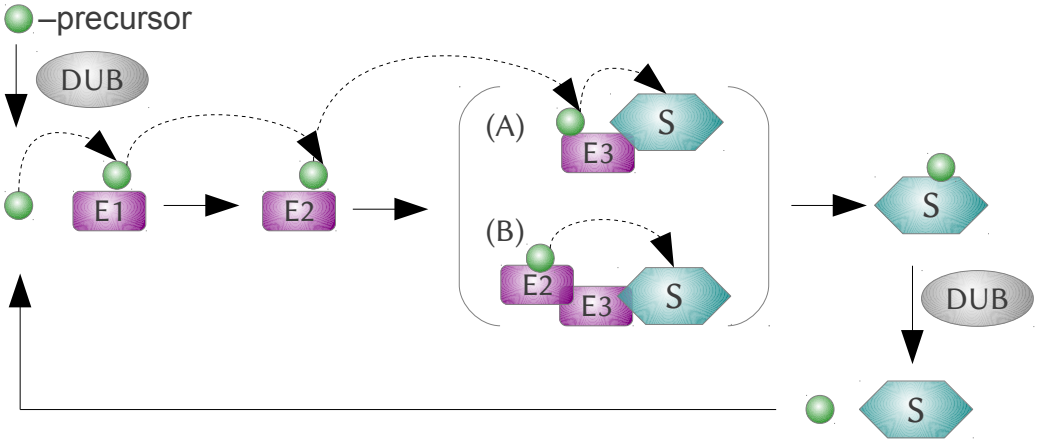

Figure 1.1.: Ub- and UbL-conjugation cascade. The posttranslational modifier Ub/UbL (green circle) is expressed as an unprocessed protein that is cleaved by DUBs to generate the GG motif. It is then activated by an E1 by thiolester bond formation in an ATP-dependent manner. Subsequently, Ub/UbL is transferred to an E2 conjugating enzyme. **(A)** Some E3 ligase, harboring a HECT domain, take over the modifier from an E2 forming by thioester bond formation to a catalytic cysteine and then mediate the ligation of the modifier to the substrate (S). **(B)** However, in most cases an E3 ligase (usually a RING ligase) brings the substrate and the E2 enzyme into close proximity facilitating the transfer of the modifier to the substrate. Generally, Ub/UbL is ligated with its C-terminus to a Lys residue on the substrate via isopeptide bond formation. The modification can be removed by an DUB resulting in unconjugated substrate and modifier.

1.2. Processing, conjugation and deconjugation

In mammals, Ub is encoded by four genes coding for fusion proteins [18]. UBA52 and UBA80 encode a single copy of Ub fused to ribosomal proteins and the UBB and UBC genes encode concatemeric Ub precursor proteins. These precursors are processed by deubiquitinating enzymes (DUBs), e. g., USP5, cleaving C-terminal of the Ub moieties (see figure 1.1) [77]. The processed Ub exposes a GG motif important for (iso)peptide formation on target proteins [77]. First of all, processed Ub is activated by an Ub activating enzyme (E1) (see figure 1.1) in an ATP-dependent manner [16]. In this process, Ub is adenylated and subsequently attacked by the catalytic cysteine of the E1 enzyme forming an thioester bond between the C-terminal glycine residue and the E1 and releasing AMP [16]. In the human proteome two Ub E1 enzymes have been identified [75]. Then, Ub is transferred via thioester bond exchange from the E1 to an conjugating enzyme (E2) [16] of which exist approximately 40 in the human proteome (see figure 1.1) [75]. In a last step, Ub is transferred to the substrate by a Ub ligase (E3) forming an isopeptide bond between the C-terminal glycine of Ub and the ϵ-N group of a Lys residue on the substrate (see figure 1.1) [75]. However, attachment to a nonlysine residue also has been reported [13].The existence of more than 600 E3 ligases lets one get a glimpse of the specificity to their substrates [75].

The multitude of E3 ligases can be divided into two families containing either a homologous to E6-AP carboxy terminus (HECT) domain or a RING domain. HECT domain E3 ligases have only few members in the human proteome (approximately 28) and directly bind Ub via thioester bond formation before ligation to the target protein, similar to E1 and E2 enzymes (see figure 1.1(A)) [144]. The vast majority of E3 ligases are RING ligases [93] (some contain an U-box which is similar to the RING domain) holding hundreds of family members [28]. The RING domain coordinates two Zn^{2+} ions (except U-box containing ligases) [28] and interacts with an E2 enzyme, thereby, bringing it into close proximity to the substrate facilitating and catalyzing the ligation the Ub/UbL (see figure 1.1(B)) [93].

Most RING E3 ligases are cullin RING ligases (CRLs). CRLs are of modular nature consisting of multiple subunits [142]. Cullin acts as a scaffolding protein and N-terminally binds RING domain containing protein RBX1 or RBX2 [142]. For instance, depending on the cullin scaffold in the E3 ligase complex they are abbreviated CRL1 for containing cullin1, CRL2 for containing cullin2 and so on. On the

C-terminus of cullin the substrate receptor does bind either diretly or via an adaptor protein [142]. The substrate receptor is put in superscript of the abbreviation, e. g., $CRL1^{SKP2}$ for SKP2 as a substrate receptor. Near to the C-terminus, cullin proteins can be posttranslationally modified with the UbL NEDD8 in a process called NEDDylation. NEDDylation of CRLs induces a structural change of the E3 ligase which enhances or activates the ligase in vitro [139]. The COP9 signalosome (CSN), a multisubunit protein complex associates with CRLs mediating their deNEDDylation [172]. Therefore, the CSN has a great impact and is considered to be a main regulator of CRL function.

The CSN consists of eight subunits (CSN1–8) and is structurally related to the regulatory lid of the 26 S proteasome and the eukaryotic translation initiation factor 3 [171, 143]. It harbors an intrinsic deNEDDylation activity which is pinpointed to CSN5, whereas CSN5 per se does not seem to have such activity [24]. The CSN has been shown to play a pivotal role in a wide range of cellular processes, e. g., DNA repair [49], protein localization [160, 85], signal transduction [170], transcription [82, 149], cell cycle [184] and development [182, 100, 182, 126, 161]. However, the most prominent biochemical function of the CSN is the deNEDDylation of CRLs [24, 99, 147] mediated by CSN5. The CRL complex is activated by NEDDylation [99], which induces a conformational change of the cullin and enhances E2 ligase binding/recruitment in vitro [139]. However, CSN-mediated deNEDDylation is important for CRL function in vivo (reviewed in [23]). There are several examples from budding yeast [24], fission yeast [94], plant [147] to human [45] which demontrated that downregulation of CSN leads to accumulation of certain CRL substrates. This suggests that the CSN positively regulates CRL activity. The contradiction of in vitro and in vivo generated data led to the proposal that cycles of NEDDylation and deNEDDylation are important for CRL function and proper substrate degradation [176, 169].

1.3. Regulation mediated by Ub- and UbL-deconjugating enzymes

Posttranslational modification of proteins by Ub or UbLs is a reversible process [77] and all enzymes counteracting these modifications are generally called deubiquitinating enzymes (DUBs) or referring to their substrate deNEDDylating, deISGylating, or deSUMOylating enzymes.

All proteases are divided into five classes based on the mechanism of catalysis (aspartic, cysteine, metallo, serine and threonine proteases) [117]. Two of these classes contain DUBs (metallo and cysteine proteases) [117]. There are 95 DUBs encoded in the human genome [155] and most of them are cysteine proteases which can be further subdivided based on their Ub protease domains like Ub-C-terminal hydrolases (UCHs), Ub-specific proteases (USPs), ovarian-tumor (OTU) domain proteases, and Machado-Joseph domain proteases. The only metalloprotease domain DUBs contain a Jab/MPN/MOV34 metalloenzyme (JAMM or MPN+) domain [117]. Of note, USPs are the largest familiy of DUBs with approximately 55 members [18] and their enzymatic activity relies on the thiol group of a cysteine in the active site [117].

The great diversity of DUBs implies the existence of considerable substrate specificity [174]. This is supported by the different specific phenotypes of mice in which single DUBs are disrupted [134, 161, 116, 79]. There exists also specificity in cleavage of certain linkages or polyUb chains or varying in efficiency [78, 9]. For instance, USP8 and USP14 cleave K48 but not K63 polymers [117], while the cylidromatosis gene product (CYLD) hydrolyses K63 linked Ub [75].

There is also a crosstalk between Ub and UbL modifiaction on the level of DUBs, in other words, some DUBs promiscuously deconjugate either Ub and UbLs from substrates. USP21 and UCH-L3 both cleave Ub and NEDD8 [43]. Another example are crossreactive DUBs in the Ub and ISG15 pathway [17]. However, it is challanging to determine the physiological specificity as DUBs often show low specificity in vitro. It has been suggested that subcellular localization [18] and scaffolding proteins influence specificity [174] or even regulate their activation. Since the interactome of DUBs is largely unknown Sowa et al. from the Wade Harper lab published a global proteomic analysis based on an unbiased approach to identify high confidence candidate interacting proteins from parallel nonreciprocal proteomic data of 75 DUBs [155]. This led to the interesting observation that most DUBs are associated with multi-protein complexes [155] supporting the notion that DUBs cooperate with other proteins enhancing their specificity. In the case of POH1 and CSN5 (both MPN domain DUBs), it seems that incorporation into protein complexes 19 S and CSN, respectively, is required for their activity [117]. DUBs can be also activated by cofactors. For example, USP1 has been shown to activated by USP1 activating factor 1 (UAF1), a WD40 repeat containing protein, that allosterically activates USP1, USP12 and USP46 [19, 20]. The fact that many USPs bind WD40 repeat containing proteins might point to a general mechanism of regulation, although this

might not be applied to all USP/WD40 intercations [8]. Interestingly, DUBs themselves can be regulated by Ub or UbL modification, e.g., Ataxin-3 is activated by ubiquitination [158], whereas SUMOylation of USP25 inhibits its activity [109], and USP5 is allosterically activated by Ub [133]. Finally, the yeast orthologue of USP14, namely Ubp6, vastly increases its activity by binding to the 19 S regulatory lid of the proteasome [86, 35].

There are three different categories of DUB function as suggested by Komander et al. [77]. Since Ub is expressed as a precursor, there are DUBs processing Ub that it can act as a posttranslational modifier. Second, Ub can be removed from ubiquitinated proteins affecting stability of the protein or affecting signaling events. And finally, Ub is removed from proteins that are subject to degradation, thus, Ub is returned to the pool of unconjugated Ub.

Many DUBs associate with E3 ligases that have the tendency to autoubiquitinate themselves. DUBs oppose this autoubiquitination stabilizing the ligase. For instance, USP8 stabilizes neuregulin receptor degradation protein 1 (NRDP1) as observed in knockdown studies [15], USP19 stabilizes Kip1 ubiquitination-promoting complex 1 (KPC1) [98] and USP15 is suggested to stabilize RBX1 [52]. There is also an example in vivo, in which USP7 (aka HAUSP) deficiency reduces steady state protein levels and half-life of the E3 ligase mouse double minute 2 (MDM2 aka HDM2) [79, 80]. Autoubiquitination of Ub E3 ligases can also result in change of activity as observed for CYLD and TNF receptor-associated factor 2 (TRAF2) [163]. However, some DUBs also have been shown to interact with E3 ligases without affecting E3 ligase stability, but the stability of the E3 ligase substrates [77]. For example, USP20 which interacts with the E3 ligase von-Hippel–Lindau protein (pVHL) has been shown to stabilze the E3 substrate Hypoxia-inducible factor (HIF)-1α [92]. Moreover, the OTU domain DUB A20 that harbors DUB and ligase activity edits Ub chains on its substrate [77]. The mechanism of E3 stabilization is also hijacked by viruses. For example, the infected cell polypeptide 0 (ICP0) which is an E3 ligase of HSV is stabilized by USP7 [14]. Therefore, E3 ligase and DUB interaction is suggested to be quite frequent but having distinct effects.

Mutations in distinct DUBs have been linked to cancer, neurological diseases and pathogenesis [187, 68, 175, 6] and the usability of DUBs as therapeutic drug targets has already been discussed [152, 27]. It is noteworthy in this context that many human pathogenic organisms carry DUBs, either with a mammalian ancestor or evolved from microbial genes [31]. This stresses the importance of DUBs in

infection and may be harnessed. However, DUBs have a limited set of substrates and distinct function in vivo and inhibition by small molecules is suggested to result in selective effects [27]. However, beside an approved proteasome inhibitor there are yet no therapeutics for humans available [27].

1.4. The ubiquitin-like modifier ISG15

ISG15 is one of the strongest induced proteins by type I interferon (IFN) and was the first UbL identified [47, 96] showing crossreactivity with antisera with selective affinity for Ub, therefore, it was named Ub crossreactive protein (UCRP) at that time. Analogous to Ub, ISG15 is conjugated to its target proteins via an enzymatic cascade using E1, E2 and E3 enzymes, in a process termed ISGylation. Since ISG15 is expressed as a precursor, prior to conjugation, it is processed by cleaving eight amino acids from the C-terminus exposing the highly conserved LRLRGG motif necessary for isopeptide bond formation [72, 186]. However, the protease for ISG15 processing has not been identified yet. Noteworthy, ISG15 and FAT10 are the only UbLs featuring a linear dimer of two Ub-like domains seperated by a short hinge region [114, 127]. In contrast to Ub, ISG15 is only present in vertebrates exhibiting a cross-species conservation to a low of 42% in mammals in contrast to Ub which appears to be 100% conserved and exists throughout all eukaryots [186]. Chain formation of ISG15 has not been reported yet. The activating enzyme for ISG15 is UBE1L (aka UbA7)[185]. Ub-conjugating enzyme in human 6 (UBCH6) and UBCH8 function as E2 conjugating enzymes [119] for ISG15 but are also crossreactive to Ub [188]. There are three E3 ligases identified for ISG15: HECT and RLD domain containing E3 ligase 5 (HERC5) in human [26, 177] (HERC6 in mice [164]), estrogen responsive finger protein (EFP or TRIM25) [191] and human homologue of *Drosophila ariadne* (HHARI) [121]. Interestingly, HERC5 is important for ISG15 conjugation in human cells [26], whereas in HERC6 seems to be the main E3 ligase in mice [67]. ISG15 conjugation is counteracted by USP18 (aka UBP43). IFN receptor 1 (*Ifnar1*) knockout mice derived bone marrow macrophages exhibit dramatically decreased ISG15 expression after lipopolysaccharide (LPS) administration [69]. Therefore, IFN signaling seems to be the most important pathway for stimulation of ISG15 expression. Importantly, the fact that the expression of the main enzymes required for ISGylation (ISG15, UBE1L, UBCH8, HERC5, EFP) including USP18 are induced by type I IFN [73, 102] suggests ISGylation to be a fine tuned

dynamic process linked to pathogene defense.

Noteworthy, there is remarkable crosstalk between ISG15 and Ub by several enzymes in their pathway that show dual specificity [73]. For example, as mentioned above UBCH6 and UBCH8 also serve as conjugating enzymes for Ub [188]. In a screen for promicuous isopeptidases using an ISG15 suicide inhibitor 22 DUBs from major clades were tested and USP2, USP5, USP13 and USP14 could be identified to also react with ISG15 [17]. Also the E3 ligase EFP is able to use Ub or ISG15 as a substrate [191] as well as the E3 ligase HHARI [121]. The physiological role of the evident crossreactivity of several enzymes observed in vitro still remains obscure.

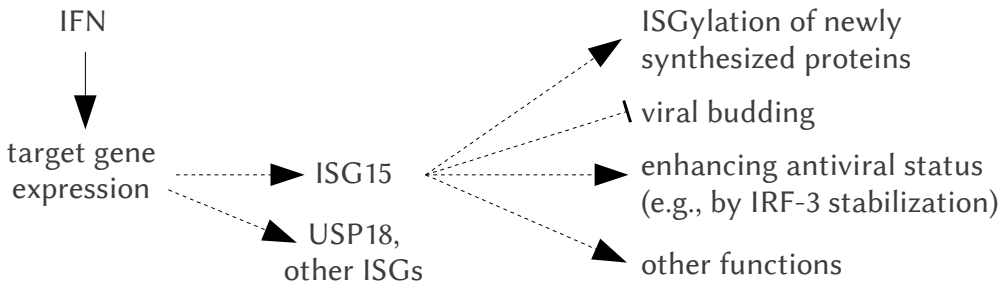

Figure 1.2.: Induction of ISG15 and its function. IFN stimulates the expression of ISG15, USP18 and many other ISGs. ISG15 is a UbL that can modify target proteins but also acts in its free unconjugated form. The most prominent function of ISG15 is to counteract infection at multiple levels.

1.5. Function of ISG15

Type I IFN secretion is a hallmark of virus infected cells [137]. Cells that receive this signal are primed to impede infection. Due to the early (approximately 4 h) and strong induction of its expression after viral [115, 64] or bacterial infection, ISG15 implies its importance in innate immunity. The first support for an antiviral function of ISG15 arose in 2001 from the observation that the nonstructural protein 1 of influenza B (NS1B) inhibits the activation step of human ISGylation in vitro [185]. However, type I IFN induces a battery of genes that act as transcription factors, pattern recognition receptors, or modulators of signaling pathways. Only a few of these proteins have been shown to act directly as antiviral effectors [137]. Today ISG15 is affiliated to the group of proteins that function to perform that task like the myxovirus resistance protein (Mx) GTPases, 2′-5′Oligo adenylate synthetase/RNaseL and protein kinase R (PKR) pathway [137]. Even though ISG15 has been known for a long time, its function was obscure until a few years ago starting with elegant

genetic experiments performed by Lenschow et al. in 2005. In this study the authors generated recombinant chimeric sindbis virus overexpressing wildtype ISG15 or an LRLRGG mutant that cannot be conjugated to target proteins [88]. Subsequent infection of knockout mice, which lack IFNα receptor (IFNAR) and are not able to undergo type I IFN-mediated induction of endogenous ISG15 expression, revealed that ISG15 overexpression attenuates infection. This attenuation was dependent on the conserved LRLRGG motif of ISG15 suggesting that conjugation is mendatory for antiviral activity [88]. In the same year *Isg15* knockout mice became available [123]. Infection of *Isg15* knockout mice demostrated that ISG15 indeed acts as an antiviral protein, since *Isg15* knockout animals were more susceptible to influenza A and B, herpes, and sindbis virus infection [89]. Of note, *Isg15* knockout mice revealed that ISG15 is not only involved in infection related processes because $Isg15^{-/-}$ animals display decreased bone formation which is the only observed spontaneous phenotype in these mice [1].

The antiviral effect of ISG15, although far from being fully understood, is apparently exerted at multiple levels of action. Examples on how free ISG15 or ISGylation interplays with viral and cellular proteins are emerging. It has been shown that *Isg15* null mouse embryonic fibroblasts (MEFs) are more permissive to vesicular stomatitis virus (VSV) replication. Moreover, the transcription factor IFN responsive factor-3 (IRF-3) which plays a critical role in establishing an antiviral state has been shown to be ISGylated and thereby protected IRF-3 against proteasomal degradation [97, 150]. Interestingly, two viral proteins, bICP0 a potential Ub E3 ligase of bovine herpes virus 1 and nonstructural protein 1 (NSP1) of rotavirus promote IRF-3 degradation [140, 4] suggesting that the viral host response is counteracted by this mechanism. This shows that ISGylation can protect proteins that are subject to proteasomal degradation.

Membrane budding is an important for enveloped viruses and some of them depend on the host machinery endosmal sorting complex required for transport (ESCRT) [57]. There exist several ESCRT complexes, i. e., ESCRT-0 to III, and some reports demostrate that ISG15 effectively inhibits viral budding by interfering with viral or host proteins and certain ESCRT complex proteins. Tumor susceptibility gene 101 (TSG101) is a protein of the ESCRT-I complex and binds the group-specific antigen (Gag) protein of human immunodeficiency virus (HIV) and Ub [120]. Ubiquitination of Gag is required for viral budding [120]. ISG15 blocks the interaction of Gag with TSG101, although ISGylation of neither Gag nor TSG101 was detected

[120]. Gag also requires NEDD4 Ub ligase and the ESCRT-II complex for budding [106]. ISG15 has been shown to inhibit interaction of E2 with the Ub E3 ligase NEDD4 diminishing its activity to ubiquitinate viral matrix proteins [106]. In turn, diminished NEDD4 activity has been shown to decrease the release of ebola virus like particles [106]. Moreover, Vacuolar protein sorting 4 (VSP4) is required for the ESCRT-III complex to induce membrane scission [81]. Interaction of VSP4 with the ESCRT-III complex gets lost by ISGylation of ESCRT-III components, most importantly CHMP5 [81]. ISGylated CHMP5 fails to recruit LIP5, another factor required for VSP4 recruitment [81]. These examples demonstrate that ISG15 inhibits viral budding at multiple sites.

Moreover, ISGylation can also affect activity of its target, e. g., protein phosphatase 2Cβ is renderd inactive by ISGylation resulting in enhanced NFκB signaling [156].

Most reports so far suggest that ISGylation and not free ISG15 is crucial in antiviral host defense which has been strengthened by data optained with *Ube1L* deficient mice [70]. These mice are unable to activate ISG15. Although ISG15 is still expressed, *Ube1L* deficient mice fail to perform ISGylation [70] and demonstrate increased susceptibility to infection with influenza B [84] and sindbis virus [41]. Nevertheless, there is an instance of ISG15 function as free unconjugated form in vivo. A recent report of Werneke et al. showed that ISG15 was critical for the control of chikungunya virus infection but is independent of UBE1L conjugation [173].

In a recent study, Durfee at al. observed that a wide range of substrates is ISGylated which is restricted to newly synthesized pools of proteins [29]. Furthermore, they could show that an ISG15 E3 ligase associates with polyribosomes which let them suggest that, in the context of an IFN-stimulated cell, newly translated viral proteins may be primary targets of ISG15 modification [29].

The mechanisms on how ISG15 counteracts infection, although not fully understood, seems to be quite diverse affecting infection at multiple sites of action (see figure 1.2).

1.6. USP18 function in vitro and in vivo

1.6.1. USP18 as an isopeptidase for ISG15

In 1999, USP18 was originally identified in a screen for differentially expressed genes in knockin mice expressing the AML1-ETO fusion protein, a model for de novo acute myelogenous leukemia in which 15% of the cases are associated with this fusion protein [95]. Prediction of its amino acid sequence revealed similarity to members of the Ub-specific protease family especially in the conserved regions that are hallmarks of this family (e. g., cysteine-box, histidine-box) [95]. Cotransformation of USP18 and Ub-β-galactosidase in *E. coli* led to cleavage of Ub from this fusion protein [95]. These initial data suggested that USP18 would be Ub-specific. Subsequently, USP18 was shown to specifically remove ISG15 from conjugated substrates [102]. Due to the fact that in other assays no proteolytic activity against Ub was observed, it was suggested that Ub may not be the proper substrate for USP18 [102]. The experimental setup in which excess of enzyme to substrate ratio was accounted for cleavage of the Ub fusion protein [102]. In contrast to a USP18 mutant lacking the catalytic cysteine residue, recombinant USP18 was able to generate free ISG15 but not free Ub from cytoskeleton enriched fractions of USP18 deficient lung tissue with detectable Ub and ISG15 conjugates [102]. Moreover, the same study showed that USP18 deficient mice displayed a massive increase in ISG15 conjugates but no change in levels of Ub modified substrates.

Nevertheless, it cannot be ruled out that USP18 might also use Ub as a substrate under physiological conditions. This notion is supported by the recent identification of ISG15-crossreactive deubiquitinating enzymes, e. g., USP5 [17]. Genetic studies showed that *Usp18* deficient mice develop severe brain injury and are hyperresponsive to poly(I:C) that mimics double stranded RNA [105]. However, these phenotypic abnormalities are also observed in the absence of ISG15 [74] clearly showing that USP18 must have additional functions beside ISG15 deconjugation and/or might be crossreactive to Ub or another UbL.

1.6.2. USP18 in IFN signaling

IFNs are pleiotropic cytokines (small proteins) that are important mediators of antiviral defense, exhibit immunomodulatory effects, and inhibit cell proliferation, among others [7]. There are three classes of IFN, i. e., type I to III [137]. Type I

IFN is the best characterized and comprises 17 subtypes in human [7], e. g., IFNα and IFNβ [137]. IFN type I signaling is mediated by their binding to a ubiquitously expressed heteromeric receptor comprised IFNAR1 and IFNAR2 [137, 7]. IFNAR1 and IFNAR2 are associated with the janus kinases tyrosine kinase 2 (TYK2) and janus kinase 1 (JAK1), respectively [7]. Binding of type I interferon to IFNAR2 recruits IFNAR1 [7] and juxtaposes these kinases leading to IFNAR1 phosphorylation [137]. Subsequently, the signal transducers and activators of transcription (STATs) STAT1 and STAT2 are recruited and phosphorylated [137]. Phosphorylated STAT1 and STAT2 heterodimerize and associate with IFN regulatory factor-9 (IRF-9) [137]. This heterotrimeric complex, also called IFN stimulated gene factor-3 (ISGF-3), translocates to the nucleus, and directly activates transcription of ISGs (e. g., ISG15, USP18, Mx, OAS, etc.) [137] by binding to IFN stimulated response elements (ISRE) on the DNA [137].

As mentioned before, ISG15 and USP18 expression is strongly induced by viral infection and type I IFN [103]. To analyze the function of USP18 in vivo, Ritchie et al. generated *Usp18* null mice [134]. According to previous observations that USP18 deconjugates ISG15, *Usp18* deficient animals display profound increase in the level of protein ISGylation after IFN stimulation. Interestingly, *Usp18* deficient animals died prematurely, were hypersensitive to intraperitoneal injection of the IFN inducing chemical poly(I:C), and developed severe brain injury [134, 103]. For *Usp18* knockout mice it has been reported that type I IFN signaling is enhanced indicated by prolonged STAT1 phosphorylation and upregulation of IFN target genes [190]. Dysregulation of protein modification by ISG15 was reported to be the cause of the observed phenotype of *Usp18* knockout mice [134]. Since knockout mice for *Isg15* are indistinguishable from wildtype mice [123], double knockout of *Usp18* and *Isg15* should lead to a rescue due to elimination of ISG15 expression. Unexpectedly, *Usp18 Isg15*double knockout mice do not differ from *Usp18* knockout animals [74]. This unequivocally shows that the severe phenotype of *Usp18* deficient mice is not mediated by ISG15. USP18 must either act as an isopeptidase for other modifiers like Ub or even perform an isopeptidase independent function. According to the assumption of a nonenzymatic function, ectopically expressed USP18 has been reported to inhibit the activation of the kinases JAK1 and TYK2 independently of its protease active site [104]. In these cell culture based experiments, using overexpressed proteins, USP18 competed with JAK1 in binding to IFNAR2, thereby, attenuating the IFN response. Lately, using *Usp18* knockout mice and investigating

IFN refractoriness in the liver, USP18 was identified to be a main regulator of this process [141, 36]. Still obscure is the mechanism on how USP18 leads to refractoriness to IFN which could be dependent or independent of the enzymatic activity. Furthermore, silencing of USP18 potentiates the antiviral activity of IFN in hepatitis C infection [132]. Recombinant IFNα is used in treatment against hepatitis B and C infection, multiple sclerosis and some forms of cancer [7]. It is well known that cells become refractory to IFN, in other words, after IFN administration they remain unresponsive for several days [141]. Therefore, it is believed that opposing refractoriness would improve the therapeutical use of IFN.

1.7. USP15 function

1.7.1. USP15 is a Ub-specific isopeptidase

USP15 was first cloned and characterized in 1999 from human cDNA [3] (and mouse [2]) and contains conserved hallmarks of USPs (e. g., cysteine-box and histidine-box). Its closest paralogues are USP4 (approximately 70% sequence identity [33]) and USP11. Interestingly USP15, USP4 and USP11 contain two UbL domains and one of them is juxtaposed to their DUSP domain [33]. In the case of USP4 this double domain (DUSP-UbL) is crucial for its association with a protein mediating substrate specificity, i. e., the substrate targeting factor called squamous cell carcinoma antigen recognized by T-cells 3 (SART3) [33]. However, how this domain contributes to USP15 function has yet not been determined. Noteworthy, USP15 contains a functional zinc finger motif which is required for binding and cleavage of polyUb [52].

USP15 has been shown to cleave a Ub-GST fusion protein, hence, it is an active member of the USP family [3, 2]. Noteworthy, activity to linear Ub-GST fusion proteins may not resemble a physiological substrate, and only recently the specificity towards more physiological substrates has been determined in vitro. In tetra-Ub assays performed in one of these studies, USP15 has been proven to be active on K63, K48, and with less activity on M1 linked Ub [78]. Interstingly, USP15 could cleave K63 and K11 linked Di-Ub but showed limited activity on K11 linked UBE2S-polyUb formed by UBE2S-mediated autoubiquitination [9].

1.7.2. USP15 is implicated in diverse cellular processes

Most studies adressing USP15 functions were so far based on experiments set up by ectopical overexpression or knockdown and might not completely reveal its function in vivo. Genetic loss of function models only exist in *Saccheromyces cerevisiae*. Using this model system demonstrated that Ubp12p, the *S. cerevisiae* orthologue of human USP15, associates with the CSN complex [189]. Furthermore, in yeast the CSN is needed to shuttle Ubp12p into the nucleus where it stabilizes the Fbox substrate receptor cullin E3 ligase protein Pop1p [189]. However, the stabilizing effect of Ubp12p on CRL components has been shown to be more pronounced for the substrate receptor Btb3p of Cul3p [145]. In conjunction with these reports USP15 was reported to stabilize RBX1 against the Ub proteasome system in human cells [52]. This suggests a general mechanism of Ubp12p or USP15 to stabilize CRL components that are prone to destabilization by autoubiquitination. As already mentioned, E3 ligase stabilization by DUBs has also been observed with other DUBs [77].

USP15 has also been related to the anticancer drug paclitaxel which is one of the most effective drugs in cancer treatment [179]. Paclitaxel disrupts microtubule dynamics leading to cell cycle arrest in G2/M phase activating mitotic spindle checkpoint and finally induces apoptosis [179]. In a high throughput screen for siRNAs that affect paclitaxel resistance, knockdown of USP15 has been reported to reduce paclitaxel induced apoptosis [179] and its overexpression stabilized procaspase-3 enhancing paclitaxel induced apoptosis.

In a high throughput proteomic approach to identify putative interaction partners of 75 investigated DUBs, USP15 associated with proteins involved in mRNA processing (possible candidates U5/U6-snRNP components PRPF4 and SART3) [155]. Beside proteins involved in mRNA processing, this proteomic approach also suggested another putative interaction partners, e. g., skeletal muscle LIM protein 1 (SLIM1). Isumi et al. [62] could verify interaction of the recombinant proteins. Interestingly, a mutant USP15 in which the catalytic cysteine is changed to serine was diminished in its ability to interact with SLIM1 in vitro. Since SLIM1 has been implicated in cardiomyopathy, the group generated a trangenic mouse strain overexpressing human USP15 in the heart [62]. Beside leading to cardial hypertrophy and stabilization of SLIM1, transgenic expression of USP15 in the heart resulted in markedly high expression of another isoform of SLIM1 that was not detectable by immunoblot in control mice. This observation and the earlier implication of USP15

in mRNA splicing raise the question if this is the consequence of USP15 affected splicing events.

There is also a report directly associating USP15 with viral infection of the human papilloma viruses (HPVs) [165]. HPVs are considered for high risk in their oncogenic potential and express the protein E6 which has been shown to interfere with p53 and retinoblastoma protein, beside other functions, affecting cell cycle and apoptosis [165]. In a screen for E6 interacting proteins in human HPV cervical cancer cells USP15 has been identified and stabilized E6 depending on USP15 catalytic activity [165]. However, the authors did not observe any alterations in p53 levels after USP15 knockdown. Thus, the consequences of USP15-mediated E6 stabilization are yet unknown.

USP15 has also been shown to be one of 13 DUBs (85 DUBs screened) that inhibit hepatocyte growth factor (HGF)-mediated scattering of epithelial cells [12]. HGF activates the Met receptor tyrosin kinase, a member of a small subfamily of growth factor receptors [37], leading to motile cells which represents one key factor for invasive growth [12]. Thus, protease inhibition of USP15 might be a suitable target for pharmacological intervention.

Recently, USP15 also has been implicated to be involved in neurodegenerative disorders. In a mouse model for spinocerebellar ataxia type 3, expression of USP15 mRNA and protein is reduced [108]. The pathological phenotype of these mice can be reverted by a rapamycin ester that enhances autophagy, leading to normal USP15 expression [108]. Of note, the changes of USP15 were admittedly low and the importance of these transcription alterations remain unclear. In another report, USP15 and the CSN have been shown to associate to the hexameric chaperone p97/VCP AAA-ATPase and processing bound polyUb substrates. The p97/VCP AAA-ATPase protects cells against toxic effects resulting from aggregation prone proteins including polyglutamine stretches (e. g., huntingtin and ataxin-3) and fulfills multiple functions in the cell in protein quality control, lysosomal degradation, signaling, and chromatin-associated functions [110].

1.7.3. USP15 in cell signaling

The NFκB family of transcription factors regulates innate and adaptive immune response [40]. Many common diseases, e. g., rheumatoid arthritis, diabetes, and cancer are associated with NFκB dysregulation [48]. Typically activation of NFκB precedes the phosphorylation of IκBα by the IκB kinase (IKK) complex consisting

of IKKα, IKKβ and the regulatory subunit IKKγ (aka NEMO) [50]. Beside IκBα, there exist other IκBs, but genetic studies in mice suggest IκBα to be the most important IκB [66]. IκBα is a stable protein that binds to NFκB and thereby inhibits its activity [66]. After stimulation with, e. g., TNF-α, the inhibitor IκBα is phosphorylated and subsequently degradated in less than five minutes [66] in a Ub-dependent manner by the proteasome [125]. Subsequently, NFκB transactivates the expression of target genes including proinflammatory cytokines, chemokines, angiogenic factors, antiapoptotic proteins and so on [48]. NFκB also induces IκBα synthesis constituting a negative feedback loop [66] in which IκBα again associates with NFκB rendering it inactive [66]. In 2007, based on knockdown studies it was reported that the CSN controls NFκB pathway by deubiquitination of IκBα mediated by USP15. Knockdown of USP15 resulted in reduced reaccumulation of IκBα post TNFα stimulation [148].

The Wnt-pathway has also been reported to be affected by USP15 [56]. Knockdown of CSN subunits resulting in decreased cellular CSN protein levels resulted in retarded degradation of of β-catenin [56]. Degradation of β-catenin is mediated by the β-catenin destruction complex constitutively [56]. After stimulation with Wnt, β-catenin is stabilized, translocates to the nucleus, and binds to certain DNA elements triggering target gene expression [56]. Adenomatous polyposis coli (APC) together with glycogen synthase kinase-3 β (GSK-3β) and axin form the destruction complex [56]. Based on knockdown and overexpression experiments, USP15 was suggested to stabilize APC reducing β-catenin levels as a consequence [56]. Interestingly, in the same study APC was degraded even faster by overexpression of a zinc finger domain mutant USP15 compared to empty vector control [56] suggesting a dominant negative effect of this mutant.

In 2011 and 2012 Inui et al. and Eichhorn et al., respectively, independently identified USP15 in an unbiased RNA interference screen to affect tumor growth factor-β (TGF-β) signaling [61, 32]. TGF-β is a cytokin controling a variety of cellular responses highly dependent on the cellular context [178]. TGF-β also acts as an oncogenic factor and recently has been suggested to play a key role in glioblastoma, the most aggressive type of brain tumor [32]. The superfamily of TGF-β ligands holds more than 30 genes in human which are divided in TGF-βs, activins, nodal, bone morphogenic proteins (BMPs) and eleven growth and differentiation factors [146]. The ligand binds as a dimer to a tetrameric receptor which gets activated and phosphorylates regulatory SMADs (R-SMADs) [22]. BMP binding to the re-

ceptor leads to phosphorylation of the R-SMADs SMAD1, SMAD5 and SMAD8 [71]. Stimulation with TGF-β results in phosphorylation of the R-SMADS SMAD2 and SMAD3 [71]. These phosphorylated R-SMADs form a complex with SMAD4, accumulate in the nucleus, and start gene transcription [146]. Inhibitory SMADs (I-SMADs) like SMAD6 and SMAD7 oppose the signal [71]. SMAD7 associates with the SMAD Ub regulatory factor 1 (SMURF1) and SMURF2, both E3 Ub HECT ligases, that induce Ub-dependent degradation of SMAD7 and associated receptors [60]. Inui et al. showed that USP15 binds to SMAD3 and opposes its ubiquitination [61]. Furthermore, USP15 was crucial for association of the SMAD complex with DNA after TGF-β stimulation. Since SMAD3 is mainly monoubiquitinated and only unubiquitinated SMAD complex binds to DNA, the authors suggested a model in that USP15 enhances TGF-β and BMP signaling by R-SMAD deubiquitination. Eichhorn et al. describe another function of USP15 in TGF-β signaling. By performing coimmunoprecipitations the authors observed an association of USP15 with SMAD2, SMAD3, SMAD4, and SMAD7, but the latter interacted most strongly. However, association of USP15 with SMAD7 was reduced after TGF-β stimulation. Their work suggested that SMAD7 acts as a scaffold protein which binds SMURF2 and USP15 in one complex. SMAD7 mediates their association with the TGF-β receptor I (TβR-I) which was stabilized against the Ub proteasome system mediated by USP15 in this context. They also observed lower p-SMAD2 levels after USP15 knockdown after TGF-β or activin stimulation, whereas BMP stimulation led to lower p-SMAD1 levels. Additionally, they inoculated the brain of immuncompromized mice with human tumor cells displaying elevated USP15 protein levels. Mice in which tumor cells were pretreated with an letiviral small hairpin RNA against *USP15* before inoculation, the number and tumor size was diminished.

Taken together, these two previous studies provided very strong evidence that USP15 enhances TGF-β signaling. However, due to the lack of *Usp15* knockout mice the physiological relevance and function within the context of the whole organism still remains elusive.

1.8. Manipulation of the mouse genome

In 2008, the Nobel Prize in physiology or medicin was awarded jointly to Mario R. Capecchi, Martin Evans, and Oliver Smithies for their discoveries of »principles for introducin specific gene modifications in mice by the use of embryonic stem cells«.

Gene targeting in mice offers the possibility to site specifically disrupt genes (see section 1.8.1), delete parts of the genome and to introduce genes or subtle changes (see section 1.8.2). This marvelous technique was even advanced and suffisticated by including the Cre/loxP system offering to knockout genes at certain time points of development or certain tissues.

1.8.1. Gene knockouts in mice

To produce a conventional knockout in mice by gene targeting, embryonic stem (ES) cells are transfected with a linearized targeting vector. This linearized targeting vector bears two sequences, that are homologous to the locus to be targeted, seperated by a positive selection marker, e. g., neomycin resistance gene under control of a constitutively active promotor (see figure 1.3). After homologous recombination, which is a cellular mechanism involved in DNA repair [68], the endogenous locus is replaced by the sequence of the targeting vector due to double reciprocal recombination between vector sequences and their homologous endogenous sequences. The positive selection marker enables to select transfected ES cells for those that integrated the vector into their genome. Since random integration of the transfected vector occurs at a much higher frequency than integration by homologous recombination (approximately 1:1000 [153]), positive selection also enriches for random integrates. To reduce the number of cells harboring random integrates, negative selection is recommended to enrich for homologous recombination. Usually, a thymidine kinase gene (TK) of herpes simplex virus (also diphteria toxin A or immunotoxin) under control of a constitutively active promotor is placed outside of the vector sequences that are homologous to the endogenous locus. TK phosphorylates thymidine analoga, e. g., gancyclovir, and anticipates DNA synthesis. Sequences outside of the homologies are not integrated by homologous recombination. Therefore, cells that underwent homologous recombination will survive negative selection, because the TK is not inserted into the genome in contrast to cells which randomly integrated the targeting vector.

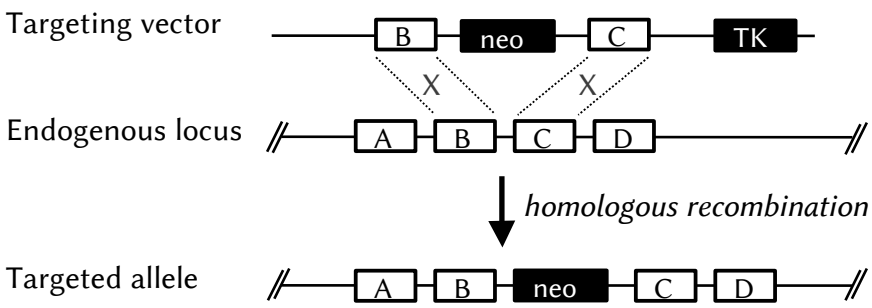

Figure 1.3.: Scheme of homologous recombination. The targeting vector harbors a positive selection marker, i. e., a neomycin resistance gene (neo), and a negative selection marker, thymidine kinase gene (TK). Flanking the neo gene are sequences that are homologous to the endogenous locus to be targeted (B&C). By homologous recombination the homologous sequences recombinate (indicated by X) inserting the sequence in between of the homologous sequences of the targeting vector. Thus, the neo gene is inserted in the targeted allele (A-B-neo-C-D).

There can be some drawbacks with conventional knockouts. Because the gene is disrupted in every cell/tissue of the organsim from the beginning of development, it does not permit to analyze the function of the gene in different cell types or certain time points of development. Moreover, the gene disrupted from beginning of development could play a crucial role in embryogenesis, and if so, no pups or adult animals would develop. In this case, one would be limited to investigate the function of the targeted gene only in embryogenesis.

The Cre/loxP technique is often used for the generation of gene knockouts in mice, though a conventional knockout might be desirable depending on the question to be examined. This technique enables to produce animals displaying the knockout only in certain tissue/cells (spatial) and/or at a certain timepoint (temporal). Such an inducible knockout greatly expands the versatility of gene targeting [83].

The common technology to generate a conditional knockout is using the Cre/loxP system. The recombinase Cre (causes recombination) is an 38 kDa protein and belongs to the λ-integrase superfamily [138] including the FLP recombinase from *S. cerevisiae* [30]. Cre originates from the bacteriophage P1 and mediates the site specific recombination of loxP sites (locus of crossover[x] in P1).

A loxP site consists of two 13 bp repeats flanking a 8 bp nonpalindromic core sequence dictating the polarity of the sequence (see figure 1.4) [162]. Cre binds to the inverted repeats and mediates the recombination of two identical loxP sites without the need of cofactors [30]. There are two ways of Cre-mediated intramolecular recombination (see figure 1.5). First, if two loxP sites in a DNA sequence are placed in the same direction according to their core sequence, Cre mediates the escision

and circularization of the sequence flanked by loxP sites both remaining one loxP site (see figure 1.5 A) [83]. Though the excision reaction is favored, Cre also catalyzes the backward reaction, i. e., the integration event [83]. Secondly, if two loxP sites are placed in opposite directions (facing each other), Cre mediates the inversion of the sequence between the loxP sites (see figure 1.5 B) [83]. The cleavage of the DNA strands occurs within the core sequence of the loxP sites via covalent 3′phosphotyrosine linkages of DNA and a conserved tyrosine residue of Cre. Subsequently, a Holliday junction intermediate is formed with a strong requirement for sequence identity in the crossover region of the loxP sites for successful recombination [30].

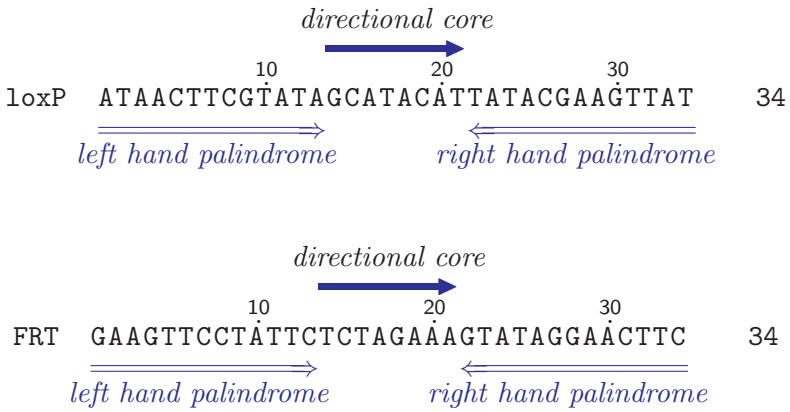

Figure 1.4.: Sequence features of loxP and FRT sites. The loxP or FRT sites are the target recognition sites for the Cre or FLP recombinase, respectively. Each consists of a 8 bp core sequence flanked by two sets of palindromic sequences. The core sequence gives the recognition site their polarity/direction. The palindromic sequences are important for Cre or FLP recognition.

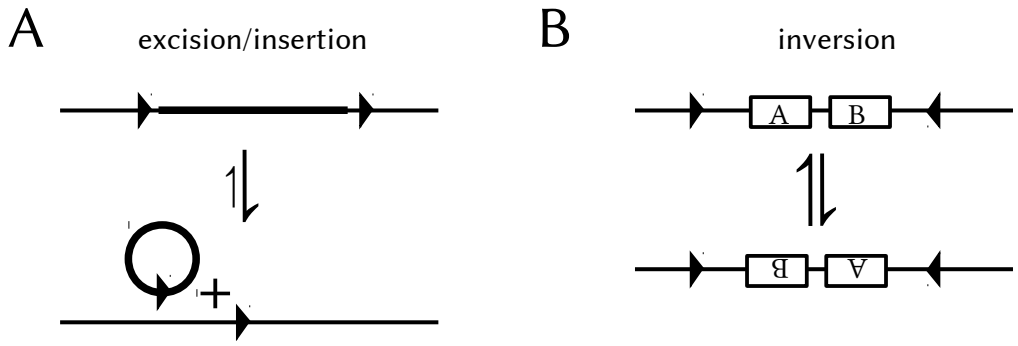

Figure 1.5.: Possible recombinations mediated by Cre/loxP or FLP/FRT. **(A)** Cre or FLP catalyze the excision of the sequence between two loxP or FRT site having the same orientation, respectively. Thus, the remaining and the excised circular sequence bear a loxP or FRT site. The backwards reaction is less favored. **(B)** If two loxP or FRT sites are placed in opposite orientation to each other, Cre or FLP catalyzes the inversion of the sequence in between, respectively. Neither forward nor backward reaction is favored. Hence, an equilibrium of both versions would establish.

These features and the fact that Cre exhibits it optimum activity a 37 °C [162] made the Cre/loxP system an excellent tool for genomic manipulation in mammalian cells.

The strategy for conditional inactivation (loss-of-function) of an endogenous gene is to flank the target gene, or at least a part of it, with loxP sites (to flox) which are inserted into the genome by homologous recombination. These genetic elements have to be inserted without disrupting splice sites or the protein coding sequence. If these mice are crossed to a transgenic mouse strain expressing Cre under the control of a certain promotor, Cre will mediate the recombination in the offspring resulting in gene ablation in a spatial or temporal manner depending on the promotor that controls recombinase expression. This strategy was first applied to conditionally knock out the DNA polymerase β gene by Gu et al. [46].

Beside the Cre/loxP system, the yeast derived FLP/FRT system is used frequently. The FLP/FRT system is analogous to the Cre/loxP system (see figure 1.4 and 1.5). It was less attractive due to the temperature optimum of 30 °C of the FLP enzyme. This was overcome by generating a FLP mutant (named FLPe) exhibiting improved thermostability for efficient use in mammalian cells at 37 °C [11]. For convenience, only the term FLP is used in this work.

Because the FLP/FRT and the Cre/loxP system are well established, they are often used in combination. The FLP/FRT system is frequently used to eliminate the neomycin resistance gene that is only needed for positive selection of targeted cells. Usually, the positive selection marker is flanked by FRT sites. If these mice

are mated with transgenic mice expressing FLP, the selection marker is excised. Because FLP and Cre only recognize FRT and loxP sites, respectively, they can be used independently.

1.8.2. Introducing subtle mutations into the mouse genome

The procedure to introduce subtle mutations (e. g., point mutation, insertion or change of short sequences) into the mouse genome is similar to the procedure for the generation of a conventional knockout. One homology bears the desired mutation close to the neomycin resistance gene. Since it is not predictable at which point in the homologous sequence the DNA will recombinate, the probability of incorporation of the mutation will rise the closer it is to the positive selection marker.

1.8.3. Procedure and general principles for gene targeting in mice

To generate genetically modified mice a strategy has to be developed, which ensures efficient targeting and the ability to screen for the mutated allele. After construction of the targeting vector according to the developed strategy, it is introduced into ES cells. Mutated ES cells are identified by Southern blotting. The ES cell clone bearing the desired mutation, also called positive ES cell clone, is injected into C57BL/6 derived blastocysts which are then implanted into pseudo pregnant foster mothers. The progeny will be chimeras generated from wildtype and mutated ES cells. Generally, ES cells derive from an agouti coat colored strain and the blastocysts derive from a black coated strain. Therefore, the grade chimerism can be estimated on the basis of the coat color. Chimeric mice are then mated with wildtype animals to hopefully achieve germline transmission, i. e., propagation of the mutation, thus, creation of a noval founder strain.

1.9. Aim of this study

DUBs are under growing interest, because it is emerging that they perform specific functions. Moreover, DUBs are considered as possible drug targets that may be attractive for future therapies. Mouse models for many DUBs are not available but are important to identify and evaluate their function in vivo. Aim of this study was to clarify the in vivo function of two DUBs: USP18 and USP15.

The previously reported massive phenotype of *Usp18* ablation, e. g., brain injury and hypersensitivity to IFN is monitored even in the absence of the ISG15 protein, thus, it cannot be ascribed to dysregulation of ISG15 protein modification. There must either be a function which is isopeptidase independent or USP18 might be a protease for another UbL or Ub. Indeed, in vitro experiments suggest that USP18 attenuates IFN signaling and causes refractoriness to repeated IFN stimulation independent of its protease activity, which is thought to hamper IFN therapy. *Usp18* knockout mice also have been reported to be more resistant to infection. Therefore, *Usp18* knockin mice lacking protease activity should be generated by gene targeting in which the USP18 protein is still expressed, specifically lacks its protease function and still is able to fulfill isopeptidase independent functions. Using such a mouse model, it will be possible to dissect enzymatic and nonenzymatic physiological functions of USP18.

USP15 has been shown to cleave preferencially K48 and K63 linked Ub chains and binds to the CSN. Moreover, USP15 is suggested to stabilize RBX1, a cullin RING E3 ligase component, and affect the NFκB pathway by ensuring proper reaccumulation of IκBα. Two recent reports provide strong evidence for USP15 enhancing TGF-β signaling. Thus, USP15 might be crucial for development and immunity. As the physiological relevance and function in vivo so far is completely unclear, it was the objective of this work to generate *Usp15* conditional knockout mice which would be valuable model system to study the function of USP15 within the context of the whole organism and to challenge previous functions ascribed to USP15 and its physiological relevance in an in vivo setting. Moreover, it should be analyzed whether mice homozygous for a *Usp15* null allele are viable and if loss of USP15 affects RBX1 and CSN protein levels. Additionally, the TNF-α and TGF-β signaling should be analyzed in *Usp15* knockout cells to evaluate the physiological relevance of prior observations.

2. Materials and methods

2.1. Materials

2.1.1. Centrifuges

Centrifuge	Company
Biofuge fresco	Heraeus, UK
Biofuge pico	Heraeus, UK
Centrikon T-124	Kontron Instruments GmbH
Megafufe 1.0R	Heraeus, UK

2.1.2. Reagents and chemicals

Product	Company
$\alpha-{}^{32}$P dATP 111 TBq/mmol 370 MBq/ml (3000 Ci/mmol 10 mCi/ml)	Hartman Analytik GmbH
$\alpha-{}^{32}$P dCTP 111 TBq/mmol 370 MBq/ml (3000 Ci/mmol 10 mCi/ml)	Hartman Analytik GmbH
β-Mercaptoethanol	SERVA Electrophoresis GmbH
3-morpholino-propanesulfonic acid (MOPS)	Carl Roth GmbH+CO. KG
Agarose	Carl Roth GmbH+CO. KG
Albumin bovine, fraction V	Carl Roth GmbH+CO. KG
Ammonium persulfate (APS)	AppliChem GmbH
Aprotinin	Sigma-Aldrich Chemie GmbH
Bovine serumalbumine (BSA)	Carl Roth GmbH+CO. KG
Bromphenol blue sodium salt	AppliChem GmbH
CasyTon®isotonic buffer	Scharfe System, Reutlingen
Chloramphenicol	Carl Roth GmbH+CO. KG
Chlorophorm	Merck KGaA
Chloroform(24):Isoamylalcohol(1)	AppliChem GmbH
Diethylpyrocarbonate (DEPC)	Sigma-Aldrich Chemie GmbH
Dimethylsulfoxide (DMSO)	AppliChem GmbH
DNA from salmon sperm	Sigma-Aldrich Chemie GmbH

dGTPs	MBI Fermentas, St.Leon Rot
dNTPs (5mM)	Roboklon GmbH
dTTPs	MBI Fermentas, St.Leon Rot
ECL™ western blotting detection reagent	Amersham Biosciences Europe GmbH
EDTA	AppliChem GmbH
Ethanol 70% (with ketones)	AppliChem GmbH
Ethanol 96% (pure)	AppliChem GmbH
Ethidiumbromid	Sigma-Aldrich Chemie GmbH
ExpressHyb™ Hybridization Solution	Clontech Laboratories Inc., USA
Ficoll®	AppliChem GmbH
Formaldehyde (37%)	AppliChem GmbH
Formamide (deionized)	AppliChem GmbH
G418 (neomycin sulfate)	Life Technologies GmbH
Gancyclovir, Cymeven®	Roche Diagnostics Deutschland GmbH
Gelatine	Carl Roth GmbH+CO. KG
Glacial acid 100%	AppliChem GmbH
Glycerol	AppliChem GmbH
Glycine	AppliChem GmbH
HEPES	Sigma-Aldrich Chemie GmbH
HEPES sodium salt	Carl Roth GmbH+CO. KG
Hydrochloric acid 37%	AppliChem GmbH
Isopropanol	AppliChem GmbH
Lipopolysaccharide (*E. coli* O55:B5)	Sigma-Aldrich Chemie GmbH
Magnesium chloride	AppliChem GmbH
Methanol	AppliChem GmbH
Mitomycin C	Carl Roth GmbH+CO. KG
Nonfat powdered milk	Carl Roth GmbH+CO. KG
Nonident P40 (NP-40)	AppliChem GmbH
PBS	PAA Laboratories
pegGOLD Trifast™ reagent	PEQLAB Biotechnologie GmbH
Phase Lock Gel™ tubes	Eppendorf AG
Phenol(25):Chloroform(24):Isoamyl-alcohol(1)	AppliChem GmbH
Phenylmethanesulfonylfluoride (PMSF)	Sigma-Aldrich Chemie GmbH
Polyoxyethylensorbitanmonolaurat (tween20)	AppliChem GmbH
Polyvinylpyrrolidone	AppliChem GmbH
Ponceau S	Sigma-Aldrich Chemie GmbH
Protease inhibitor cocktail tablets (PIT)	Roche Diagnostics Deutschland GmbH
Roti®-Load1 (1×)	AppliChem GmbH
Salmon sperm nuclei	Sigma-Aldrich Chemie GmbH
Sodium acetate	AppliChem GmbH
Sodium azide	AppliChem GmbH

Sodium citrate	AppliChem GmbH
Sodium chloride	AppliChem GmbH
Sodium hydroxide	Carl Roth GmbH+CO. KG
Sodium lauryl sulphate (SDS)	Serva electrophoresis GmbH
Tetramethylethylenediamine (TEMED)	AppliChem GmbH
Trichloroacetic acid (TCA)	Sigma-Aldrich Chemie GmbH
Tris-(hydroxymethyl)-aminomethane (TRIS)	AppliChem GmbH
Trypan blue	Sigma-Aldrich Chemie GmbH
Xylene cyanol	Carl Roth GmbH+CO. KG

2.1.3. Buffers and solutions

All buffers and solutions were prepared in deionized H_2O, unless otherwise noted.

Buffer or solution	Components
Aprotinin	10 mg/ml
APS	10% amonium persulfate
Blocking solution (western blot)	5% milk in PBS
Blotting buffer	25 mM TRIS 192 mM Glycin 10% Methanol pH 8.3
Church buffer	586 mM phosphate buffer (Na_2HPO_4/NaH_2PO_4, pH 7) 1.17 mM EDTA 8.2% SDS
ColHyb denaturation solution	0.5 N NaOH 1.5 M NaCl
ColHyb neutralization solution	1.5 M NaCl 0.5 M TRIS/HCl pH 7.4
ColHyb wash I	40 mM phosphate buffer (Na_2HPO_4/NaH_2PO_4, pH 7) 0.25 mM EDTA 5% SDS

ColHyb wash II	40 mM phosphate buffer (Na_2HPO_4/NaH_2PO_4, pH 7) 0.25 mM EDTA 1% SDS
Denhardt's solution (100×)	2% BSA 2% ficoll 2% polyvinylpyrrolidone
DEPC-H_2O	1 ml DEPC in H_2O autoclaved
DNA lysis buffer	50 mM TRIS pH 8 100 mM EDTA 100 mM NaCl 1% SDS 400 µg/ml proteinase K
DNA sample loading buffer (10×)	0.4% bromphenol blue 0.4% xylencyanol 50% glycerol 0.1 mM EDTA
Electrophoresis buffer	25 mM TRIS 192 mM Glycin 0.1% SDS
ES cell lysis buffer	100 mM TRIS/HCl pH 8.5 0.1% tween20 100 µg/ml proteinase K
MOPS (10×)	0.2 M MOPS 0.05 M sodium acetate 0.01 M EDTA pH 5.5–7.0
OLB buffer	100 µl OLB solution A 250 µl OLB solution B 150 µl OLB solution C
OLB solution A	1 ml OLB solution O 18 µl β-mercaptoethanol 5 µl dGTP and dTTP each (0.1 M)

OLB solution B	2 M Hepes pH 6.6
OLB solution C	random hexamers in TE (OD_{260} 90 U/ml)
OLB solution O	1.25 M TRIS/HCl pH 8 125 mM $MgCl_2$
PBS (10×)	1.37 M NaCl 120 mM phosphate 27 mM KCl pH 7.4
PBS-T	0.05% tween20 in PBS
Phenylmethanesulfonylfluoride	50 mM in methanol
Ponceau S solution	0.2% ponceau S in 5% trichloroacetic acid
Prehybridization solution	5×SSC 0.5% SDS 100 µg sheared and denatured salmon sperm DNA 5×Denhardt's solution
Premix	2.5 ml 10×MOPS running buffer 4.4 ml 37% formaldehyde (pH>4.0<7.0) 12.5 ml formamide deionized
Protease inhibitor cocktail	protease inhibitor tablet (Roche) dissolved in 1 ml H_2O
Proteinase K	10 mg/ml
RIPA buffer	50 mM TRIS-HCl pH 7.4 150 mM NaCl 1% NP-40 0,5% sodium deoxycholate 0,1% SDS 5 mM EDTA 1×protease inhibitor cocktail

RNA loading buffer (10 ml)	20 µl 0.5 M EDTA 25 µl saturated bromphenol blue solution 25 µl saturated xylene cyanol solution 5.0 ml glycerol (100%) 4.93 ml DEPC-H_2O
Southern blot wash solution I	2×SSC 0.2% SDS
Southern blot wash solution II	1×SSC 0.2% SDS
Southern blot wash solution III	0.2×SSC 0.2% SDS
SSC (20×)	3 M NaCl 300 mM sodium citrate
Stripping solution (Southern blot)	0.5% SDS
Stripping solution (western blot)	62.5 mM TRIS pH 6.7 100 mM β-mercaptoethanol 2% SDS
TAE (50×)	2 M TRIS 2 M acetic acid 50 mM EDTA
TE	10 mM TRIS-HCl, pH 7.5 or pH 8 1 mM EDTA
Transfection buffer	10 mM HEPES in PBS
Transfer solution (Southern blot)	0.4 N NaOH
Tripple lysis buffer	50 mM TRIS pH 8.0 150 mM NaCl 0.5% sodiumdeoxycholat 0.1% SDS 1% NP-40 0.02% sodium azid 10 µg/ml aprotinin (directly before use) 1 mM PMSF (directly before use)

2.1.4. Protein and DNA markers

Marker	Company
1 kb ladder	Fermentas GmbH
100 bp ladder	Fermentas GmbH
High molecular weight marker	Fermentas GmbH
Prestained protein ladder	Fermentas GmbH

2.1.5. Vectors

Vector	Company/Producer
BAC RPCIP711F18214Q3 (USP15)	imaGenes GmbH
BAC RPCIP711G10332Q2 (USP18)	imaGenes GmbH
pBlu2KSP[USP15_3′homo_Spe/Avr kl]Rev_loxP	Ronny Hannß
pBlu2KSP[USP15_3′subfragment]	Ronny Hannß
pBlu2KSP[USP15_5′homo Spe/Avr kl]Rev	Ronny Hannß
pBluescript II KSP (pBlue2KSP)	Stratagene GmbH
pCMV-Tag3B-USP15	Hetfeld et al. [52]
pPNT-frt3	Obtained from Dr. Klaus-Peter Knobeloch
pPNT-frt3[5′homo UBP43]	Ronny Hannß
pPNT-frt3[UBP43TV]	Ronny Hannß
pPNT-frt3[USP15_5′homo]	Ronny Hannß
pPNT-frt3[USP15_TV]	Ronny Hannß
pZErO™-2	Life Technologies GmbH
pZErO™-2[UBP43 KpnI frag]	Ronny Hannß
pZErO™-2[UBP43 PmlI3-5]	Ronny Hannß
pZErO™-2[UBP43 PmlI C61]	Ronny Hannß
pZErO™-2[UBP43 PmlI C61A]	Ronny Hannß
pZErO™-2[USP15_5′SpeI]	Ronny Hannß

2.1.6. Primary antibodies

Antibodies were diluted as indicated in PBS containing 5% milk. Dilution marked by asterisk was prepared in 3% BSA in PBS-T.

Antigen	Dilution	Host	Company/Producer
γ-Tubulin	1:3000	Mouse	Santa Cruz Biotechnology Inc., USA
CSN5 (8H8.5)	1:2000	Mouse	GeneTex Inc., USA
CSN8 (PW8290)	1:4000	Rabbit	Biomol GmbH
GAPDH	1:7500	Mouse	HyTest Ltd., Finland

IκBα	1:2000	Rabbit	Cell Signaling Technology Inc., USA
p-SMAD2	1:1000	Rabbit	New England Biolabs GmbH
RBX1 (Rockland)	1:2000	Rabbit	Biomol GmbH
USP15 (polyclonal)	1:750–1000*	Rabbit	Abcam plc, UK

2.1.7. Secondary antibodies

Antibodies were diluted as indicated in PBS containing 5% milk.

Name	Final concentration	Company/Producer
Anti-goat-IgG-HRP conjugate	0.5 µg/ml	Seramun diagnostics GmbH
Anti-mouse-IgG-HRP conjugate	0.5 µg/ml	Seramun diagnostics GmbH
Anti-rabbit-IgG-HRP conjugate	0.5 µg/ml	Seramun diagnostics GmbH

2.1.8. Cytokines

All cytokines were diluted according to the manual supplied by the providing company.

Cytokine	Company
TGF-β1 (recombinant, active, human)	Abcam plc, UK
TNF-α1 (recombinant, murine)	ImmunoTools GmbH

2.1.9. Kits

Kit	Company
EURx PCR / DNA CleanUp Kit	Roboklon GmbH
First Strand cDNA Synthesis Kit	Fermentas GmbH
GeneMATRIX Agarose-Out DNA Purification Kit	Roboklon GmbH
GeneMATRIX PCR/DNA Clean-Up Purification Kit	Roboklon GmbH
Invisorb®Spin Plasmid Mini Two kit	STRATEC Molecular GmbH
NucleoBond®Xtra Midi kit	MACHEREY-NAGEL GmbH+Co. KG
QuikChange™ Site-Directed Mutagenesis Kit	Stratagene GmbH
Rediprime™ II DNA Labeling System	Amersham Biosciences Europe GmbH

2.1.10. Equipment and devices

Device	Company
Automated cell counter CASY®	Roche Innovatis AG
Contamination monitor LB122	BERTHOLD TECHNOLOGIES GmbH+Co. KG
Copier 7115	Konica Minolta Business Solutions Deutschland GmbH
Electroporator Gene Pulser	Bio-Rad Laboratories GmbH
Freezer −86C	FORMA SCIENTIFIC ltd., UK
Freezers, refridgerators	Robert Bosch Hausgeräte GmbH
Gased incubator	Heraeus, UK
GenAmp®PCR System 9700	Perkin Elmer, Wellesley, USA
Hemocytometer, Neubauer (improved)	VWR International GmbH
Homogenizer	PEQLAB Biotechnologie GmbH
Horizontal electrophoresis chamber	Bio-Rad Laboratories GmbH, USA Renner GmbH
Ice machine	SCOTSMAN ICE SYSTEMS, Italy
Incubator Certomat®HK	Sartorius AG
Laminar flow bench	Heraeus, UK
Mastercycler®Gradient	Eppendorf AG
Microscope	Helmut Hund GmbH
Microwave	Robert Bosch Hausgeräte GmbH
Mini-gel system for vertical electrophoresis	Bio-Rad Laboratories GmbH
pH meter	WTW GmbH
Phosphoimager and screens	Amersham Biosciences Europe GmbH
Photometer GeneQuant	Amersham Biosciences Europe GmbH
Pipets	Eppendorf AG Gilson Inc., USA
Pipetus®	Hirschmann Laborgeräte GmbH+Co. KG
Power supply	Bio-Rad Laboratories GmbH Biometra GmbH
Scanner	EPSON EUROPE ELECTRONICS GmbH
Shaker ST5 CAT, Centromat®, Swip KL-2	Neolab, Edmund Bühler
Special accuracy weighing machine BP221S and BP610	Sartorius
Thermocycler Tpersonal	Biometra GmbH
Thermomixer Comfort	Eppendorf AG
UV gel documentation system	UV systems Intas GmbH
UV-linker, Stratalinker®2400	Stratagene GmbH
Varioklav®steam sterilizer	H+P Labortechnik GmbH

Waterbath C10/5P	Thermo Haake GmbH

2.1.11. Enzymes

Enzyme	Company
Alkaline phosphatase FastAP™	Fermentas GmbH
AvrII (XmaJI)	Fermentas GmbH
BamHI	Fermentas GmbH
BsrBI (MbiI)	Fermentas GmbH
Collagenase	Sigma-Aldrich Chemie GmbH
EcoRI	Fermentas GmbH
EcoRV	Fermentas GmbH
FseI	Fermentas GmbH
Klenow fragment	Fermentas GmbH
	New England Biolabs GmbH
KpnI	Fermentas GmbH
KpnI, HC	Fermentas GmbH
NotI	Fermentas GmbH
OptiTaq polymerase	Roboklon GmbH
PacI	Fermentas GmbH
PfuTurb™ DNA polymerase	Stratagene GmbH
PmeI	Fermentas GmbH
PmlI	Fermentas GmbH
Proteinase K (10 mg/ml)	PAN Biotech GmbH
SmaI	Fermentas GmbH
SpeI (BcuI)	Fermentas GmbH
SpeI, HC	New England Biolabs GmbH
T4 DNA ligase	Fermentas GmbH
XhoI	Fermentas GmbH

2.1.12. Expendable materials

Consumable	Company
15/50 ml tubes	Greiner bio-one GmbH
6/12/48/96 well plates	Nunc, Greiner bio-one GmbH
6/10/15 cm dishes	Greiner bio-one GmbH
Cell cultur flasks	Greiner bio-one GmbH
Cell scraper	Carl Roth GmbH+CO. KG
Cuvettes	Carl Roth GmbH+CO. KG
Pipet tips	SARSTEDT AG+Co.
Pasteur pipets	Carl Roth GmbH+CO. KG

Pipets, one-way	SARSTEDT AG+Co.
Reaction tubes	SARSTEDT AG+Co. Eppendorf AG
Safe seal 1.5 ml tubes	SARSTEDT AG+Co.
Scalpel	Carl Roth GmbH+CO. KG
X-Omat UV films	Kodak GmbH

2.1.13. Filters and membranes

Filter/membrane	Company
Nitrocellulose membrane	Carl Roth GmbH+CO. KG
Nylon membrane Biodyne®B 0.45 µm PALL Gelman Laboratory	VWR International GmbH
Sterile filters	Carl Roth GmbH+CO. KG
Whatman 3 MM chromatography paper	VWR International GmbH

2.1.14. Media and supplements for eukaryotic cells

Medium or supplement	Company
β-Mercaptoethanol	Life Technologies GmbH
DMEM high glucose	Cambrex
ES cell medium	500ml DMEM 15% FCS 0.2 mM glutamine 0.2 mM nonessential amino acids 0.1 mM β-mercaptoethanol 6 ml nucleoside solution 100 u/ml penicillin 100 u/ml streptomycine 2000 u/ml LIF
Feeder medium	500 ml DMEM 10% FCS 0.2 mM glutamine 0.2 mM nonessential amino acids 0.1 mM β-mercaptoethanol 100 u/ml penicillin 100 u/ml streptomycine

Fetal calf serum (FCS, heat inactivated 30 min at 56 °C)	Biochrom AG
Freezing medium	20% DMSO in FCS
Gancyclovir, Cymeven®	Roche Diagnostics Deutschland GmbH
Gelatine	10% gelatine in PBS
L-Glutamine	Cambrex, Verviers, Belgium
Leukemia inhibitory factor (LIF)	Bioscience Research Reagents, USA
Mitomycin C	0.5 mg/ml in PBS
Neomycine sulfate (G418)	Life Technologies GmbH
Nonessential amino acids	Cambrex Corp., USA
Nucleoside solution	80 mg adenosine 85 mg guanosin 73 mg cytidin 73 mg uridine 24 mg thymidine (steril filtered)
Penicillin/Streptomycin	Cambrex Corp., USA
Starving medium	500 ml DMEM 0.2 mM glutamine 0.2 mM nonessential amino acids 0.1 mM β-mercaptoethanol 100 u/ml penicillin 100 u/ml streptomycine
Trypsin-EDTA (0.05%), Gibco®	Life Technologies GmbH
Zell Shield™	Minerva Biolabs GmbH

2.1.15. Media and supplements for bacteria

Media or supplement	Concentration in LB	Company
Ampicillin	100-120 µg/ml	Sigma-Aldrich Chemie GmbH
LB broth (Luria Miller)	10 g/l tryptone 5 g/l yeast extract 10 g/l sodium chloride pH 7	Carl Roth GmbH+CO. KG
LB agar (Luria Miller)	Recipe is equivalent to LB broth but contains 15 g/l agar	Carl Roth GmbH+CO. KG
Kanamycin	30–50 µg/ml	Sigma-Aldrich Chemie GmbH
X-Gal		Agilent Tech. GmbH+Co. KG

2.1.16. Bacteria

Strain	Company
DH5α	Life Technologies GmbH
TOP10	Life Technologies GmbH
XL2blue	Agilent Technologies GmbH+Co. KG

2.1.17. Eukaryotic cells

ES cells E14 (Hooper et al. 1987)
Mouse adult fibroblasts *Usp15*$^{-/-}$ and *Usp15*$^{+/+}$ generated in this study

2.1.18. Animals

ACTB::FLPe transgenic deleter strain
CMV::FLPe transgenic deleter strain
C57BL/6
Isg15$^{+/-}$
Usp15$^{+/\mathrm{fl}}$ generated in this study (mixed background)
Usp18$^{+/\mathrm{C61A}}$ generated in this study (mixed background)

2.1.19. Mouse genomic library

Mouse genomic DNA (gDNA) containing P1 artificial chromosome (PAC) library, obtained from RZPD, originated from the Roswell Park Cancer Institute, created by Pieter J. de Jong and Kazutoyo Osoegawa [124].

2.1.20. Software

Software	Company/Provider
CAP3 Sequence Assembly Program	X. Huang & A Madan [55]
FinchTV	Geospiza, USA
GelQuantNET	http://BichemLabSolutions.com, affiliates University of California, San Francisco UCSF
ImageQuant	Amersham Biosciences Europe GmbH
JabRef	http://sourceforge.net/
LaTeX and BibTeX	Comprehensive TeX Archive Network (CTAN)
LibreOffice	The Document Foundation
Primer3	S. Rozen & H. Skaletsky [135] Source code available at http://fokker.wi.mit.edu/primer3/
Repeatmasker	A. F. A. Smit, R. Hubley & P. Green RepeatMasker at http://repeatmasker.org
Texmaker	Texmaker at http://www.xm1math.net/texmaker/
VectorNTI®	Life Technologies GmbH

2.1.21. DNA primers

Generally, primers were diluted in H_2O to a final concentration of 50 µM, unless otherwise noted.

Usp18 primers and corresponding sequences

Name	Sequence
UBP43 Protease EXs	TAGACCCCAGAAAAACATC
UBP43 Protease EXa	CGGCATTGGAAAGGAGAC
UBP43_mRNA_C61A_verif_F	GTCATTTGTCTCCGGCTTGT
UBP43_mRNA_C61A_verif_R	CACATGTCGGAGCTTGCTAA

Usp18 **primers for site directed mutagenesis and corresponding sequences**

Name	Sequence
upC61A	GGTTTACACAACATCGGACAGACGgcTTGCCTTAACTCCTTGC
loC61A	GCAAGGAGTTAAGGCAAgcCGTCTGTCCGATGTTGTGTAAACC

Usp15 **primers for Southern blot probe amplification and corresponding sequences**

Name	Sequence
USP15 5′ Spe probe3 F	TAGCCTCACCCCTGTACCTG
USP15 5′ Spe probe3 R	CCCAGGACTTTTCCCCTAAC
USP15 3′ Spe probe1 F	ATGAGGCAGCACTGACTTGA
USP15 3′ Spe probe1 R	CCCACTTCCTGGTGACACTT

Usp18 **primers for Southern blot probe amplification and corresponding sequences**

Name	Sequence
KpnI_5′extern_up	CACACCCTCCTCAACTGGAT
KpnI_5′extern_lo	GTGGTGTGGAAAAGCTGGTT
KpnI_3′extern_up	CGGGAATGCCATAGATTTTG
KpnI_3′extern_lo	GCGGACAGACAGAACCCTAA

Usp15 **oligos containing loxP site and corresponding sequences**

Name	Sequence
P-S-LoxP-P_Sense	5'-AAAAAATTAATTAAACTAGTATAACTTCGTATAGCATACA-TTATACGAAGTTATTTAATTAAAAAAAA-3'
P-S-LoxP-P_AntiS	5'-TTTTTTTTAATTAAATAACTTCGTATAATGTATGCTATAC-GAAGTTATACTAGTTTAATTAATTTTTT-3'

Usp15 **primers for amplification of probes for colony hybridization and corresponding sequences**

Name	Sequence
USP15 5′homo_F	GGGTAAACAGGCTGAAACCA
USP15 5′homo_R	GCCCTTCCCTGTCCTAAGAG

USP15 3′homo_F	TGAGCTATGTCCAAGCAACG
USP15 3′homo_R	GGGAAGTTTCCCTAGGCTTG

Primers for genotyping by PCR and corresponding sequences

Name	Sequence
USP15_PacI_F	GCAGGTTGCTCCATTTCCTA
USP15_PacI_R	CTCCCGGCCTAGATACATCA
USP15_5′homo-1	CCAAGCTCGGAATGATTGAT
USP15_5′homo-4	TCTTAGGCCGAACTTGAACG
USP15_ScreenIIR	GCCAGAGGCCACTTGTGTAG
Cre1	ccgggctgccacgaccaa
Cre2	ggcgcggcaacaccattttt

2.1.22. Colony hybridization probes

Diverse probes for colony hybridization and their corresponding primers used for amplification. Amplificate size in base pairs (bp).

Name of probe	Forward primer	Reverse primer	Probe size
USP15_5′homo	USP15_5′homo_F	USP15_5′homo_R	283 bp
USP15_3′homo	USP15_3′homo_F	USP15_3′homo_R	324 bp

2.1.23. Southern blot probes

Diverse probes for Southern blot and their corresponding primers used for amplification. Amplificate size in base pairs (bp).

Name of probe	Forward primer	Reverse primer	Probe size
Usp15 5′	USP15 5′ Spe probe3 F	USP15 5′ Spe probe3 R	495 bp
Usp15 3′	USP15 3′ Spe probe1 F	USP15 3′ Spe probe1 R	367 bp
Usp18 5′	KpnI_5′extern_up	KpnI_5′extern_lo	325 bp
Usp18 3′	KpnI_3′extern_up	KpnI_3′extern_lo	552 bp

2.2. DNA and RNA methods

2.2.1. DNA isolation from eukaryotic cells and mouse tail biopsies

Tail cuts of approximately 5 mm or 20 mg tissue were lysed overnight at 56 °C adding 700 µl DNA lysis buffer. Subsequently, the DNA was extracted and purified by phenol chloroform extraction (see section 2.2.2). The precipitated DNA was eluted in 100–150 µl TE overnight at 56 °C.

2.2.2. Phenol chloroform extraction

When DNA had to fulfill special requirements of purity, e. g., linearized targeting vectors used for transfection, or DNA used for Southern blots from tail cuts, it was cleaned by phenol chloroform extraction. 10 mM TRIS pH 8.5 were added to the DNA containing solution to a final volume of 300 µl. Subsequently, 300 µl of phenol(25):chloroform(24):isoamylalcohol(1) was added to the solution. After vigorous vortexing, the tube was centrifuged for 5 min at full speed (≥15000×g). For better phase separation also Phase Lock Gel™ (Eppendorf AG) tubes were used according to the manufacturer's protocol. The aqueous upper phase was transferred into a new tube and 300 µl of chloroform/isoamylalcohol (Chl/IAA) were added followed by vigorous vortexing. The solution was centrifuged for 5 min at full speed and upper phase was transferred to a new tube. Subsequently, the DNA was precipitated with isopropanol (see section 2.2.3). In every moment working with chloroform and phenol, eye protection and appropriate skin protection was used.

2.2.3. DNA precipitation using isopropanol

For precipitation of DNA 0.7 volume of isopropanol was added to the solution which was then centrifuged at 4 °C for 15–30 min at full speed (≥15000×g). The supernatant was dicarded, and the precipitated DNA was washed by adding 300–1000 µl of 70% ethanol followed by another centrifugation step at 4 °C for 10 min at full speed. The DNA was washed 2–3 times. In the last step, the DNA pellet was air dried. For sterile preparation of the DNA, it was air dried under a laminar flow box. The DNA pellet was then eluated by adding sterile PBS and incubation at either 3–4 h at room temperature or 1 h 56 °C. The DNA concentration and purity was

evaluated by photometrical mesurements (see section 2.2.6).

2.2.4. DNA agarose gel electrophoresis

Agarose gels were used to seperate DNA fragments according to their fragment size. The appropriate amount of agarose was boiled in 1×TAE buffer until the agarose powder was completely dissolved keeping in mind retardation of boiling. Depending on the size of the fragment of interest 0.7% (for large fragments, ≥6 kb) up to 2.5% (for small fragments, ≤0.5 kb) agarose gels were used. After cooling down to approximately 60 °C, ethidiumbromide was added to a final concentration of 1 µg/ml. The agarose solution was poured into horizontal casting chambers with combs. The comb was removed after complete cool down and polymerization of the formed gel. Before loading the samples, they were mixed with appropriate volume of 10×DNA sample loading buffer. The DNA fragments were electrophoretically seperated in 1×TAE buffer at constant voltage of 25–120 V depending on gel chamber size and agarose concentration.

2.2.5. Isolation of DNA from agarose gels

The DNA bands were visualized on a UV light transilluminator and excised using a scalpel or glas slide. The gel slices were transferred into a tube. The DNA was isolated with the GeneMATRIX Agarose-Out DNA Purification Kit (Roboklon GmbH) according to the manufacturer's protocol.

2.2.6. Photometric determination of DNA/RNA concentration and purity

The DNA/RNA concentration of solutions with ≥50 ng/µl DNA/RNA was determined by UV photometry. The absorption at OD_{260} and OD_{280} was measured using the solvent as reference. The DNA/RNA sample was diluted so that the OD_{260} was in the range of 0.1 to 1 in order to assure accurate measuring values. An OD_{260} of one is equivalent to 50 µg/ml dsDNA, 40µg/ml RNA, 33 µg/ml ssDNA and 20 µg/ml oligonucleotides. Therefore, the obtained value was multiplicated with the dilution factor and the above mentioned multiplication factor to calculate the concentration. The ratio of OD_{260}/OD_{280} gives information about the contamination with proteins measured at OD_{280}. In a sample free of proteins the ration of OD_{260}/OD_{280}

is expected to be between 1.8 and 2.0.

2.2.7. Determination of DNA concentration by agarose gel electrophoresis

Noncircular DNA in soultion with a concentration of 5–200 ng/µl was quantified via agarose gel electrophoresis. Different volumes of DNA solution (usually 1–5 µl) were loaded on an agarose gel. After seperation of DNA fragments, the DNA amount was estimated by comparison to a DNA ladder with defined DNA amounts per band.

2.2.8. Estimation of DNA concentration by dot quantification

The DNA concentration of solutions with a concentration of 1–50 ng/µl was estimated using a petri dish filled with 1% agarose gel containing 100 µg/ml ethidium-bromide. An advantage of this methods is that little volumina of solution with low DNA concentration can be evaluated. Therefore, 1 µl of DNA sample were pipetted on the gel together with DNA solutions of defined concentration. After a short incubation time of about 5 min, DNA on the petri dish was visualized on a UV transilluminator and the DNA concentration was estimated comparing illumination intensity of the sample to the DNA standards.

2.2.9. Isolation of genomic DNA from ES cells

To isolate genomic DNA (gDNA) from ES cells the cells were cultivated in 24-well plates. The medium of confluent clones was discarded subsequently adding 500 µl ES cell lysis buffer. The cells were incubated at 37 °C for ≥3 h. When all clones were lysed the DNA was precipitated by adding 500 µl isopropanol and shaking for 10 min. Subsequently, the solution was discarded and the precipitated DNA was washed by adding 70% ethanol. The washed and precipitated DNA was transferred to a 96-well plate using a 200 µl pipet tip. Subsequently, the DNA was eluted in 100–120 µl TE at 56 °C overnight.

2.2.10. Preparation of plasmid DNA from small bacterial cultures

For small scale preparation of plasmid DNA (miniprep), 2–10 ml LB medium containing the appropriate antibiotic was inoculated with a single bacterial clone picked from a selection agar plate. The inoculated LB medium was incubated overnight shaking at 37 °C. The DNA was extracted using Invisorb®Spin Plasmid Mini Two kit (STRATEC Molecular GmbH) according to the manufacturer's protocol. Optionally, instead of using the provided spin columns, the DNA was directly precipitated with isopropanol (see section 2.2.3).

2.2.11. Preparation of plasmid DNA from large bacterial cultures

Extraction of plasmid DNA from large bacterial cultures (midiprep) was performed using the NucleoBond®Xtra Midi kit (MACHEREY-NAGEL GmbH & Co. KG) according to the manufacturer's protocol. For extraction of high copy number plasmids single bacterial clones obtained from a selection agar plate were grown in 50–150 ml LB medium including the appropriate antibiotic shaking overnight at 37 °C. For extraction of plasmids from P1 artificial chromosomes (PAC) clones a higher volume of LB (500ml) was used due to the low the copy number.

2.2.12. Digestion of DNA with restriction enzymes

Per 1 µg of DNA 10 u of enzyme were used together with the appropriate buffer provided by the manufacturer. Usually, the final volume depended on the concentration of the DNA solution. For molecular cloning, usually 1–4 µg DNA were digested in a final volume of 20 µl. Because restriction enzymes are usually stored in 50% glycerol which inhibits the DNA digestion if exceeding 10% in the reaction mixture, the final reaction mix was adapted to keep the gycerol concentration below 10% of glycerol.

2.2.13. Blunting DNA with 5′protruding termini

The large fragment of *E. coli* polymerase I, called Klenow fragment, exhibits $5' \longrightarrow 3'$ polymerase activity and $3' \longrightarrow 5'$ proofreading exonuclease activity, but lacks $5' \longrightarrow 3'$ exonuclease activity. Thus, the Klenow fragment was used to fill up 5′ protruding ends. The Klenow fill-in reaction was performed according to the manufacturer's

protocol (Fermentas GmbH). 0.1–4 µg DNA were mixed with 0.05 mM dNTPs each and 1–5 u Klenow fragment and the provided buffer in a final reaction volume of 20 µl. If possible, the reaction was performed directly in the restriction enzyme digest mix. The reaction mix was incubated at 37 °C for 10 min followed by inactivation of the Klenow fragment at 75 °C for 10 min. Subsequently, the DNA in the reaction mix was purified using the EURx PCR / DNA CleanUp Kit (Roboklon GmbH).

2.2.14. Dephosphorylation of DNA 5′termini

When a vector was cut for cloning with only one restriction enzyme or the DNA ends were compatible, subsequent religation was avoided by dephosphorylation of the 5′ end of the vector DNA. Therefore, 1 µl of FastAP™ (an alkaline phosphatase) was added to 1–5 µg of DNA directly into the restriction enzyme mix or after purification of the linear DNA according to the manufacturer's protocol (Fermentas GmbH). To 1–5 µg DNA of cut and purified vector 5 µl of 10×FastAP™ buffer were mixed to a final volume of 49 µl. Desphosphorylation was started by adding 1 µl of FastAP™ and vigorous vortexing. The reaction mix was incubated at 37 °C for 10 min. The reaction was stopped by heating at 75 °C for 5 min.

2.2.15. Ligation of DNA fragments

For ligation of sticky end DNA fragments, e. g., compatible 5′ or 3′protruding ends, 30–100 ng of a linearized vector were used with equimolar amounts of insert. The ligation reaction was perfomed using 2.5–5 u T4 DNA ligase (Fermentas GmbH) according to the manufacturer's protocol. Ligation of blunt end fragments was performed using a vector insert ratio of 1/3 and 5 u T4-DNA ligase. The ligation mixes were incubated at room temperature for 1 h or overnight at 14 °C. Optionally, the T4-DNA ligase was inactivated 65 °C for 10 min. For tranformation of 50-150 µl competent bacteria, 2–4 µl reaction mix were used. Grown bacteria were screened for the desired vector. Vectors were sequenced by Seqlab – Sequence Laboratories Göttingen GmbH or Eurofins MWG GmbH.

2.2.16. Annealing of DNA oligomeres

For the generation of short DNA sequences, sense and antisense strand were designed and synthesized (BioTeZ Berlin-Buch GmbH). The DNA sequences were flanked by

the desired restriction enzyme cleavage sites and the necessary poly(A)$_n$ overhangs for efficient cleavage to the close termini of the fragments according to (Fermentas GmbH). Each 25 µl of 50 µM sense and antisense oligomeres were mixed in aquimolar amounts addings 25 µl of Dubelcco's PBS. The final mixture was heated to 95 °C, subsequently, decreasing the temperature in steps 5 °C/5 min until 4 °C. The annealed oligomeres were purified as described in section 2.2.24 and cut with the appropriate restriction enzymes followed by another purification step.

2.2.17. Site directed mutagenesis

For site directed mutagenesis, the QuikChange™ Site-Directed Mutagenesis Kit (Stratagene GmbH) was used according to the manufacturer's protocol. The cycling parameters for the QuikChange Site-Directed Mutagenesis method were adapted to 16 cycles of amplification with PfuTurb™ DNA polymerase.

2.2.18. Isolation of RNA from mammalian cells

The pegGOLD Trifast™ reagent (PEQLAB Biotechnologie GmbH) was used to isolate RNA from mammalian cells. Medium from cells grown on 10 cm cell culture dish was removed and 1 ml pegGOLD Trifast™ was added and incubated for 5 min at room temperature. The solution was transferred into a tube adding 0.2 ml chloroform. After vigorous vortexing the tube was centrifuged at 12000×g in order to obtain phase seperation. The clear aqueous upper phase containing the RNA was transferred into a fresh tube. In order to precipitate the RNA, 0.5 ml isopropanol was added. After vigorous vortexing and incubation on ice for 5–10 min, the tube was centrifuged at 12000×g at 4 °C for 10 min. The supernatant was removed and the pellet was washed two times with 1 ml of 75% ethanol by vortexing and subsequent centrifugation using latter conditions. The RNA pellet was air dried and eluted in 40 µl of RNase free, DEPC treated water at 56 °C. The RNA concentration was determined by photometrically analysis (see section 2.2.6).

2.2.19. Synthesis of cDNA

The cDNA was synthesized using the First Strand cDNA Synthesis Kit (Fermentas GmbH). Therefore, 2 µg (0.1–5 µg) of RNA were mixed with 1 µl 100 µM oligo(dT)$_{18}$ primer filled up to a final volume of 11 µl with nuclease free water. The mixture was

heated to 65 °C for 5 min and immediately chilled on ice. The following components were added to the mix in the mentioned order: 4 µl of 5×Reaction Buffer, 1 µl of (20 u/µl) RiboLock™ RNase Inhibitor, 2 µl of 10 mM dNTP mix and 2 µl of (20 u/µl) M-MuLV Reverse Transcriptase. The mix was incubated at 37 °C for 60 min. The reaction was terminated at 70 °C for 5 min. The prepared cDNA was directly used for PCR or stored at ≤ -20 °C.

2.2.20. Generation of competent bacteria using $CaCl_2$

For the generation of heat shock competent bacteria 500 ml LB medium were inoculated with 5 ml overnight culture obtained from a single colony. The inoculated LB medium was incubated shaking at 37 °C until an OD_{600} of 0.4–0.6 (3–4 h). Subsequently, the bacteria suspension was kept 3 min on ice mixed with NaCl to cool down. The bacteria were peleted by centrifugation at 4000–6000×g for 8–12 min. The supernatant was removed, the bacterial pellet was resupsended in ice cold 0.1 M $MgCl_2$, and again centrifuged at 4000–6000×g for 8–12 min. The supernantant was discarded, the bacteria were resuspended in ice cold 0.1 M $CaCl_2$, and incubated on ice for 30 min. Subsequently, the bacteria were pelleted by centrifugation at 4000–5500×g for 8–12 min. After discarding the supernatant, the bacteria were resuspended in ice cold 15 ml 0.1 M $CaCl_2$, mixed with approximately 2 ml of autoclaved 87% glycerol, and stored in aliquots of 50–100 µl at −80 °C.

2.2.21. Transformation of competent *E. coli* by heat shock

To introduce a DNA vector, chemocompetent *E. coli* bacteria were thawn on ice for 15 min. For transformation of 100 µl competent bacteria, generally, 1–30 ng vector were used (for coexpression of plasmids up to 1 µg). For ligation mixtures, the volume did not exceed 5 µl per 100 µl bacteria. After adding the DNA, the bacteria DNA suspension was gently mixed and kept on ice for 15 min. Subsequently, the mix was immediately heated at 42 °C for 45–90 seconds and directly placed on ice for additional 2 min. In case of ampicillin selection, the bacteria were directly plated on agar plates. If not ampicillin, 500-1000 µl of LB medium were added and the bacteria were put on a shaker at 37 °C for 45 min. Subsequently, the bacteria were plated on a selection agar plate containing the appropriate antibiotic.

2.2.22. Polymerase chain reaction (PCR)

PCR was used to specifically amplify DNA using vectors, gDNA or cDNA as template. For all PCR reactions, Opti*Taq* DNA polymerase (Roboklon GmbH) was used. Opti*Taq* DNA polymerase is a mixture of thermostable DNA polymerases and exhibits a $3' \longrightarrow 5'$ proofreading activity, so that the obtained amplified DNA could be used for cloning. For DNA amplification, components were mixed as shown in table 2.28. If the amplified DNA was used for cloning, the amount of template DNA was used as high as possible but not exceeding 200 ng DNA per 25 µl PCR reaction mix. The general PCR program used can be seen in table 2.27. Annealing temperature (T_a) depended on the primers that were used to amplify the DNA. Generally, all primers were designed by the primer3 algorithm and were optimized for $T_a = 60\,°C$. The duration of the extension step depended on the DNA to be amplified expecting synthesis speed of 1 kb per minute.

Table 2.27.: PCR temperature protocol.

Temperature	Time (min)		
95 °C	5	Initial denaturation	
95 °C	0.5	Denaturation	
T_a	0.5	Annealing	25–35 cycles
72 °C	kb/min	Extension	
72 °C	5–10	Terminal extension	

Table 2.28.: General PCR pipetting scheme.

Component	Ammount/Volume
DNA template	0.1–200 ng
10×Buffer C	2.5 µl
dNTPs (5 mM)	1 µl
5′primer (50 µM)	0.25 µl
3′primer (50 µM)	0.25 µl
H_2O	*ad* 25 µl
	25 µl

2.2.23. Genotyping of *Usp15* mutants by PCR

Usp15 mutant mice generated in this study were genotyped by PCR as shown in table 2.29 using 1 µl of 1/4 diluted DNA derived from tail biopsies as template. To

detect the different alleles, appropriate primers (section 2.1.21) were used in a PCR program shown in table 2.29. The different *Usp15* alleles detected are wildtype (wt), neomycin-floxed (neo-fl), floxed (fl), and deleted (del) indicated in conjunction with their expected amplificate size (see table 2.30) using the above mentioned PCR protocol.

Table 2.29.: PCR protocol for genotyping of *Usp15* mice.

Temperature	Time		
95 °C	5 min	Initial denaturation	
95 °C	30 s	Denaturation	
T_a	30 s	Annealing	35 cycles
72 °C	37 s	Extension	
72 °C	10 min	Terminal extension	

Table 2.30.: Genotyping of *Usp15* mutants. Primers and size expected amplificates in base paires.

Primer 1	Primer 2	wt	neo-fl	fl	del
USP15_PacI_F	USP15_PacI_R	219	267	267	—
USP15_5′HOMO-1	USP15_PacI_R	—	—	—	513
USP15_5′HOMO-1	USP15_ScreenIIR	—	585	—	—
USP15_5′HOMO-1	USP15_5′HOMO-4	483	—	616	—

2.2.24. Purification of DNA fragments and PCR products

DNA fragments derived from digestion with restriction enzymes or reactions with other DNA modifying enzymes were isolated with the EURx PCR / DNA CleanUp Kit (Roboklon GmbH) according to the manufacturer's protocol.

2.2.25. Southern blotting

The gDNA was digested with the appropriate restriction enzyme and separated on a 0.7% agarose gel. The DNA was visualized on a UV transilluminator and photographed together with a ruler, allowing size assignment of detected fragments. The Southern blot was assembled by placing 1–2 layers of Whatman 3 MM paper on a glass plate. The glas plate was put on a tank filled with 0.4 N NaOH serving as transfer solution. The protruding ends of the Whatman 3 MM paper were soaking in the 0.4 N NaOH. The agarose gel was mounted upside down on the Whatman 3 MM

paper. The membran was directly placed on the gel followed by 2 layers of Whatman 3 MM paper. A stack of paper towels placed on top and pinned down by a glass plate with a weight on top permitted DNA transfer by upward capillary action. The transfer was performed at room temperature for 6–24 h. Afterwards, the membrane was rinsed with 2×SSC, to remove the NaOH, and dried.

2.2.26. Northern blotting

The gel was prepared by boiling 4.68 g agarose in 340 ml water subsequently adding 39 ml 10×MOPS and 11.7 ml 37% formaldehyde. After pouring the gel, the gel chamber was filled with 1×MOPS. 44 µg of RNA were prepared in 11 µl of DEPC treated H_2O. 39 µl premix, 10 µl of RNA loading buffer and 2 µl (0.5 µg/µl) ethidiumbromide were mixed, incubated at 65 °C for 15 min and quenched on ice. The sample was loaded on the gel and run at approximately 120 V for several hours. The gel chamber was continously stirred. Afterwards the gel was rinsed in 2×SSC. The blotting apparatus was assembled like for Southern blots (see section 2.2.25) except 20×SSC was used as transfer solution. Blotting was performed over night. Subsequently, the membrane was washed in 2×SSC and crosslinked with UV light. The membrane was prehybridized in ExpressHyb™ Hybridization Solution. The radiolabeled DNA probe was added and incubated for several hours at 68 °C. The membrane was subsequently washed and exposed as Southern blots (see section 2.2.28).

2.2.27. Preparation of radiolabeled probes by single labeling

For the generation of single labeled DNA probes the Amersham Rediprime™ II DNA Labeling System was used. 50–100 ng of unlabeled DNA was heated to 95 °C for 5 min and than cooled on ice for additional 5 min. The DNA solution was mixed with 10 mM TRIS buffer pH 8 to a final volume of 45 µl and gently mixed in an Amersham Rediprime™ II DNA Labeling System tube without pipetting up and down. Subsequently 5 µl (1.85 MBq) of [$\alpha-^{32}$P]dCTP were transferred to the mix and the tube was incubated at 37 °C. After 30–60 min the labeled probe was purified (see section 2.2.24) and eluted in 50–150 µl elution buffer. The labeled DNA probe was denatured for hybridization by heating to 95 °C for 5 min and immediately cooled on ice for 5 min. The probe was then transferred to the hybridization solution.

2.2.28. Preparation of radiolabeled probes by double labeling

For double labeling of DNA probes with [$\alpha-^{32}$P]dCTP and [$\alpha-^{32}$P]dATP, 50 ng of DNA were heated to 95 °C for 5 min and instantly cooled down for 5 min on ice. The DNA was transferred to a reaction mix containing 10 µl OLB buffer containing 3 µl of [$\alpha-^{32}$P]dCTPs (1.11 MBq) and 3 µl of [$\alpha-^{32}$P]dATPs (1.11 MBq). Finally, 1 µl of Klenow and H_2O was added to a final volume of 30 µl. In table 2.31 the pipetting scheme is summarized. The reaction mix was incubated at 30 °C for 3 h. Subsequently, the labeled probe was purified (see section 2.2.24). The labeled DNA probe was eluted in 50–150 µl and denatured for hybridization by heating to 95 °C for 5 min and immediately cooled on ice for 5 min. The probe was then transferred to the hybridization solution.

Table 2.31.: Preparation of radiolabeled probes by double labeling

Content	Volume
DNA probe (50–100 ng)	1 µl
OLB buffer	10 µl
$\alpha-^{32}$PdCTPs (1.11 MBq)	3 µl
$\alpha-^{32}$PdATPs (1.11 MBq)	3 µl
Klenow	1 µl
H_2O	*ad* 30 µl

Prehybridization, hybridization, washing and exposure

For prehybridization (blocking), the membrane was incubated in a hybridization tube rolling at 63 °C for at least 4 hours with prehyb buffer containing denatured single-stranded salmon sperm DNA (ssDNA) as blocking agent (see section 2.2.31). The radioactively labeled DNA probe was denatured and added to the hybridization solution. The prehybridization solution was discarded and the membrane was incubated with the labeled DNA probe containing hybridization solution. In order to remove the unspecifically bound labeled probe, the membrane was washed with 2×SSC conatining 0.1% SDS for 10 min. This step was repeated at least three times but was repeated as often as necessary to achieve the membrane to have less than 100 IPS (Berthold LB 122, contamination monitor). The membrane was wrapped into plastic and placed on a phosphoimager screen and exposed overnight. Finally, the screen was scanned with a phosphoimager.

Table 2.32.: Contents of prehybridization and hybridization solution in ml for approximately 15 ml solution, according to Rosel.

Content	Prehybridization	Hybridization
20×SSC	3.75	3.75
100×Denhardt's	0.75	—
20% SDS	0.37	0.37
ssDNA (10 mg/ml)	0.15	0.15
H_2O	10	10

2.2.29. Colony hybridization

To screen a large quantity of bacterial clones, for carrying a desired DNA fragment or insert, bacteria were picked with a pipet tip and transferred on two agar plates one covered by a 0.45 µm nylon membrane on top of the agar. The agar plates were incubated at 37 °C overnight or 3 days at room temperature. The agar plate without nylon membrane was kept as backup and the bacteria grown on the membrane were lysed and the DNA was fixed on the membrane. Therefore, the membrane was placed with the lower site on top of Whatman 3 MM paper soaked with ColHyb denaturation solution for 5 min. Afterwards, the membrane was transferred to Whatman 3 MM paper soaked in ColHyb neutralization solution and incubated for 5 min. In a last step the membrane was transferred to Whatman 3 MM paper soaked in 2×SSC and incubated for 5 min. To remove excessive bacterial debris the membrane was put between two layers of Whatman 3 MM paper, squeezed and dried. Subsequently, it was placed into a hybridization tube containing 10–15 ml church buffer and incubated rotating at 65 °C. After a period of 30–60 min, the radioactively labeled DNA probe directed against the desired fragment was added (see section 2.2.27 and 2.2.28). The Membrane was incubated with the labeled probe, for at least 30 min up to 3 days. To wash the membrane and remove unbound probe, the hybridization solution was discarded and the membrane was washed for 10 min with 10–50 ml wash buffer I at 65 °C. Subsequently, the wash buffer I was discarded and the membrane was washed in two additional washing steps using wash buffer II and wash buffer III. The last washing step was repeated as often as necessary to achieve the membrane to have less than 100 IPS (Berthold LB 122, contamination monitor). The membrane was wrapped into plastic and placed on a phosphoimager screen and exposed for at least one hour. Finally, the screen was scanned with a phosphoimager.

2.2.30. Stripping and reprobing of colony hybridizations and Southern blots

For stripping of probed nylon membranes, a 0.5% SDS solution (in H_2O) was heated until cooking and poured onto the membrane. Subsequently, the membrane was rinsed in 2×SSC and was ready for reprobing.

2.2.31. Generation of sheared and denatured salmon sperm ssDNA

Sheared, single-stranded, and denatured salmon sperm DNA was used in prehybridization and hybridization solutions to reduce background signal. In order to prepare sheared DNA, 1 g of salmon sperm nuclei was dissolved in 100 ml 0.4 NaOH stirring overnight at room temperature. The vessel containing the solution was placed into a boiling water bath for 45 min to shear the DNA. Subsequently, the solution was chilled on ice and neutralized to pH 7.0 with glacial acetic acid. To remove debris, the solution was centrifuged at 3345×g for 20 min. The supernatant was mixed with 2 volumes of 95% ethanol, placed at −20 °C for 1 h, and centrifuged at 3345×g for 20 min. The pellet was rinsed with 70% ethanol. Afterwards, the pellet was dried and dissolved in 50 ml TE. The ssDNA quantity was determined by photometric analysis (see section 2.2.6), diluted to 10 mg/ml, and stored in aliquots at −20 °C. Before use, the aliquot was denatured by heating to 95 °C for 5 min and chilling on ice for additional 5 min.

2.3. Protein methods

2.3.1. Preparation of protein extracts

Protein extracts from eukaryotic cells

For protein extraction from mammalian cells, the adherent cells were cultivated in a cell culture dish. The medium was discarded and the cells were washed with PBS. After completely removing the PBS, the cell culture dish was put on ice and the cells were lysed by adding ice cold tripple lysis buffer ($\geq$100 µl/10^6 cells) containing 10 ng/ml aprotinin and 0.1 mM PMSF both added freshly. Subsequently, the cells were collected with a cell scraper and transferred to a reaction tube followed by a

centrifugation step at ≥15000×g at 4 °C for 5 min. Half of the tripple lysis buffer volume used was transferred from the supernatant to a fresh tube. Protein extracts were directly mixed with Roti®-Load1 or stored at −80 °C.

Protein extracts from mouse tissue

Tissue was prepared from sacrificed mice and stored in liquid nitrogen. Subsequently, the tissue was homogenized in RIPA buffer followed by a centrifugation step at ≥15000×g at 4 °C for 5 min. Half of the RIPA buffer volume used was transferred from the supernatant to a fresh tube. Protein extracts were directly mixed with Roti®-Load1 or stored at −80 °C.

2.3.2. SDS polyacrylamide gel electrophoresis (SDS-PAGE)

To seperate proteins according to their size, protein samples were seperated in vertical polyacrylamid gels containing SDS in a Bio-Rad system. The buffer chambers were filled with electrophoresis buffer. The polyacrylamid gels consisted of two parts. The seperation gel (see table 2.34) was of high polyacrylamid percentage and high pH (7.5%–16%, pH 8.8) and the stacking gel (see table 2.33) with low polyacrylamid concentration and low pH (5%, pH 6.8). The stacking gel ensures focusing (simultaneous entry) of proteins into the separation gel. Proteins loaded onto the gel were denatured by prior heating at 95 °C with final concentration of approximately 1×Roti®-Load1. Roti®-Load1 contains β-Mercaptoethanol and SDS reducing disulfide bonds in proteins and gives the proteins an equal negative charge, respectively. The proteins were then separated in the electric field.

Table 2.33.: Recipe for stacking gel.

5% stacking gel (ml)	
H_2O	0.688
0.5 M TRIS, pH 6,8	0.300
PAA[1] (30%)	0.200
SDS (10%)	0.012
APS (10%)	0.006
TEMED	0.0024

Table 2.34.: Recipe for seperation gel.

	seperation gel (ml)						
	5.0%	7.5%	10%	12.5%	13%	14%	15%
H_2O	2.87	2.45	2.03	1.62	1.53	1.37	1.2
1.5 M TRIS, pH 8.8	1.25	1.25	1.25	1.25	1.25	1.25	1.25
PAA[1] (30%)	0.83	1.25	1.67	2.08	2.17	2.33	2.5
SDS (10%)	0.05	0.05	0.05	0.05	0.05	0.05	0.05
APS (10%)	0.05	0.05	0.05	0.05	0.05	0.05	0.05
TEMED	0.005	0.005	0.005	0.005	0.005	0.005	0.005

2.3.3. Western blotting

Proteins, seperated using SDS-PAGE, were transferred and immobilized on a nitrocellulose membrane in an electric field using the wet-blotting technique. The gel containing the seperated proteins was placed on the nitrocellulose membrane. On each site two layers of Whatman 3 MM paper were placed. All the assembly was done in blotting buffer. Subsequently, a roller was used to assure that the gel lays on the membrane void-free. The system was mounted in the blotting chamber filled with blotting buffer and ran at constant amperage of 250–300 mA (not exceeding 100 V) for 1.5–2 h at 4 °C or at 110 mA for overnight blotting at 4 °C. Subsequently, the system was disassembled and the membrane was rinsed with H_2O.

Ponceau S staining of proteins immobilized on membranes

Directly after blotting, proteins to a nitrocellulose membrane the transferred proteins were stained with ponceau S solution. Therefore, the membrane was rinsed in H_2O and incubated in ponceau S solution for approximately 5 min. Subsequently, the membrane was rinsed again with H_2O to destain parts of the membrane not containing protein. The membrane was dried, photographed and archived.

Detection of Proteins immobilized on membranes

After blocking the membrane with 5% milk in PBS for 30–60 min, the membrane was rinsed in PBS. Subsequently, the membrane was incubated with the primary antibody shaking overnight at 4 °C or 1–2 h at room temperature. The membrane

[1] PAA, Polyacrylamid

was washed three times for 5 min in PBS to remove unbound antibody followed by incubation with secondary antibody (peroxidase cupled) for 1 h at room temperature. Excessive antibody was removed by washing at least three times for 5 min in PBS. The membrane was then incubated with fresh ECL™ solution (Amersham Biosciences Europe GmbH) according to the manufacturer's protocol. The bands were visualized with X-Omat UV films (Kodak GmbH) and scanned.

2.4. Cell culture methods

For working with eukaryotic cells a laminar flow work bench was used. All used equipment was sprayed with 70% ethanol to avoid contamination. All used media and solutions were bought sterile, autoclaved or sterilized by filtration. Only one-way expendable items were used. Cells were either counted with a Casy®cell counter or stained with trypan blue and subsequently counted in an improved Neubauer hemocytometer.

2.4.1. Preparation of mouse embryonic fibroblasts

Mouse embryonic fibroblasts (MEFs) were prepared at day 13.5 of embryonical development (E 13.5) assessed by plug formation. Gestating mice were sacrificed and the fur was sprayed with 70% ethanol. Individual embryos were extracted from the uterus. Head and internal organs were removed and the torso of the embryo was washed with PBS. Subsequently, the torso was minced and dispersed in a 12 or 24-well dish and incubated with 2 ml trypsin at 37 °C for 15 min. Each dispersed embryo was then transferred to a 10 cm dish containing 9 ml feeder medium. Every day, the medium was changed. Two days after preparation, the cells were splitted 1/3 and frozen four days post preparation or directly used.

2.4.2. Preparation of mouse adult fibroblasts

Mouse adult fibroblasts (MAFs) were prepared by taking ear biospies which were briefly incubated in 70% ethanol and rinsed in PBS containing 100 µg/ml kanamycin. The tissue was minced in a 24-well plate containing 0.3 ml of collagenase neutral protease (4 mg/ml) in DMEM. After incubation at 37 °C for 45 min 1.5 ml feeder medium was added followed by another incubation at 37 °C over night. The tissue was dissociated by pipetting and the cell suspension was passed through a

cell strainer. Harvested cells were peleted by centrifugation and cultured in MAF medium containing Zell shield™. MAFs were immortalized via SV40 large T antigen according to standard protocols by Dr. Klaus-Peter Knobeloch (Neuropathology, Universitätsklinikum Freiburg, Germany).

2.4.3. Stimulation of MAFs with TNF-α or TGF-β

Prior to stimulation, 0.5×10^6 MAFs were seeded on 6 well plates in 2 ml of starving medium. The next day, TNF-α to a final concentration of 20 ng/ml or TGF-β to a final concentration of 10 ng/ml was added.

2.4.4. Cryopreservation of mammalian cells

Mammalian cells can be stored in liquid nitrogen for many years. At the cryopreservation process cells to be frozen were in exponential growth phase. The cells were harvested with trypsin, dispersed and diluted 1/10 in medium containin FCS. Afterwards, the cell suspension was centrifuged at 200×g (should not exceed 400×g). The cells were resuspended in growth medium at room temperature to a concentration 2×10^6—2×10^7 cells per ml.

To avoid damage to the cell during freezing, the cryoprotectant DMSO was used. FCS containing 20% DMSO was added to the cells to be frozen, to a final concentration of 10%. The final concentration of viable cells was in the range of 10^6 and 10^7 cells per ml. Subsequently, the cell suspension was transferred to cryopreservation vials and the vials were initially cooled by storing the vials in a freezer boy filled with isopropanol. This aparature was put in a −80 °C freezer allowing a cooling rate of 1 °C per minute in the range from room temperature to −80 °C. Two to seven days later, the vials were stored in liquid nitrogen at −196 °C.

The thawing process was performed as quickly as possible. The vial containing frozen cells was placed directly into a 37 °C water bath until completely thawed. If liquid nitrogen has entered the cryopreservation vial, it will explode after warming. Therefore, the vials were handled with care and eye protection was worn. The cryopreservation vials were sprayed with 70% ethanol, before, they were transferred to the laminar flow bench. The cells were then washed with warm medium by 1/10 dilution. The cells were pelleted by centrifugation and resuspended in fresh medium.

2.4.5. Cell culture methods for ES cells

To generate genetically modified mice, ES cells were cultivated and ES cells were cultivated and transfected with a targeting vector. After homologous recombination of the genome with the targeting vector, ES cells were screened for positive (mutated) clones by Southern blotting. Positive clones were injected into mouse embryos to generate chimeric animals. To pass the mutation to the offspring, the manipulated clone had to be pluripotent that it could generate cells of the germline. In order to assure this sophisticated process to work, some facts are important.

ES cells were grown on a layer of feeder cells (MEFs) that were resistant to G418 to withstand the selection process of ES cells. Another crucial factor was to use a low passage number of ES cells from a stock tested to be germline transitive to assure high possibility of germline transmission. ES cells had be split early enough to prevent differentiation of the clones and ES cells were provided with new medium daily.

Inactivation of feeder cells with mitomycin C

For the growth inactivation of fibroblasts used for ES cell culture, 150 µl of 0.5 mg/ml mitomycin C was added to feeder cells in a 10 cm dish with 7.5 ml feeder medium (final concentration 1 µg/ml mitomycin C). The cells were incubated 2–3 hours at 37 °C. The cells were washed twice with PBS, trypsinized, and transferred on the appropriate cell culture dishes that were gelatinized. For gelatinization of cell culture dishes, the surface was covered by 10% gelatine which was removed immediately before seeding the cells into the dish.

Electroporation of ES cells and selection

ES cells were tranfected by electroporation. Therefore, ES cells grown on a 10 cm dish were washed 3×with DMEM and trypsinized with 2.5 ml trypsin at 37 °C. Singularization (decollaction) of ES cells was checked microscopically. Then, trypsinization was stopped by adding feeder medium (20 ml/5 ml cell suspension). The cell number was evaluated with a CASY cell counter and the cells were pelleted by centrifugation at 200×g for 5 min. The medium was discarded and the cells were resuspended in ice cold transfection reagent to a final cell concentration of 20×10^6/800 µl. 800 µl of the cell suspension were transferred into a precooled electroporation cuvette containing 5–25 µg phenol chloroform extracted, sterile, and linearized vector

in PBS. The mix was incubated at room temperature for 10 min followed by electroporation at 400 V and 250 µF (time rate should be around 3.7 s). Subsequently, the cells were transferred into 10 ml feeder medium followed by centrifugation at 200×g for 5 min. 2–3×10^6cells were plated each on a 10 cm dish with settled, inactivated feeder cells containing ES medium.

Every day, the cells were provided with fresh ES cell medium. From the second day after electroporation, the medium contained selective ES cell medium (280–360 µg/ml G418). On the fifth day the double selective medium was used containing 2 µM gancylovir. At day seven and eight post electroporation ES cell clones were picked.

Picking of single ES cell clones and production of a replica plate

A 10 cm dish with ES cells was washed two times with DMEM medium only (without additionals) remaining 10 ml of that medium. A 96-well plate was prepared for trypsinization of ES cell clones by adding 15 µl of trypsin to each well. The clones were picked from the 10 cm dish with a 20 µl pipette in a volume of 7 µl by detaching a single clone and snipping the knob of the pipette to rapidly aspirate the clone. Subsequently, the picked clone was transferred to a well of the 96-well plate containing trypsin. Afterwards, to each well 200 µl ES cell medium were added and the singularized cells were transferred to a 96-well plate containing inactivated feeder cells. At day two after having picked a clone it was washed twice with DMEM medium only, subsequently, adding 40 µl trypsin to each well. After 5 min incubation at 37 °C, trypsinization was stopped by adding 200 µl ES cell medium. Subsequently, 120 µl cell suspension were transferred to a 96-well plate containing 120 µl freezing medium. This replica plate was wrapped into air bubble film and put into a foamed polystyrene box. The box was placed into a freezer at −80 °C. To the remaining 120 µl cell suspension 120 µl ES cell medium were added and were placed back into a 37 °C incubator. After three to five additional days of cell culture, the ES cell clones were washed, trypsinized, and transferred to 24-well plates without feeder cells but gelatinized wells (see 2.4.5).

After three to five more days when the medium turns yellow although changed daily, the cells were lysed and the DNA was precipitated. The DNA was eluted in 120 µl of TE buffer in U-bottom shaped 96-well plates.

2.4.6. Preparation of ES cells for blastocyst injection

In order to prepare the ES cells for blastocyst injection, the medium was changed and they had to be singularized and seperated from the feeder cells. Therefore, the cells were washed with DMEM medium only and trypsinized for 3 min at 37 °C. For optimal singularization, a Pasteur pipet tip was melt to obtain a smaller aperture, the cells were singularized, and taken up in 10 ml of ES cell medium. After centrifugation the cells were resuspended in 10 ml of ES cell medium and plated on a dish and incubated at 37 °C for 20 min. The supernatant was then transferred to a fresh dish. After 15 min of incubation, the supernatant was centrifuged and the obtained cell pellet was resuspended in 2 ml feeder medium containing 20 µl HEPES/ml. The cells were cooled to 4 °C for 3 min on ice to let sediment potentially existing clots of cells. Approximately 1.5 ml of cell suspension from the top were transferred in a 15 ml tube cooled on ice. The prepared ES cells were injected into mouse blastocysts.

2.5. Bioinformatical methods

2.5.1. Primer design

All primers were designed using the primer3 algorithm (v 0.4.0) that is available at http://fokker.wi.mit.edu/primer3/ using standard parameters. The primer3 source code is available at http://fokker.wi.mit.edu/primer3/. For primers that were designed to amplify DNA from gDNA or subcloned parts of gDNA the mispriming Library (repeat library) was adapted to `HUMAN` or `RODANT_AND_SIMPLE` for human or mouse template, respectively.

2.5.2. Design of probes for Southern blotting

For the design of Southern blot probes, the gDNA region that came in consideration was run through the RepeatMasker algorithm open-3.0 licensed under the Open Source License v2.1 available at http://www.repeatmasker.org/. Standard parameters were used adapting `Speed/Sensitivity` to `slow`, and the DNA source to `Rodent` and `Mouse`. Obtained sequences, which were not disrupted by repeats, were run through the primer3 algorithm (see section 2.5.1). The `Product Size Ranges` was set to `200-600` to allow the algorithm to find the primer pair producing a DNA probe of optimal size.

2.5.3. Alignments

All alignments were done using BLAST, Clustal W [157], or the T-Coffee algorythm [118] using default parameters, if not specified. The alignments were typeset and shaded using TeXshade, an alignment shading software completely written in TEX/LATEX by E. Beitz [5].

3. Results

3.1. Generation of mice expressing catalytically inactive USP18

3.1.1. Targeting strategy

The sequence similarity shared by all USP members is largely restricted to six conserved domains [95] including the cysteine box (see figure 3.1). Members of the USP familiy share a highly conserved cysteine crucial for enzymatic function. This is confirmed by fact that USP18 is able to cleave ISG15-gsPEST sequence in contrast to a mutant with a serine instead of a cysteine at position 61 (Cys61) [102] and has also been reported in other publications for this mutation [69, 104]. Therefore, a targeting strategy was developed to introduce an amino acid exchange within the *Usp18* locus at the position encoding the Cys61.

The murine *Usp18* gene is located on the forward strand of chromosome 6: 121,-195,924-121,220,934 and encoded by eleven exons in the genome (see figure 3.2). The Cys61 critical for enzyme activity is encoded in the third exon (see figure 3.2). To generate an catalytically inactive USP18 mutant, the triplet `TGT` encoding Cys61 should be changed to `GCT` leading to an amino acid exchange from cysteine to alanine. This mutation will be referred to as C61A in this work.

The developed targeting strategy to insert the desired mutation by homologous recombination is shown in figure 3.3. Pml restriction enzyme cleavage sites were used for the construction of the 5′ and the 3′homology of the targeting vector. The 3′homology harbors the third exon with the codon mutation. Between the 5′ and 3′homology a neomycin resistance gene was placed, flanked by FRT sites for positive selection. The thymidine kinase gene of herpes simplex virus inserted adjacent to the 3′homology is used for negative selection in the presence of the thymidin analogon ganciclovir. The herpes simplex virus thymidine kinase has a higher affinity to the thymidine analogon than it has to the cell's dTTPs. As a

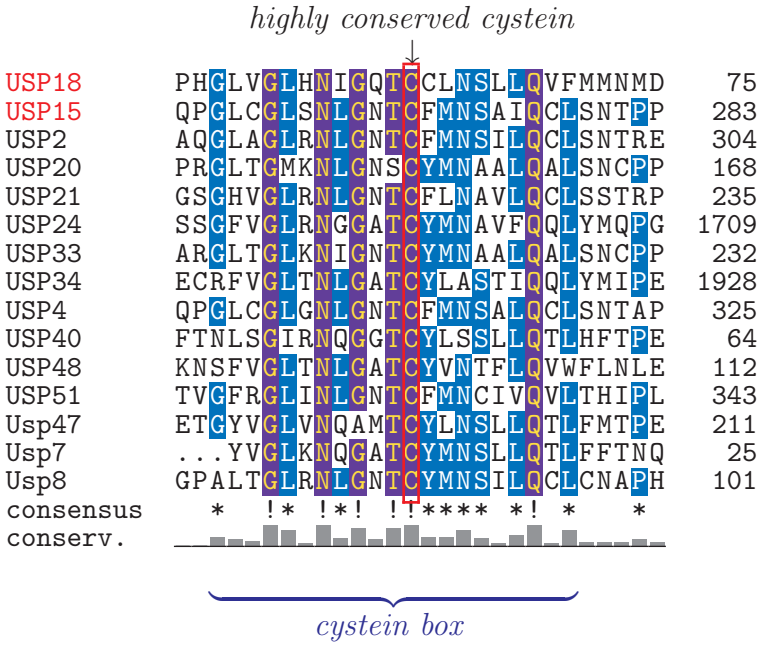

Figure 3.1.: Alignment of the cysteine box of USP15 and USP18 with other USPs. USP15 and USP18 are highlighted in red. The alignment was done using T-Coffee. 5% identity are shaded in bright blue and ≥80% identity in dark blue. The red box highlights the highly conserved cysteine residue, a hallmark of USPs. The degree of protein sequence conservation (conserv.) is indicated by a bar graph.

consequence, DNA synthesis is blocked due to failure in DNA polymerization. After homologous recombination has occurred, only the sequence between the homologous sequences would be inserted into the genome in contrast to randomized insertion of the targeting vector with high possibility of integration of the whole targeting vector. Hence, stable integration events can be enriched by positive selection with G418 (neomycin), whereas enrichment of random integration events can be reduced by negative selection using gancyclovir.

To screen for homologous recombination events, Southern blot probes were designed binding DNA sequences upstream and downstream of the homologies. These probes (*Usp18* 5′ and 3′probe, see figure 3.3) detect a genomic KpnI digested DNA fragment of 11.9 kb. After homologous recombination has occurred, an additional KpnI cleavage site is inserted. Thus, the *Usp18* 5′ and 3′probe detect additional DNA fragments of 3.4 kb and 10.3 kb, respectively. The modified gene locus will be referred to as $Usp18^{\text{neo-C61}}$ in this study. FLP-mediated excision of the neomycin resistance gene can be monitored with the *Usp18* 3′probe which detects a 8.7 kb fragment. After FLP-mediated recombination the allele will be referred to as $Usp18^{\text{C61}}$.

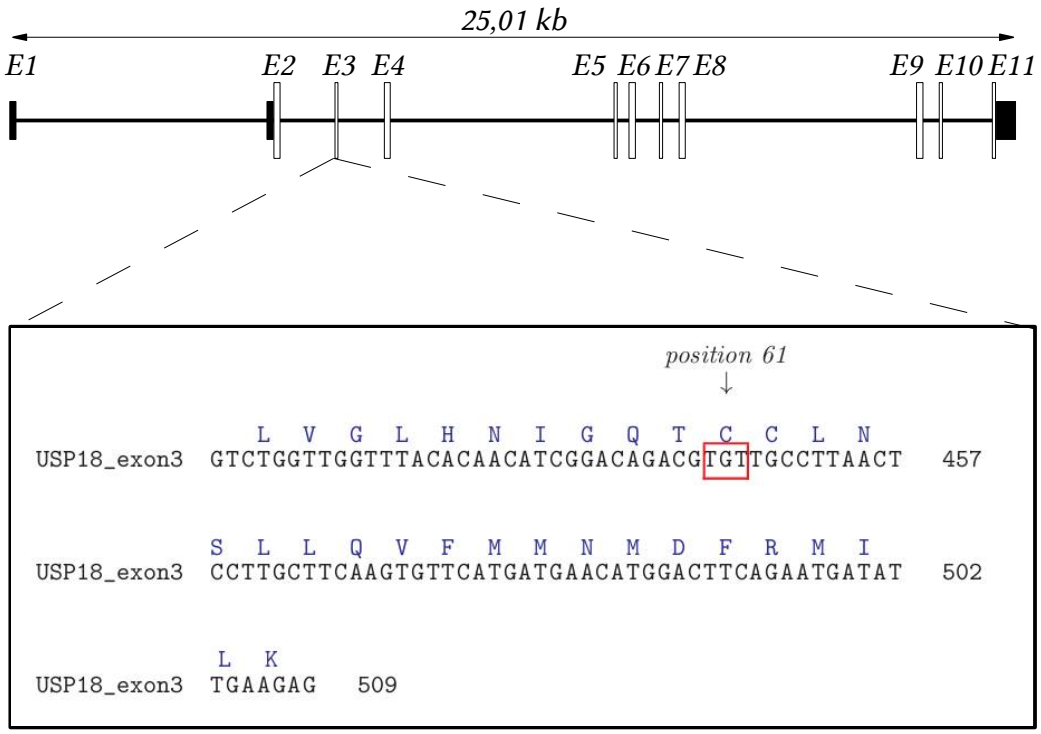

Figure 3.2.: Genomic structure of *Usp18* and sequence of the third exon encoding the cysteine residue at amino acid position 61. *Usp18* is encoded by eleven exons (E1-E11). The 5′ and 3′untranslated region are indicated by black boxes. Protein coding regions are indicated by white boxes. The third exon includes the codon for Cys61 highlighted by a red box.

3.1.2. Construction of *Usp18*^{C61A} targeting vector

A mouse genomic DNA (gDNA) containing P1 artificial chromosome (PAC) library, obtained from RZPD, originated from the Roswell Park Cancer Institute, created by Pieter J. de Jong and Kazutoyo Osoegawa [124], was screened by colony hybridization with a radiolabeled *Usp18* probe amplified with primers flanking the Cys61 coding region (UBP43 Protease EXs and UBP43 Protease EXa). Subsequently, a bacterial clone `RPCIP711G10332Q2` was identified to contain the desired *Usp18* gene locus. A KpnI fragment containing the Cys61 coding region was subcloned by shotgun cloning of the KpnI cut PAC vector into pZErO™-2. Obtained clones were subsequently screened by colony hybridization. The vector containing the desired KpnI fragment was designated pZErO™-2[UBP43 KpnI frag] and was digested with PmlI resulting in an ≈1.9 kb upstream and an ≈3.2 kb downstream gDNA fragment used as 5′ and 3′homology, respectively. For targeting vector construction, the 5′PmlI cut fragment was cloned blunt into EcoRV digested pZErO™-2 in antisense orientation (pZErO™-2[UBP43PmlI3-5]). The fragment was cloned via NotI

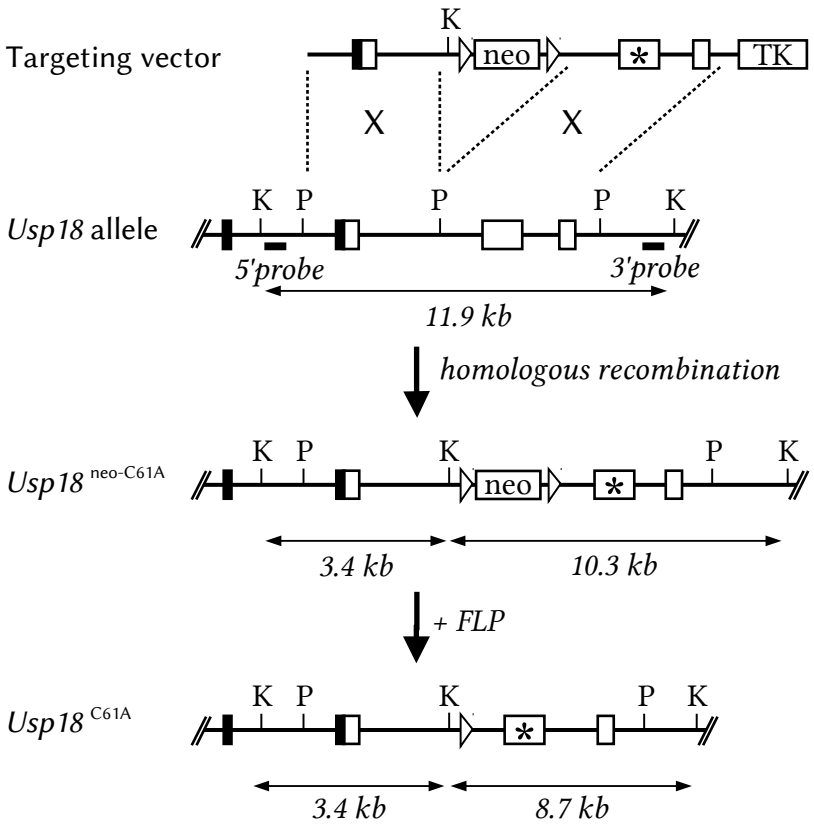

Figure 3.3.: Targeting strategy for *Usp18*^{C61A} knockin. The targeting vector was constructed using PmlI (P) fragments as homologies. The 5′homology includes exon two with untranslated-(black box) and translated region (white box). The 3′homology harbors exon three and exon four. For positive and negative selction in ES cells, the vector contains a neomycin resistance gene flanked by FRT sites and a thymidine kinase gene, respectively. Exon three of *Usp18* within the 3′homology is mutated in the codon which encodes the active site cysteine (Cys61) and is replaced by an an alanine encoding codon (C61A, asterisk). Homologous recombination of the allele (*Usp18*$^{neo\text{-}C61A}$) is detected by Southern blot analysis of KpnI digested genomic DNA using the *Usp18* 5′ and 3′probe to validate correct 5′ and 3′integration, respectively. Subsequently, the neomycin resistance gene can be excised using a FLP expressing mouse deleter strain resulting in *Usp18*^{C61A} mice. Recombination events can be detected by Southern blot analysis with the 5′ and 3′probe by changes in fragment sizes for KpnI digested genomic DNA as indicated (double-arrows with kb designation) due to the introduction of an additional KpnI restriction enzyme cleavage site in the mutated allele.

and KpnI sites into pPNT-frt3, upstream from the neomycin resistance gene (pPNT-frt3[5′homo UBP43]) via directed sticky end ligation. pPNT-frt3 harbors a neomycin resistance gene which is flanked by FRT sites. The 3′homology was generated by subcloning the 3′PmlI gDNA fragment into EcoRV digested pZErO™-2 resulting in pZErO™-2[UBP43 PmlI C61]. Subsequently, the vector was mutated using the Quickchange site directed mutagenesis kit and appropriate DNA oligos (upC61A and loC61A), purified by high performance liquid chromatography, according to the

manufacturer's protocol. Two bases were mutated to alter the codon TGT to GCT (Cys to Ala). Subsequently, the 3′homology containing the mutation was excised by BamHI and XhoI digestion, blunted via a Klenow fill-in reaction, and ligated into vector pPNT-frt3[5′homo UBP43] that was opened by PmlI digestion resulting in the targeting vector (pPNT-frt3[UBP43TV]).

3.1.3. Manipulation and identification of mutated ES cells

The targeting vector pPNT-frt3[UBP43TV] was linearized with the restriction enzyme FseI, purified by phenol chloroform extraction, and was inserted into ES cells by electroporation. After positive and negative selection with G418 and gancyclovir, respectively, single ES cell clones were isolated. Each clone was expanded and cryoconserved, before, replicas were split for DNA extraction. The DNA was extracted from each clone and was digested with the restriction enzyme KpnI for detection of homologous recombination events by Southern blotting according to the developed strategy (see figure 3.3). Successful gene targeting via homologous recombination was identified in ES cell clone 2.3.7C by Southern blotting using the *Usp18* 5′probe (see figure 3.4 A). Additionally to the wildtype band of 11.9 kb a diagnostic fragment at approximately 3.4 kb, as expected from the targeting strategy, was detected in ES cell clone 2.3.7C. ES cells carry to alleles of every gene and since homologoues recombination is a rare event only one allele was modified. ES cell clone 2.3.7C was thawed and rechecked by Southern blot using the *Usp18* 5′ and 3′probe to verify correct integration by homologous recombination (see figure 3.4 B). As expected, the *Usp18* 5′ and 3′probes detected DNA fragments of 3.4 kb and 10.3 kb, respectively, in addition to the wildtype band of 11.9 kb. The desired mutation was verified by sequencing of cDNA (see figure 3.4 C). Therefore, RNA of LPS (100 mg/ml for 18 h) stimulated ES cells was isolated and cDNA was synthesizes. Subsequently, the cDNA was used as template in a PCR with primers flanking the Cys61 coding region (UBP43_mRNA_C61A_verif_F and UBP43_mRNA_C61A_verif_R). The obtained amplificate was isolated and sequenced using the same primers. In the mutant, the bases TG which are part of the Cys61 codon were changed to GC as desired.

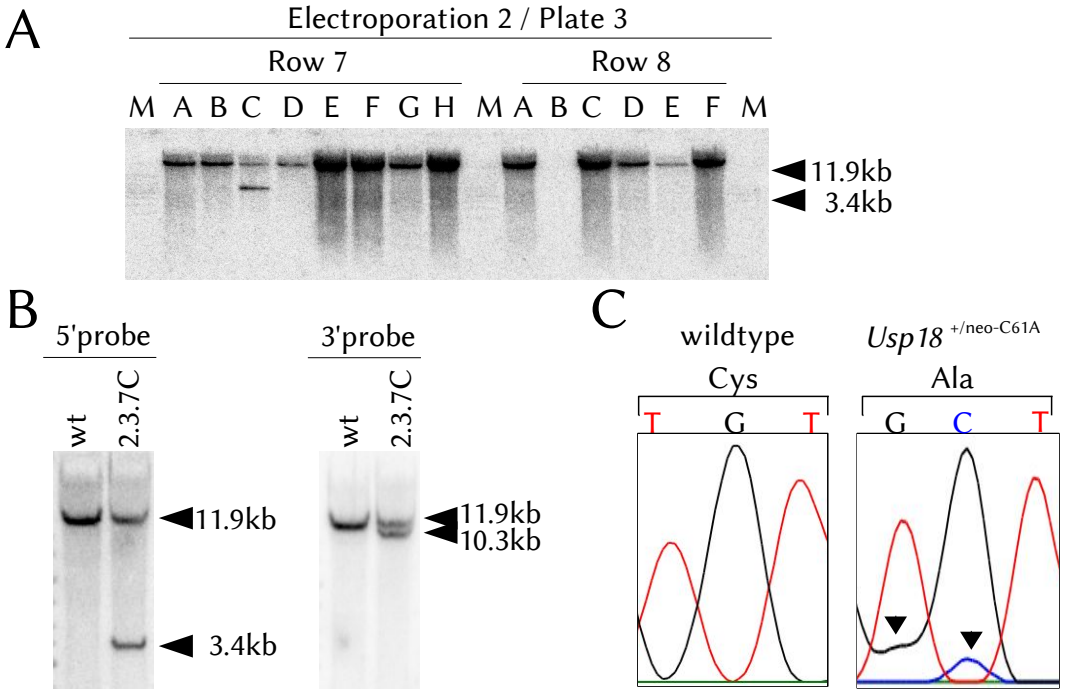

Figure 3.4.: Successful mutation of *Usp18* in ES cells. **(A)** Part of the *Usp18* screen for homologous recombination events using the *Usp18* 5′probe. The clone C in row 7 on plate 3 of the second electroporation (2.3.7C) is positive for homologous recombination, indicated by an additional signal at 3.4 kb. Marker (M). **(B)** ES cell clone 2.3.7C was thawed and rechecked using the *Usp18* 5′ and 3′probe. The *Usp18* 3′probe detected an 11.9 kb and a 10.3 kb fragment corresponding to the wildtype and mutated allele, respectively. In contrast, only an 11.9 kb fragment was detected in wildtype (wt) ES cells. **(C)** Chromatographs of cDNA sequence of wildtype and *Usp18*$^{+/\text{neo-C61A}}$ ES cell clone. The base pair exchange is indicated (black triangles). The basepair exchange results in a triplet encoding alanine (Ala, `GCT`) instead of a cysteine (Cys, `GCT`). The manipulated ES cell clone is heterozygous for the mutation.

3.1.4. Generation of chimeric mice and identification of germline transmission

The mutated ES cells were injected into C57BL/6 morulae (early stage embryos) using laser assisted injection at the Max-Planck-Institut in Dresden by Ronald Naumann. The obtained chimera was interbred directly with a FLP deleter strain. Thus, germline transmission may directly lead to FLP-mediated deletion of the neomycin resistance gene. Germline transmission was identified by Southern blotting (see figure 3.5 A) and could be detected in littermates 307, 312 and 314. However, the *Usp18* 5′probe only detected successful germline transmission, while FLP-mediated deletion could only be monitored by the *Usp18* 3′probe. Detection of neomycin resistance gene deleted allele with the *Usp18* 3′probe resulted in a smaller fragment of 8.7 kb as compared to 10.3 kb before FLP-mediated deletion (FRT flanked

sequence is ≈1.6 kb in size). Therefore, Southern blots were hybridized with the *Usp18* 3′probe. Beside successful germline transmission, FLP-mediated deletion of the neomycin resistance gene could also be detected in several animals, e. g., animal number 317 and 396–398 (see figure 3.5 B).

A mouse mutant expressing USP18 under control of the endogenous promotor, which lacks protease function, could be successful generated in this work. This novel mouse strain provides a valuable tool to unequivocally discriminate between protease dependent and independent function of USP18.

Due to the fact that the lab moved to the Universitätsklinikum Freiburg (Germany) the project could not be continuously pursued. The *Usp18*$^{+/\mathrm{C61A}}$ mice generated in this study are currently under investigation in collaboration with Dr. Klaus-Peter Knobeloch (Neuropathology, Universitätsklinikum Freiburg, Germany).

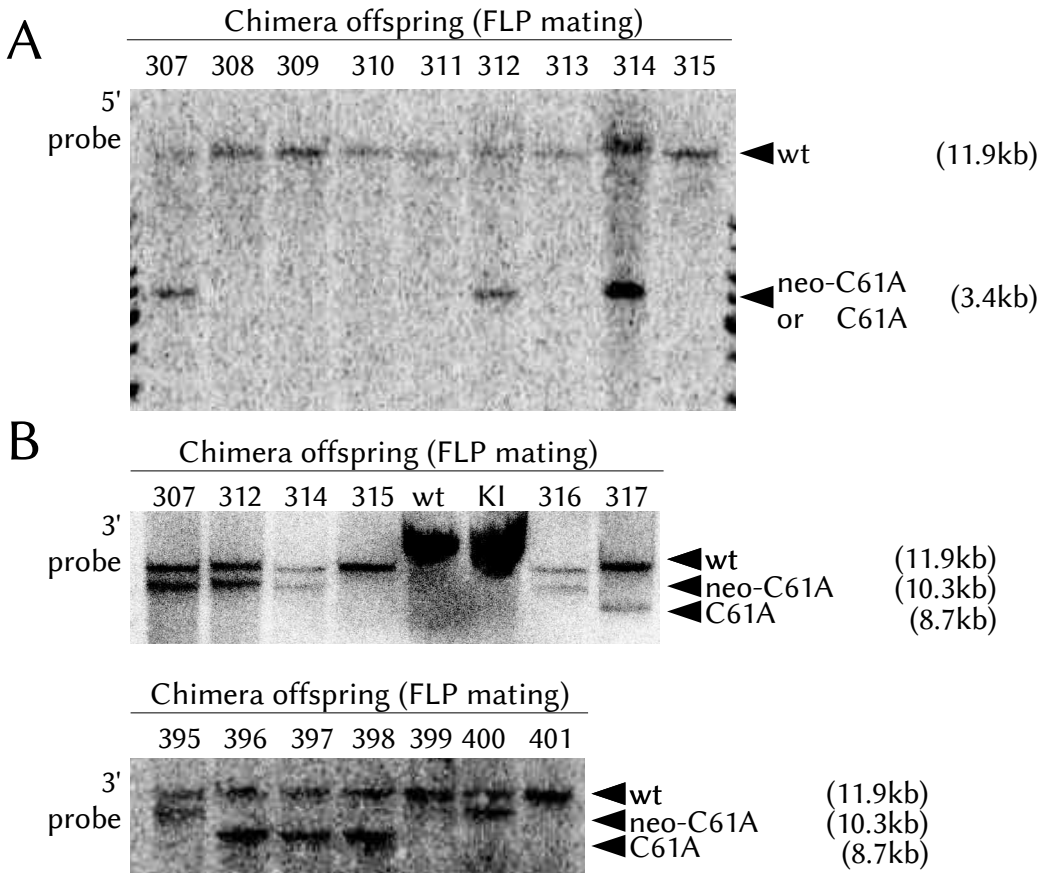

Figure 3.5.: Detection of germline transmission for the mutated *Usp18* allele and deletion of the neomycin resistance gene using a FLP deleter strain. **(A)** Southern blot using the *Usp18* 5′probe to detect germline transmission of offspring littermates from chimera crossed with a FLP deleter strain. Animals 307, 312 and 314 carry the mutated allele (neo-C61A or C61A) as indicated by the additional band at 3.4 kb. However, FLP-mediated deletion of the neomycin resistance gene (C61A) could only be determined using the *Usp18* 3′probe. **(B)** Detection of germline transmission and deletion of the neomycin resistance gene using the *Usp18* 3′probe. Approximately half of the offspring carrying the mutant allele display FLP-mediated deletion of the neomycin resistance gene, revealed by a faster migrating band at 8.7 kb. Wildtype DNA (wt). Positive ES cell clone (KI).

3.2. Generation of conditional *Usp15* knockout mice

3.2.1. Targeting strategy

The murine *Usp15* gene is encoded by 22 exons on the reverse strand of chromosome 10: 122,550,286-122,634,017. As for all USPs, the conserved cysteine residue within the cysteine box is crucial for catalytic activity. Alignments of USP15 with other USPs clearly shows the high conservation of the cysteine box reflecting a hallmark

of USPs (see figure 3.1). The catalytically active cysteine residue is encoded in exon eight (see figure 3.6). To generate a conditional knockout of *Usp15*, the aim was to flank the exon encoding the cysteine residue, which is crucial for enzymatic function, with loxP sites. Hence, Cre-mediated deletion of the exon eight should result in a loss of function of the protein. Furthermore, ideally a frameshift should be achieved after deletion of exon eight. This frameshift should lead to premature stop codons on the mRNA potentially leading to nonsense-mediated mRNA decay (see figure 3.6).

The strategy to flank the exon eight of the genomic *Usp15* locus with loxP sites is illustrated in figure 3.7. An approximately 6.7 kb genomic fragment from an intrinsic SpeI to an AvrII restriction enzyme cleavage site was used as 3′homology, which encompasses exon eight. As 5′homology the 1.7 kb fragment from the SpeI site to an EcoRI site more upstream was used. In the constructed targeting vector the SpeI site should be deleted for better screening possibilities (see figure 3.7). Between the 5′ and 3′homology, the planned targeting vector carries a neomycin resistance gene flanked by FRT sites. Thus, elimination of the neomycin resistance gene can be mediated by FLP. However, the neomycin resistance gene and the exon eight in the 3′homology is flanked by loxP sites. There is a SpeI site introduced upstream juxtaposing the 3′loxP, which is used for convenient screening by Southern blotting. A thymidine kinase was located downstream of the 3′homology allowing negative selection of ES cells.

After homologous recombination of the targeting vector with the *Usp15* locus, the SpeI site seperating the homologies used for target vector construction is disrupted. Simultaneously, two SpeI sites are inserted into the genome resulting in a change of SpeI fragment sizes. One SpeI site juxtaposes the neomycin resistance gene and the other juxtaposes the 3′loxP site (see figure 3.7). Deletion of the intrinsic SpeI site on the one hand and introduction of two additional SpeI sites on the other hand, makes the detection of recombination events via Southern blot more convenient. Recombination events result in distinct fragment sizes for SpeI cut gDNA (see figure 3.7). Southern blot probes were designed and tested for detection of SpeI fragments of which the *Usp15* 5′ and 3′homology used for vector construction are part of. The *Usp15* 5′ and 3′probe detect fragments of 6.2 kb and 9.7 kb, respectively. After homologous recombination, the *Usp15* 5′ and 3′probe detect a diagnostic 6.6 kb and a 7.9 kb fragment, respectively. Deletion of the neomycin resistance gene by FLP-mediated FRT recombination also causes loss of the SpeI site,

which is located between the FRT sites, resulting in a DNA fragment of 8.1 kb detected by the *Usp15* 5′probe. Cre-mediated deletion eliminates the introduced SpeI sites that both the *Usp15* 5′ and 3′probe detect an SpeI fragment of 14.1 kb. Thus, the *Usp15* 3′probe can be used to distinguish between the 9.7 kb wildtype and the fragment generated by Cre-mediated deletion of 14.1 kb. However, it is not suitable to distinguish between targeted (neo-fl) and FLP-deleted (fl) allele, because both are of 7.9 kb. Deletion of the neomycin resistance gene has to be monitored by detection of a 8.1 kb diagnostic DNA fragment using the *Usp15* 3′probe (see figure 3.7).

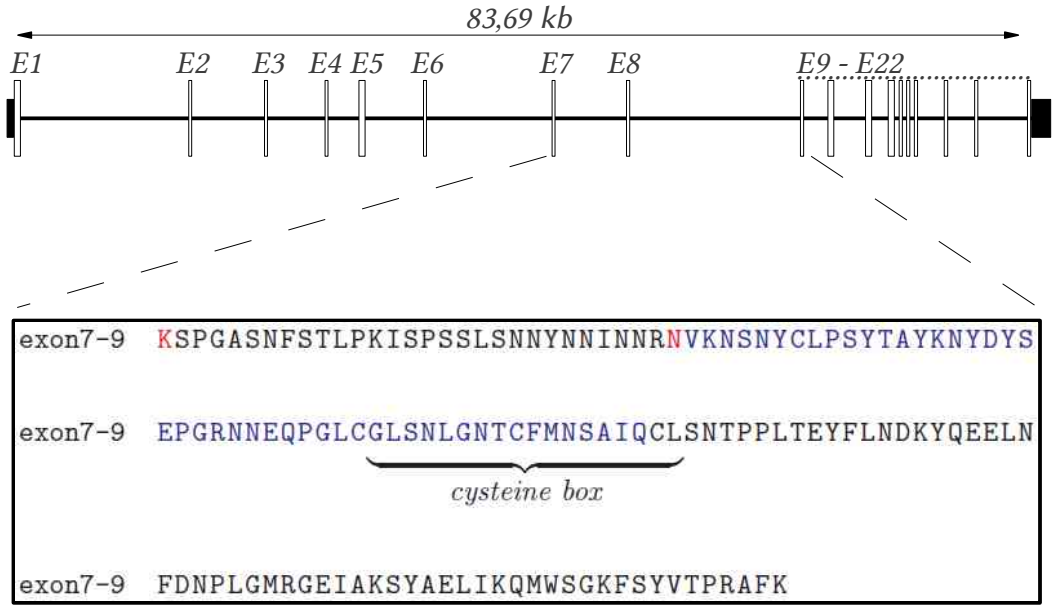

Figure 3.6.: Genomic structure of *Usp15* and exon seven to nine. *Usp15* is encoded by 22 exons (E1-E22) spanning approximately 83.69 kb of the genome. The 5′ and 3′untranslated region are indicated by black boxes, whereas protein coding parts are indicated by white boxes. A part of the mRNA sequence, from exon seven to nine, is shown in the lower box. Sequence of exon eight is indicated by blue letters partially encoding the cysteine box. Residues overlapping the splice site are highlighted in red. An asparagine residue (N) is encoded partially by exon seven and eight, thus, deletion of exon nine would lead to a frameshift. Thus, the generated mRNA is suggested to be degraded by nonsense-mediated mRNA decay.

3.2.2. Generation of a targeting vector

For the generation of the targeting vector a mouse gDNA containing PAC library, obtained from RZPD originated from the Roswell Park Cancer Institute, created by Pieter J. de Jong and Kazutoyo Osoegawa was screened [124]. The pCMV-Tag3B-USP15 vector [52] was cut with HindIII and SalI and the cDNA of *Usp15*

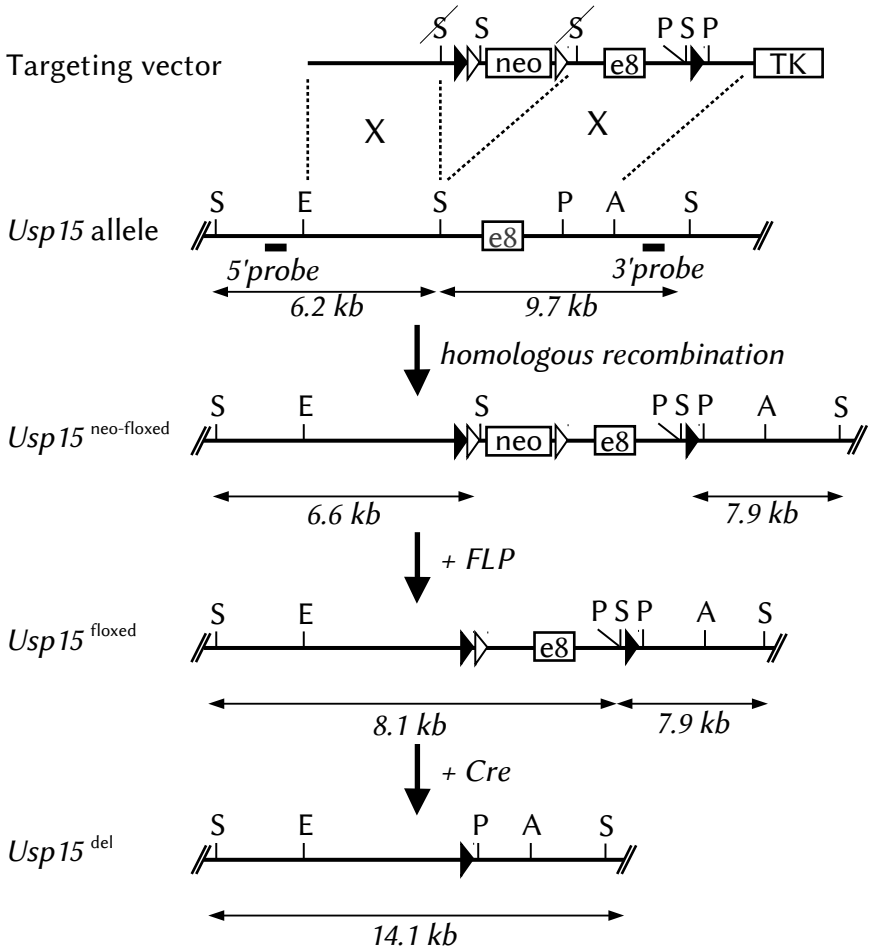

Figure 3.7.: Targeting strategy for *Usp15*. Targeting vector was constructed using EcoRI (E)/SpeI (S) and SpeI/AvrII (A) fragments as homologies. The SpeI cleavage sites were destroyed during the cloning processes. The 3′homology harbors exon three. For positive and negative selection in ES cells the vector contains a neomycin resistance gene in control of a constitutively active promotor (neo) flanked by FRT sites (white triangles) and a thymidine kinase gene (TK), respectively. Downstream of exon three of *Usp15*, a loxP site carrying an additional cleavage site (SpeI-loxP) was introduced into a PacI cleavage site. Homologous recombination was detected by Southern blot analysis with SpeI digested gDNA using the *Usp15* 5′ and 3′probe to validate correct 5′ and 3′ integration, respectively ($Usp15^{\text{neo-floxed}}$). Subsequently, the neomycin resistance gene can be excised using FLP expressing mouse deleter strain (+FLP) resulting in floxed exon three of *Usp15* ($Usp15^{\text{floxed}}$). The floxed allele can be deleted ($Usp15^{\text{del}}$) by usage of a Cre deleter strain (+Cre). Recombination events are verified by Southern blot analysis with mentioned probes by changes in fragment sizes for SpeI digested gDNA as indicated (double-arrows with kb designation).

was isolated, radiolabeled, and subsequently used as DNA probe. The bacterial clone `RPCIP711F18214Q3` was identified on two independent PAC library membranes. The identified bacterial clone was ordered and rechecked by hybridization with the radiolabled probe. The plasmid was extracted and digested with SpeI isoschizomere BcuI. The generated DNA fragments were cloned via shotgun cloning

into SpeI cut pZErO™-2 and pBlue2KSP. Bacterial clones containing the pZErO™-2 vector with the genomic sequence of the 5′homology were identified by screening via colony hybridization using an appropriate DNA probe (USP15_5′homo). In analogy, the bacterial clones containing the pBluKSP with genomic sequence of the 3′homology were identified by screening via colony hybridization with an appropriate DNA probe (USP15_3′homo). The pZErO™-2 containing the 5′homology (namely pZErO™-2[USP15_5′SpeI]) was cut with EcoRI and SpeI, blunted by a Klenow fill-in reaction, and subsequently ligated into NotI cut pPNT-frt3 vector (named pPNT-frt3[USP15_5′homo]) that also was blunted by a Klenow fill-in reaction prior to ligation destroying the SpeI site. The pBluKSP vector containing the 3′homology (named pBlu2KSP[USP15_3′subfragment]) was SpeI and AvrII (isoschizomere XmaJI) cut. In order to disrupt the endogenous SpeI restriction enzyme cleavage site, the fragment was SpeI and AvrII cut, blunted with Klenow fragment, and introduced in reverse orientation into EcoRV digested pBlu2KSP resulting in pBlu2KSP[USP15_5′homo Spe/Avr kl]Rev. Thus, after integration of the final targeting vector into the endogenous *Usp15* allele via homologous recombination, the genomic SpeI cleavage site would be lost. Hence, it is easier to screen recombination events by Southern blotting. To insert a loxP site into the 3′homology, the PacI restriction enzyme cleavage site was chosen, which is located within an intron downstream of the exon eight. Therefore, oligos were synthesized and annealed that beared the DNA sequence of an SpeI restriction enzyme cleavage site and the loxP site flanked by PacI sites (P-S-LoxP-P-Sense and P-S-LoxP-P-AntiS). The annealed oligo was PacI cut, ligated into PacI cut pBlu2KSP[USP15_3′homo Spe / Avr kl]Rev, and validated for correct orientation. The resulting vector was was named pBlu2KSP[USP15_3′homo_Spe / Avr kl]Rev_loxP. The 3′homology was cut out by SmaI and BsrbI digestion and ligated into PmlI cut (isoschizomere Eco72I) pPNT-frt3[USP15_5′homo] in the same orientation as the 5′homology producing the final targeting vector (pPNT-frt3[USP15_TV]).

3.2.3. Manipulation and identification of mutated ES cells

129P2/OlaHsd derived E14.1 ES cells and Bruce4 C57BL/6 ES cells were electroporated with the PmeI linearized pPNT-frt3[USP15_TV] targeting vector construct. Subsequently, ES cells were screened by Southern blotting using the *Usp15* 3′probe. Four ES cell clones were identified that displayed the expected additional fragment of 7.9 kb, i. e., C1, C2, D12 and F12 (see figure 3.8 A). Clone C1 is derived from

Bruce4 C57BL/6 cells and during the project this clone was not further worked with. Remaining positive ES cell clones were thawed and rechecked by Southern blotting using both *Usp15* 5′ and 3′probe to confirm correct homologous recombination. In figure 3.8 B SpeI-digested DNA of ES cell clone C2, D12 and F12 was hybridized with the *Usp15* 5′ and 3′probe. As expected, the *Usp15* 3′probe detected 9.7 kb and 7.9 kb DNA fragments corresponding to the wildtype and homologous recombinated allele, respectively. Interestingly, there was only the 6.2 kb wildtype DNA fragment detectable for ES cell clone F12 using the *Usp15* 5′probe, indicating only partial integration of the targeting vector. Nevertheless, for clone C2 and D12, two bands could be detected with expected sizes of 6.2 kb and 6.6 kb corresponding to the wildtype and homologous recombinated allele, respectively (see figure 3.8 B). These clones were used for blastocyst injection. Herein I refer to this locus type as neomycin-floxed (neo-fl).

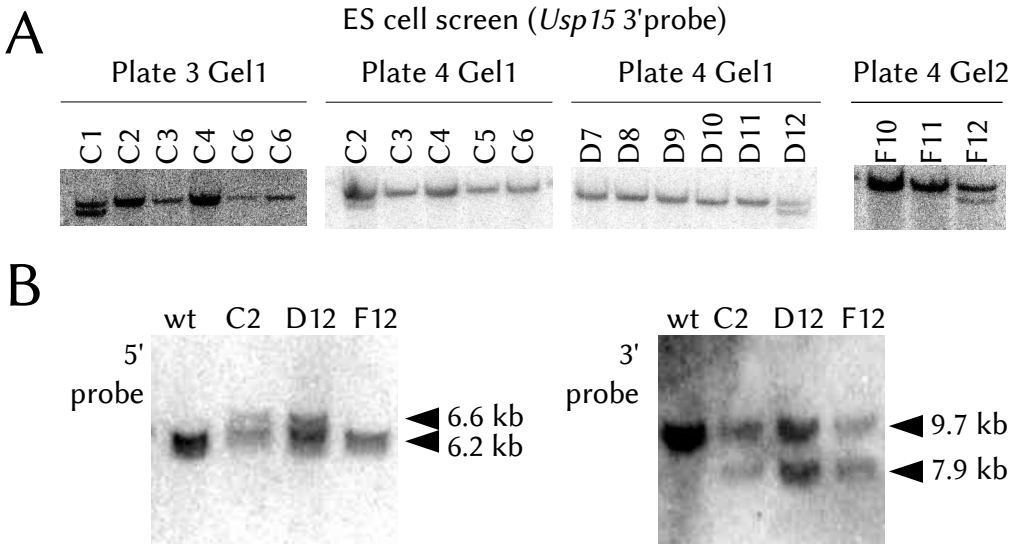

Figure 3.8.: Successful manipulation of the *Usp15* gene locus. **(A)** Part of the Southern blot screen for homologous recombinants using the *Usp15* 3′probe. Four clones (C1, C2, D12 and F12) could be detected in a screen for homologous recombinants using the *Usp15* 3′probe. **(B)** Positive ES cells were rechecked with *Usp15* 5′ and 3′probe by Southern blotting. Detected fragments in clones C2 and D12 correspond to the expected sizes according to the targeting strategy.

3.2.4. Generation of chimeric mice and identification of germline transmission

After confirmation of successful gene targeting of the *Usp15* locus, positive ES cells were prepared for blastocyst injection. Finally, two independent clones, i. e., C2

and D12, were used for injection into C57BL/6 blastocysts to generate chimeras at the core facility conditional gene targeting, at the University of Mainz (Germany). Subsequently, generated chimeras were bred with wildtype mice and the progeny was tested for germline transmission of the mutated *Usp15* allele. Germline transmission was verified by PCR. Therefore, primers were designed flanking the PacI restriction enzyme cleavage site that was used to introduce the additional SpeI and loxP site (see figure 3.7 and 3.9). These primers would amplify a DNA fragment of 219 bp or 267 bp for wildtype or the modified locus, respectively (see figure 3.9 A). To establish the PCR reaction, it was tested with wildtype, ES cell DNA, and the targeting vector only (see figure 3.9 B). The PCR resulted in amplification of a 219 bp fragment corresponding to the wildtype allele that was detectable in wildtype DNA, all ES cell clones, but not the targeting vector only. In contrast, amplification of an additional DNA fragment of 267 bp was observed in C2 and D12 which have been proven for correct homologous recombination before (see figure 3.9 B). However, wildtype DNA or the targeting vector only led to an amplification of a single fragment of 219 bp or 267 bp, respectively. Hence, these experiments verify solid identification of both alleles, wildtype and successful germline transmission. Noteworthy, clone F12 tested by Southern blotting with the *Usp15* 3′probe two bands of expected size were identified but only the wildtype fragment was detectable using the *Usp15* 5′probe. In the designed PCR for genotyping also two fragments could be amplified from the ES cell clone F12 indicating complete integration of the SpeI cleavage site adjacent to the loxP site. However, clone F12 was only shown to have the SpeI/loxP insertion. For that reason F12 was discarded.

After blastocyst injection of positive ES cells and implantation into foster mothers, chimera were obtained. These chimera were bred with C57BL/6 animals and offspring was tested for germline transmission (see figure 3.10). Two litter were tested by PCR as mentioned before, and two animals carrying the mutated allele could be detected (see figure 3.10 A and B), which were used for further breeding.

3.2.5. Deletion of the neomycin resistance gene

The created mouse strain with the floxed (fl) *Usp15* allele still carried the neomycin resistance gene which could alter normal expression of the endogenous locus. Since the neomycin resistance gene ist flanked by FRT sites, it can be easily excised. Therefore, heterozygous neo-fl animals ($Usp15^{+/\text{neo-fl}}$) were bred with a FLP deleter strain. Animals could be identified by Southern blotting, in which the neomycin

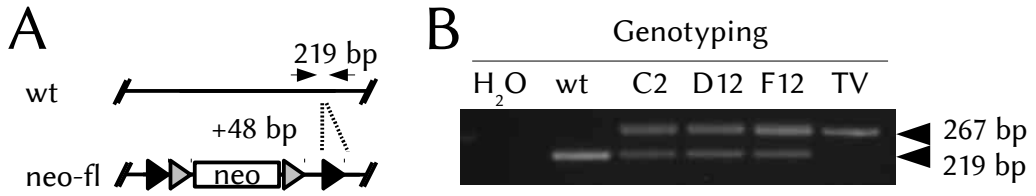

Figure 3.9.: Established PCR to detect germline transmission. **(A)** Primers were chosen flanking the region that is used for SpeI-loxP integration. Thus, the amplificate is larger after SpeI-loxP integration (+48 bp) than from the wildtype allele. **(B)** Verification of solid performance of the PCR to detect the wildtype allele and germline transmission. Wildtype (wt), ES cell DNA (C2, D12 and F12) and targeting vector only were tested. Using either wildtype DNA or the targeting vector led to amplification of single bands of 219 bp or 267 bp, respectively. Whereas, modified ES cell DNA led to amplification of both bands corresponding to wildtype and the neo-fl allele.

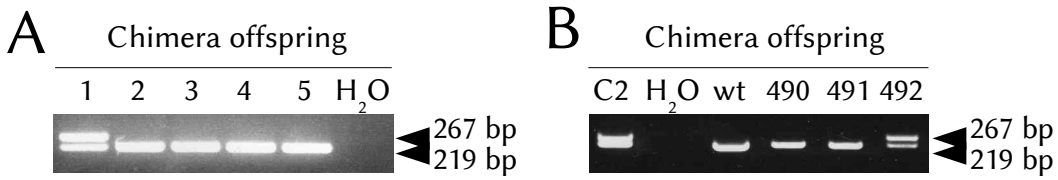

Figure 3.10.: Detection of germline transmission for *Usp15*. The primers flank the region in which the loxP site is inserted. The wildtype allele results in amplification of a 219 bp and the neo-fl allele in a 267 bp amplificate. **(A)** Animal 1 was successful tested for germline transmission. Negative control (H_2O) **(B)** Animal 492 was succesfully tested for germline transmission. ES cell clone C2 was used as positive control. Negative controls H_2O and wildtype gDNA (wt).

resistance gene was excised (see figure 3.11 B). In FLP deleted animals the fragment size detected by the *Usp15* 3′probe remains unchanged. However, the *Usp15* 5′probe could detect a fragment of 8.1 kb in size corresponding to the FLP deleted allele in which the introduced SpeI restriction enzyme cleavage site got lost resulting in a larger DNA fragment compared to 6.6 kb for the neo-fl allele.

These animals were used for subsequent breeding and creation of a mouse colony.

3.2.6. Deletion of *Usp15* using Cre deleter mice

Animals that carried the modified locus (neo-fl) were directly bred with a Cre deleter strain expressing Cre under the control of a constitutively active CMV promotor, to verify the functionality of the introduced loxP sites. Cre-mediated deletion of *Usp15* could be detected testing the offspring by Southern blot using the *Usp15* 5′ and 3′probe (see figure 3.11 A). After Cre-mediated deletion, the SpeI sites introduced into the genome would get excised. Loss of the mentioned SpeI restriction enzyme cleavage sites results in a single large DNA fragment of 14.1 kb in size that is detected using the *Usp15* 5′probe as well as the 3′probe.

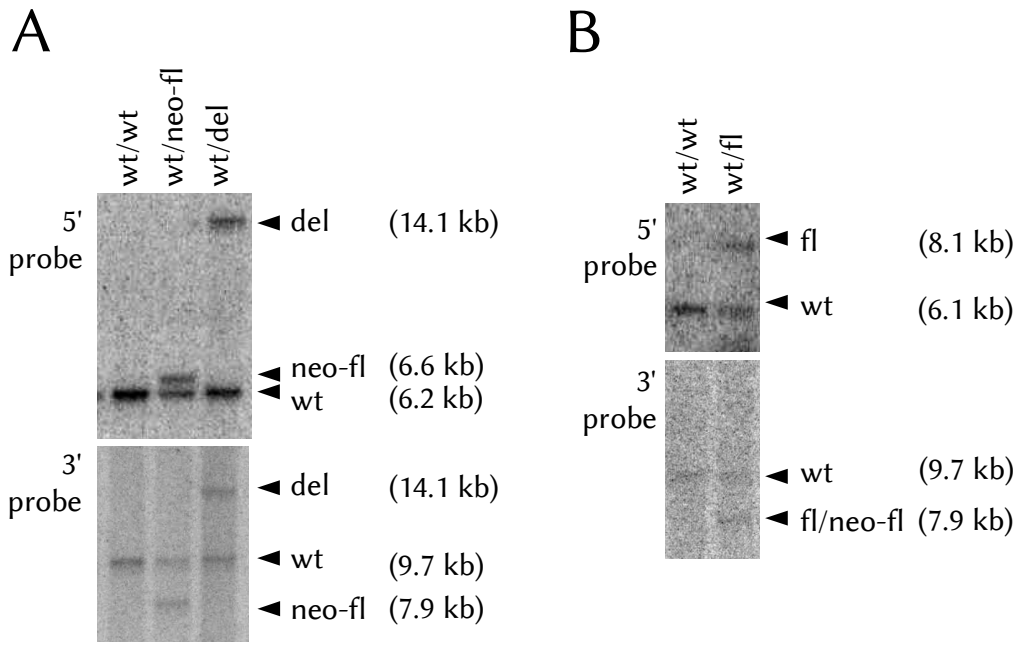

Figure 3.11.: Verification of Cre- and FLP-mediated deletion by Southern blotting. (**(A)** Genotyping of the offspring of an *Usp15*$^{+/\text{neo-fl}}$×Cre-deleter mating. All bands matched expected band sizes using the *Usp15* 5′(upper panel) and 3′probe (lower panel). **(B)** Genotyping of the offspring of an *Usp15*$^{+/\text{neo-fl}}$×FLP-deleter mating. All bands matched expected band sizes using the *Usp15* 5′(upper panel) and 3′(lower panel) probe.

At this stage the *Usp15* gene locus in heterozygous animals is referred to as *Usp15*$^{+/-}$ or *Usp15*$^{\text{wt/del}}$.

3.2.7. Design of PCRs for genotyping

To clearly identify the genomic *Usp15* gene locus in newborn mice, it is cheaper, more rapid, and easier to screen by PCR and not by Southern blotting. Therefore, a strategy was developed to detect every recombination event by PCR, thus, appropriate primers were designed. For convenient performance, all genotyping PCRs were designed to run at 60 °C annealing temperature and 37 seconds of elongation time. For further information on PCR parameters, see section 2.2.22 and 2.2.23.

To demostrate accurate determination of the different genomic recombination events, PCRs were tested using samples that were genotyped before by Southern blotting (see figure 3.11).

For the detection of wildtype and either neo-fl or fl animals, two primers (i. e., USP15_PacI_F and USP15_PacI_R) were designed that bind the endogenous locus flanking the loxP site on the mutated allele. The obtained PCR band for neo-fl

or fl animals is 48 bp larger than the 219 bp fragment obtained from wildtype DNA, because of the introduced SpeI restriction enzyme cleavage and loxP site (see figure 3.12 ❶ and 3.13 ❶). This PCR is identical to the PCR which was used to detect germline transmission as previously described in this study (see section 3.2.4). However, one cannot distiguish between animals that still bear the neomycin resistance gene (neo-fl) or animals in which the neomycin resistance gene is excised (fl), because both result in an amplificate of 267 bp (see figure 3.12 ❶). Thus, additional PCRs were mandatory to detect either the neo-fl or fl allele.

For detection of the fl allele, a PCR was designed with one primer binding upstream from the 5′loxP site (USP15_5′homo-1) and the other binding downstream between the 3′ FRT and 3′loxP site (USP15_5′homo-1) as shown in figure 3.12 ❷. FLP-mediated deletion juxtaposes the primer pair making the amplification easy. Thus, under mentioned conditions only the fl allele leads to the amplification of a 616 kb DNA fragment (see figure 3.12 ❷ and 3.13 ❷). In the wildtype the amplificate is smaller because loxP and FRT site are absent leading to the amplification of a 483 kb fragment (see figure 3.12 ❷ and 3.13 ❷).

For detection of the neo-fl allele, the same forward primer as for fl detection was used (USP15_5′homo-1) but with a reverse primer binding downstream of the 5′ FRT site (USP15_ScreenII_R) as shown in figure 3.12 ❸. Thus, there is an amplificate in neo-fl animals that gets lost as the binding sequence of the reverse primer is deleted after FLP-mediated recombination (see figure 3.12 ❸). This results in amplification of a 585 kb fragment from the neo-fl allele (see figure 3.13 ❸).

Finally, to detect Cre-mediated deletion primers were chosen that flank the region that is flanked by loxP sites (USP15_5′homo-1 and USP15_PacI_R). The binding motifs of the primers are relatively far away from each other so an amplificate using PCR parameters as mentioned is rather unlikely (see figure 3.12 ❹). However, if the sequence between the loxP sites is deleted this would lead to a amplificate of 513 kb (see figure 3.12 ❹ and 3.13 ❹).

3.2.8. Cre-mediated deletion of *Usp15* results in a null allele

Usp15$^{-/-}$ animals were obtained from *Usp15*$^{+/-}$ intercrosses. RNA from the liver was extracted and analyzed by Northern blotting. Therefore, pCMV-Tag3B-USP15 [52] was digested with HindIII and SalI, subsequently, the *Usp15* cDNA was isolated, radiolabeled and used as probe. In wildtype animals *Usp15* transcript was clearly visible, whereas *Usp15*$^{-/-}$ animals almost lack *Usp15* expression (see figure 3.14 A).

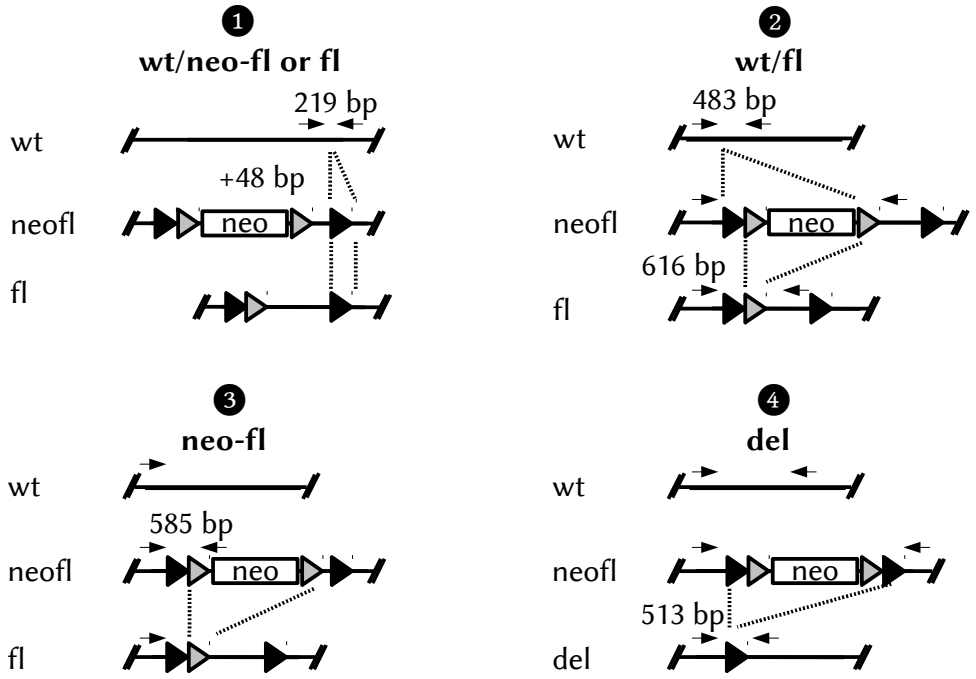

Figure 3.12.: Strategy for genotyping by PCR. ❶ For the detection of wildtype and either neo-fl or fl two primers (indicated by arrows) were designed flanking the loxP site (black triangle) on the mutated allele. The obtained PCR band for neo-fl or fl animals is 48 bp larger than the 219 bp fragment obtained from wildtype DNA. ❷ The fl allele was detected with one primer binding upstream from the 5′loxP site and the other binding downstream between the 3′FRT (grey triangle) and 3′loxP site resulting in 484 bp and 616 bp for wildtype and fl, respectively. ❸ For detection of the neo-fl allele primers were chosen that amplify a 585 kb fragment. ❹ To detect Cre-mediated deletion, the primers flank the region that is flanked by loxP sites. Thus, an amplificate of 513 bp is produced in the knockout allele.

As loading control *28S* and *18S* ribosomal RNA is shown. More importantly, in wildtype animals USP15 protein expression was detectable in whole liver protein extracts, whereas there was no USP15 detectable in the knockout (see figure 3.14 B).

In conclusion, deletion of exon eight leads to a *Usp15* null allele.

3.2.9. *Usp15*$^{-/-}$ mice are viable

Usp15$^{+/-}$ animals were intercrossed and the offspring was genotyped. Animals, which were homozygous for exon eight deletion, could be detected and were born at expected mendelian ratio (see table 3.1). However, *Usp15*$^{-/-}$ animals were retarded in growth as compared to heterozygous and wildtype littermates (see figure 3.15).

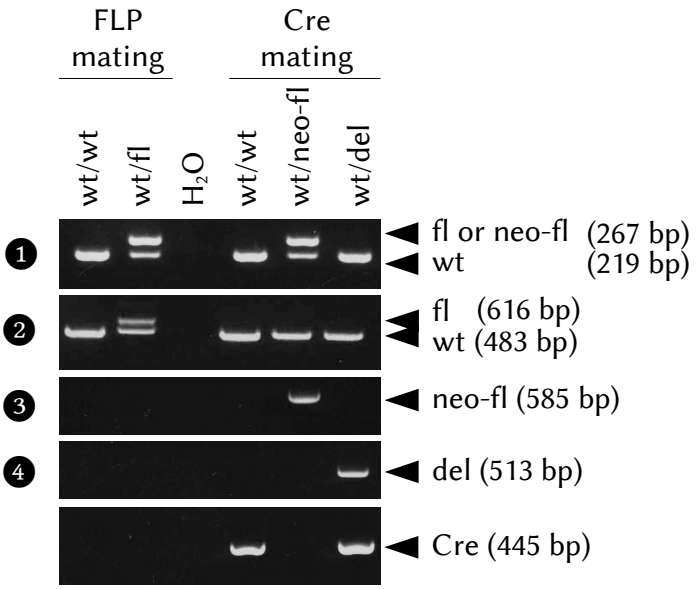

Figure 3.13.: Established PCRs for genotyping. Designed PCRs for *Usp15* genotyping work with high accuracy. ❶ PCR to detect wildtype (wt) and floxed (fl) or neo-floxed (neo-fl) allele. ❷ PCR to detect wt and fl allele. ❸ PCR to detect neo-fl allele only. ❹ PCR to detect deleted (del) allele only. Lowest panel shows genotyping PCR for Cre positive animals.

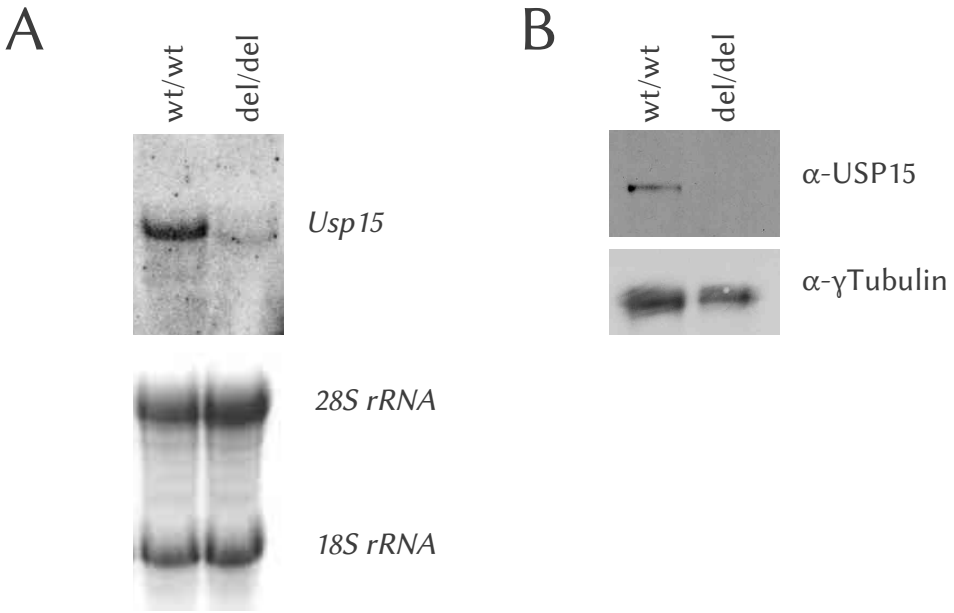

Figure 3.14.: Transcript and protein expression in the liver of *Usp15* knockout animals. **(A)** Northern blot of RNA from the liver of wildtype (wt/wt) and *Usp15* knockout (del/del) animals. *28 S* and *18 S* ribosomal RNA (*rRNA*) served as loading control. **(B)** Western blot analysis of USP15 protein levels of whole liver protein extract prepared from $Usp15^{-/-}$ and wildtype. γ-tubulin served as loading control.

Figure 3.15.: Picture of littermates from *Usp15*$^{+/-}$ intercross. *Usp15* knockout mouse (del/del) compared to wildtype (wt/wt) and heterozygous (wt/del) littermate. *Usp15* knockout mice were apparently smaller.

Table 3.1.: Mice were born at expected mendelian ratio (1:2:1). Number of mice and their genotype obtained from *Usp15*$^{+/-}$ intercrosses. 35 animals were genotyped. χ^2 equals 4.371 with 2 degrees of freedom. The two tailed p value equals 0.1124.

Genotype	*Usp15*$^{+/+}$	*Usp15*$^{+/-}$	*Usp15*$^{-/-}$
Observed number of mice	14	15	6
Expected number of mice (ratio of 1:2:1)	8.75	17.5	8.75

3.2.10. Analyses of MAFs

Fibroblasts generated from mice are an excellent tool to easily address certain questions of cell signaling, among others. However, since knockout animals were viable, fibroblasts could be directly generated by using small pieces of the ear. MAFs were generated and immortalized by SV40 large T transduction according to standard protocols by Dr. Klaus-Peter Knobeloch at the Neuropathology at the Universitätsklinikum in Freiburg (Germany). Two independent lines of *Usp15*$^{-/-}$ and *Usp15*$^{+/+}$ from littermates were established (see figure 3.16 A). Both wildtype cell lines express USP15 protein in contrast to both cell lines generated from *Usp15*$^{-/-}$ animals in which USP15 protein is not detectable by western blotting (see figure 3.16 B).

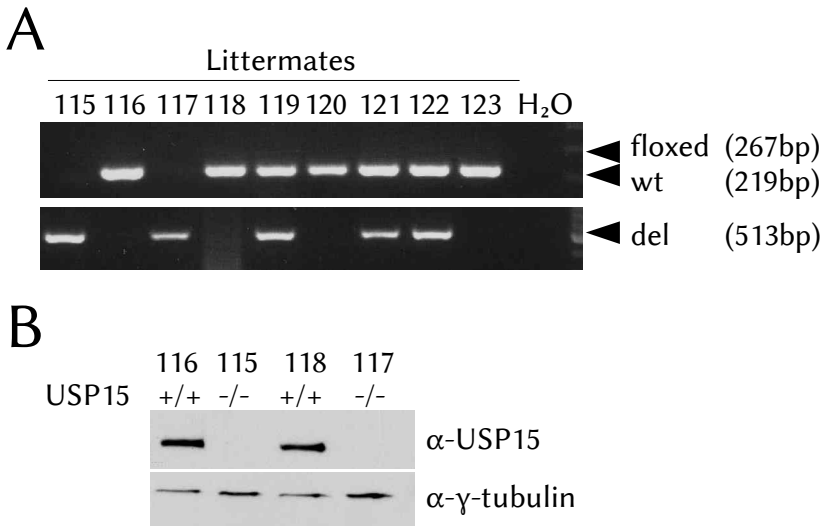

Figure 3.16.: MAFs derived from wildtype and *Usp15* knockout littermates obtained from *Usp15*$^{+/-}$ intercrosses were generated. The cells were analyzed by western blot for USP15 expression. **(A)** Littermates from *Usp15*$^{+/-}$ intercross were genotyped. In the upper panel the result obtained from a PCR that detects the wildtype (wt) and/or floxed (fl) allele is shown. In the lower panel the PCR detecting the deleted allele (del) is shown. Two independent cell lines were created by immortalization of ear fibroblasts each of homozygous wildtype (mouse number 116 and 118) and homozygous *Usp15*$^{-/-}$ animals (mouse number 115 and 117). **(B)** Immortalized MAFs were analyzed for USP15 protein expression by western blot. USP15 is not detectable in MAFs prepared from *Usp15*$^{-/-}$ animals 115 and 117 in contrast to MAFs prepared from wildtype animals 116 and 118. γ-tubulin served as loading control.

3.2.11. Loss of USP15 does not reduce protein steady state levels of the endogenous RING box protein RBX1

Some DUBs have been shown to protect E3 Ub ligases from autoubiquitination [77, 14]. USP15 has also been reported to stabilze the E3 ligase component RBX1 by deubiquitination [52] as determined by overexpression experiments. However, to address the question if loss of USP15 leads to RBX1 instability in vivo resulting in lower RBX1 protein levels, two independent MAF cell lines were analyzed for RBX1 protein levels. As shown in figure 3.17, RBX1 protein steady state levels were not altered in MAFs generated from *Usp15*$^{-/-}$ animals compared to MAFs generated from wildtype littermates. This suggests that loss of USP15 has no effect on endogenous RBX1 stability in vivo under employed experimental conditions.

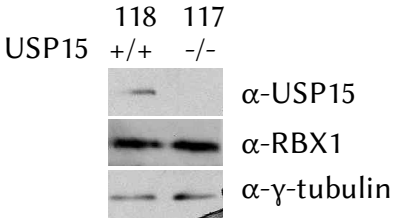

Figure 3.17.: Protein steady state levels of the RING box protein RBX1 is not altered in MAFs prepared from *Usp15*$^{-/-}$ and wildtype littermates. γ-tubulin served as loading control. Two independent cell lines derived from littermates were tested and resembled results from wildtype MAFs generated from the same litter.

3.2.12. IκBα degradation and reaccumulation is not altered in *Usp15* deficient MAFs

USP15 has been reported to affect NFκB signaling by deubiquitination ensuring proper reaccumulation of the NFκB inhibitor IκBα [148]. The data suggesting that USP15 affects IκBα reaccumulation were obtained by USP15 knockdown experiments. It was interesting to know how IκBα degradation and reaccumulation after TNF-α stimulation is altered in MAFs generated from *Usp15*$^{-/-}$ animals. Protein levels of IκBα were determined by western blot without and 10, 20 and 60 minutes after TNF-α administration. Interestingly, neither IκBα degradation nor reaccumulation was altered in MAFs generated from *Usp15*$^{-/-}$ animals although USP15 is not detectable by western blot in these cells (see figure 3.18). The experiments were performed using two independent cell lines both resembling IκBα degradation kinetics and amounts of cells prepared from wildtype animals.

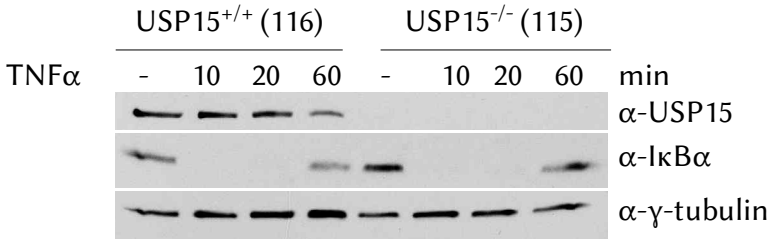

Figure 3.18.: Determination of IκBα degradation kinetics in MAFs prepared from *Usp15*$^{-/-}$ and wildtype littermates. Protein levels of IκBα were determined without, 10, 20, and 60 minutes after TNF-α administration. Neither IκBα degradation nor its reaccumulation was affected in MAFs generated from *Usp15*$^{-/-}$ animals compared to MAFs derived from wildtype littermates. γ-tubulin served as loading control. Two independent cell lines derived from littermates were tested and resembled results from wildtype MAFs generated from the same litter.

3.2.13. TGF-β induced SMAD2 phosphorylation is not altered in *Usp15*$^{-/-}$ MAFs

Recently, two papers were published suggesting that USP15 positively affects TFG-β signaling [32, 61]. Eichhorn et al. [32] reported that USP15 stabilizes TGF-β receptor I and thereby promotes oncogenesis through the activation of TGF-β signaling in glioblastoma. Moreover, in their studies phosphorylation of SMAD2 is inhibited by USP15 knockdown. Therefore, MAFs generated from *Usp15*$^{-/-}$ should display reduced responsiveness to TGF-β stimulation compared to control cells generated from wildtype littermates. Although Eichhorn et al. reported inhibition of SMAD2 phosphorylation by USP15 knockdown, neither a difference in intensity nor kinetics of SMAD2 phosphorylation was observed analysing *Usp15*$^{-/-}$ and *Usp15*$^{+/+}$ MAFs generated from littermates as shown in figure 3.19. Experiments were validated in two independent MAFs derived from littermates.

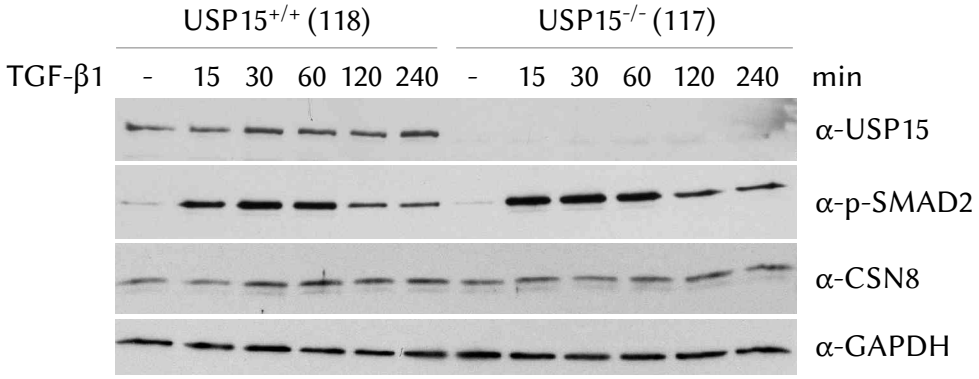

Figure 3.19.: *Usp15* deficient MAFs respond normally to TGF-β. TGF-β1 stimulated *Usp15* deficient MAFs did not differ from wildtype MAFs monitored by SMAD2 phosphorylation. Cells were harvested without or after indicated time (min) of TGF-β1 stimulation. Kinetics and intensity of phosphorylation of the SMAD2 degradation was not affected by loss of USP15 in MAFs generated from *Usp15*$^{-/-}$ animals compared to MAFs derived from wildtype littermates. Also the CSN subunit CSN8 protein levels were not altered in the analyzed time course. GAPDH served as loading control. Two independent cell lines derived from littermates were tested and resembled results from wildtype MAFs generated from the same litter.

3.2.14. USP15 does not influence protein steady state levels of neither CSN5 nor CSN8

Until recently, USP15 was the only DUB known to bind the CSN [52, 34]. Although association of USP15 and the CSN is often described in literature [52, 56, 148], little

is known about how USP15 binds to the CSN and if USP15 affects the stability of the CSN complex or single subunits. Therefore, it was investigated whether lack of USP15 in MAFs prepared from *Usp15*$^{-/-}$ animals had an effect on steady state levels of single CSN subunits. Protein levels of CSN5 and CSN8 were analyzed by western blotting of protein extracts from *Usp15*$^{-/-}$ and *Usp15*$^{+/+}$ derived MAFs. Loss of USP15 had no effect on protein levels of neither CSN5 nor CSN8 compared to MAFs prepared from wildtype littermates as shown in figure 3.20. The experiments were performed by examination of two independent cell lines generated from two *Usp15*$^{-/-}$ and two wildtype littermates.

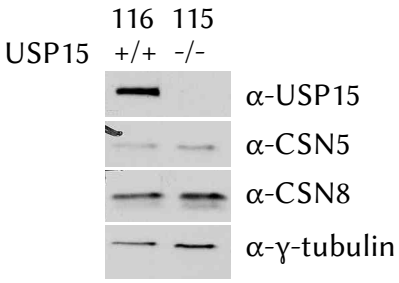

Figure 3.20.: Loss of USP15 does not influence CSN5 or CSN8 steady state levels. Protein levels of CSN subunits CSN5 and CSN8 in *Usp15*$^{-/-}$ MAFs compared to MAFs generated from wildtype littermates. Neither CSN5 nor CSN8 differed in protein steady state levels. γ-tubulin served as loading control. Two independent cell lines derived from littermates were tested and resembled results from wildtype MAFs generated from the same litter.

4. Discussion

4.1. USP18

4.1.1. Generation of mice expressing catalytically inactive USP18

Mice that lack ISG15 expression are more susceptible to infection with influenza A and B, herpes, and sindbis virus infection [89]. Moreover, *Isg15*$^{-/-}$ MEFs are more permissive to VSV replication [97] clearly demonstrating the profound antiviral effect of ISG15. Animals that lack UBE1L, the E1 for ISG15, fail to activate ISG15 [70]. As a consequence ISG15 cannot be conjugated to target proteins [70]. Mice, which lack UBE1L, enable to investigate the role of conjugated ISG15 versus free ISG15. Like *Isg15* deficient animals, *Ube1L* deficient mice were more susceptible to infection with influenza B [84] and sindbis virus [41]. Thus, ISGylation exerts at least partially its antiviral effects through its conjugation to target proteins. For example, in vivo studies demonstrated that ISG15, without its conjugation to target proteins, is critical to control chikungunya virus infection [173]. However, strong evidence has been provided that USP18 is the main enzyme responsible for ISG15 deconjugation due to prior observations that USP18 knockout mice display a massive increase in ISGylation [134]. Interestingly, these animals are hyperresponsive to IFN, die prematurely and developed severe brain injury [134, 105]. Originally, loss of deISGylation function was accounted for these phenotypical alterations. However, loss of *Isg15* in *Usp18* knockout mice does not rescue the phenotype of *Usp18* knockout mice [134]. Thus, it was suggested that USP18 either is reactive to Ub or other UbLs. Alternatively, the observed phenotypical alterations could be due to a nonenzymatic functions of USP18 [74]. And quite so, based on in vitro studies, a nonenzymatical function of USP18 has been suggested. USP18 competed in binding to the receptor IFNAR2 with the kinase JAK1 [104], thus, inhibited IFN signaling.

In the present study, a novel mouse strain was generated by gene targeting of

the endogenous *Usp18* locus, which serves as an ideal tool to differentiate between enzymatic and nonenzymatic function of USP18 in vivo. USPs are cysteine proteases and USP18 variants mutated in cysteine residue at position 61 have been shown to fail in cleaving linear ISG15 fusion proteins and ISGylated proteins in vitro [102, 69, 104]. In this study, an amino acid exchange of cysteine to alanine at this position was introduced in the germline to generate mice expressing an enzymatically inactive USP18 protein. Therefore, a strategy was developed to introduce this mutation by gene targeting via homologous recombination in ES cells. Coexistent with the mutation encoding the amino acid exchange, a restriction enzyme cleavage site was introduced to allow to screen for homologous recombination events by Southern blotting. Subsequently, a positive ES cell clone has been identified by Southern blotting. To validate the mutation, the positive ES cell clone was stimulated with LPS to induce expression of endogenous *Usp18* mRNA. Subsequently, cDNA was prepared and sequenced with primers flanking the mutated region on the cDNA. Both wildtype and base exchange could be detected by sequencing (see figure 3.4 C). In the mutated ES cells, beside the mutated locus also one wildtype allele still exists, as also has been shown on the genomic level by Southern blotting (see figure 3.4 A and B). Hence, the wildtype allele was expressed in response to LPS stimulation explaining the peaks of the wildtype bases in the chromatograph. Homologous recombination is a rare event, therefore, only one allele can be targeted at a time. The chromatograph peaks detecting the exchanged bases were notably lower. However, this technique does not allow to draw a conclusion on the expression level. Nevertheless, the neomycin resistance gene in the intron of *Usp18* could in principle provoke hypomorph expression, as previously reported for other gene loci [53, 168]. To circumvent this possible disadvantage, the positive selection marker was removed by mating chimeras with a FLP deleter strain (see figure 3.5). In the upper pannel of figure 3.5B, gDNA from wildtype (wt) and the positive ES cell clone (KI) were used as control. Unfortunately, these samples were probably not digested completely, so that the different fragments derived from positive ES gDNA were not seperated on this Southern blot. Nevertheless, germline transmission and FLP-mediated deletion of the neomycin resistance gene could be unequivocally identified. In line with the later analysis, mutated and wildtype USP18 protein was expressed at similar levels (Dr. Klaus-Peter Knobeloch, personal communication).

The *Usp18*$^{+/C61A}$ mice generated in this study were mated to homozygosity and are currently under investigation in collaboration with Dr. Klaus-Peter Knobeloch

(Neuropathology, Universitätsklinikum Freiburg, Germany).

4.1.2. *Usp18*$^{C61A/C61A}$ mice as a tool to dissect enzymatic functions in vivo

The mouse model generated in this study is a valuable tool, because it is indispensable to discriminate between catalytic and noncatalytic function of USP18 in vivo. Moreover, endogenous expression of enzymatically inactive USP18 mimics pharmaceutical inhibition of USP18 enzyme activity. Lack of USP18 protease activity should result in higher ISGylation levels, since USP18 is the main deISGylation enzyme [134, 186]. Therefore, it will be investigated, whether there are more ISG15 conjugates in *Usp18*$^{C61A/C61A}$ as compared to wildtype, before and after IFN-mediated induction.

Usp18$^{-/-}$ mice die prematurely, develop severe brain injury, and are hyperresponsiveness to poly(I:C) [134, 105]. These phenotypical alterations are not connected to ISG15, as it cannot be rescued by loss of ISG15 in *Usp18 Isg15* double knockout mice [74]. To identify, whether USP18 might be a protease for another Ub/UbL or if these alterations are due to loss of a protease independent function, *Usp18*$^{C61A/C61A}$ mice will be analyzed and compared to the previous observations of *Usp18*$^{-/-}$ animals. Therefore, it will be monitored, whether *Usp18*$^{C61A/C61A}$ die prematurely, are hyperresponsive to poly(I:C), or develop severe brain injury.

Usp18$^{-/-}$ mice have also been reported to be more resistant to infection with *Salmonella typhimurium* than wildtype mice [69] and *Usp18*$^{-/-}$ derived MEFs are slightly more resistant against VSV induced cytopathic effect [74]. *Usp18*$^{-/-}$ mice, however, are hyperresponsive to IFN signaling and fail to deconjugate ISG15 [105]. It is not clear, if enhanced resistance is a consequence of boosted IFN signaling or due to failure of deISGylation. *Usp18*$^{C61A/C61A}$ mice should reveal which effect depends on the enzymatic activity of USP18. For instance, ISG15 has been shown to be important to counteract influenza A/B and sindbis virus infection in vivo [89]. At least for some infections it was investigated, whether free ISG15 (Chikungunya virus [173]) or ISGylation (influenza B [84], sindbis virus [41]) is necessary to establish resistance. *Usp18*$^{C61A/C61A}$ mice are expected to accumulate ISG15 conjugates what especially should be beneficial, if ISGylation rather than free ISG15 mediates the antiviral effect. Thus, it will be interesting to see, whether resistance can even be boosted by the catalytically inactive USP18 mutant compared to wildtype

(e. g., influenza A/B, sindbis virus). This would demontrate, at least in principle, if targeting USP18 protease activity would be a promising, novel, antiviral therapeutical concept. Therefore, *Usp18*$^{C61A/C61A}$ animals and *Usp18*$^{C61A/C61A}$ MEFs will be tested in infection experiments with viral and bacterial pathogens for their ability to restrict infection.

Recently, USP18 has been shown to be involved in refractoriness of IFN signaling [141, 36]. It was suggested that USP18-mediated refractoriness of IFN signaling is independent of its enzymatic activity [36]. To understand the mechanism of USP18-mediated refractoriness to IFN signaling in vivo, *Usp18*$^{C61A/C61A}$ will be analyzed and compared to *Usp18* knockout mice.

Recently, *Usp18* knockout mice have been shown to have a defect in dendritic cell development demonstrated by reduced (approximately 50%) CD11b^{+} cells in the liver [21]. The same study also provided evidence that boosted IFN signaling is the cause for this effect. Therefore, CD11b^{+} cells in the liver will be investigated. If boosted IFN signaling is the cause for the reduction of this cell population in mice lacking USP18, then *Usp18*$^{C61A/C61A}$should reveal no alteration compared to wildtype mice.

Usp18$^{C61A/C61A}$ mice are also valuable, since they mimic inhibition of USP18 enzymatic activity. USPs are generally believed to be drugable. If the *Usp18*$^{C61A/C61A}$ mutation would be beneficial to overcome refractoriness of IFN signaling or beneficial against infection, this would point out the promising benefit of developing USP18 inhibitors. Recombinant IFN is used for the treatment in some diseases (e. g., hepatitis C [101]) and cells become insensitive to IFN for some time. Overcoming this refractoriness might enhance IFN therapy.

Usp18$^{C61A/C61A}$ mice will also reveal, whether targeting of USP18 enzymatic activity might be beneficial in case of osteoporosis, a prevalent bone disorder. A study published in 2011, by Albers et al. [1], revealed that *Isg15* deficient mice display decreased bone formation. Unfortunately, it is not clear, whether free ISG15 or ISGylation is important for bone formation. One might speculate that *Usp18*$^{C61A/C61A}$ animals display increased bone formation which would point to promising effect of pharmaceutically block USP18 enzymatic activity.

4.2. USP15

4.2.1. Generation of mice carrying a conditional *Usp15* allele

In the present study, a conditional *Usp15* gene knockout mouse strain was generated via gene targeting in ES cells. This novel mouse strain enables to analyze USP15 function in a spatial and temporal manner in vivo. There is a large variety of transgenic Cre expressing mice available [113], which can be used to analyze the function of USP15 in vivo.

The gene locus was targeted according to the targeting strategy (see figure 3.7) and *Usp15*$^{+/\text{neo-fl}}$ mice were generated. It is known that the positive selection marker, namely the neomycine resistance gene, can disrupt normal interactions between local and long-distance regulatory regions affecting gene expression of various genes even at distances greater than 100 kb from the mutation [130]. It has also been reported that the neomycin resistance gene placed in an intron can reduce gene expression (hypomorph allele) [53] or affect mRNA processing [168]. Hence, the developed strategy for construction of a conditional *Usp15* allele included the subsequent ablation of the neomycin resistance gene by using the FLP/FRT system. *Usp15*$^{+/\text{neo-fl}}$ were mated with a FLP deleter strain. Accordingly, the neomycin resistance gene could be successfully excised (see figure 3.11 B).

To produce a *Usp15* knockout allele, the exon eight was be removed by Cre-mediated deletion (see figure 3.11 A). Accordingly, cells lack *Usp15* transcript and USP15 protein (see figure 3.14). Deletion of exon eight creates a frameshift resulting in a stop codon in exon nine. Thus, premature termination of translation and nonsense-mediated mRNA decay would be the expected outcomes. Nonsense-mediated mRNA decay is an intrinsic cellular mechanism that degrades transcripts that terminate 50–55 bp upstream of an exon-exon junction [107]. Exon eight of *Usp15* is followed by several exons and splice sites downstream of the transcript. Hence, deletion of exon eight should activate nonsense-mediated mRNA decay. Such a strategy has been successfully applied to conditionally knockout various other proteases, e. g., USP7 [79], USP8 [116], CSN5 [126].

Usp15$^{+/-}$ and *Usp15*$^{+/fl}$ mice generated in this study have a mixed background and will be backcrossed to a pure C57BL/6 background for further analyses. Therefore, animals have to be backcrossed for at least ten generations.

4.2.2. *Usp15* deficient mice are viable

In *S. cerevisiae*, cullin E3 ligase components are stabilized by Ubp12p [189, 145], the orthologue of USP15. Based on a cell culture experiment, it was reported that human USP15 stabilizes the RING box protein RBX1 [52], a component of CRLs. RBX1 binds to cullins recruiting the E2 to the E3 ligase complex. Moreover, USP15 binds to the CSN [189, 34], which is thought to be an important regulator of CRL function. Therefore, loss of USP15 might lead to dysregulation of a vast number of CRLs. All knockout mice for CSN subunits that have been generated so far are embryonically lethal [182, 100, 161, 87]. Because the CSN is suggested to be the main regulator for CRLs, their dysregulation might be an explanation for embryonic lethality in these animals. Even disruption of single cullins in mice results in embryonic lethality [167, 151, 91, 63]. These facts suggested that loss of USP15 might also be lethal in mice. Additionally, beside affecting the stability of CRL components, USP15 has been reported to enhance TGF-β and BMP signaling [61, 32]. Many players in the TGF-β signaling are also important for embryonic development [71]. Hence, loss of USP15 might result in dysregulation of CRLs and TGF-β signaling further pointing to its pontential importance in embryonic development.

It was not known, whether mice homozygous for a *Usp15* null allele still would survive embryonic development. Mice in which exon eight of *Usp15* was deleted were genotyped by PCR. These animals resulted from intercrosses of USP15$^{+/-}$ parents genotyped by Southern blotting. Interestingly, *Usp15* knockout animals were viable and born at expected mendelian ratio suggesting USP15 not to affect embryonic development. However, animals homozygous for *Usp15* exon eight deletion were retarded in growth.

4.2.3. *Usp15* deficient mice lack transcript and protein

As discussed earlier (see section 4.2.1), deletion of exon eight suggests the remaining transcript to be subject to nonsense-mediated mRNA decay. Hence, one would expect loss of transcript and protein. To prove the absence of *Usp15* transcript and USP15 protein, RNA and protein was extracted from the whole liver. Transcript of *Usp15* was detectable in wildtype, whereas it was almost lost in the *Usp15* knockout. This suggests that the transcript, in which exon eight was deleted, was degraded by nonsense-mediated mRNA decay. To assess, whether USP15 is also lost on protein level, whole liver protein extract was tested for USP15 expression. USP15 could

only be detected in liver extract prepared from wildtype but not from the *Usp15* knockout.

Additionally, MAFs were generated from ear tissue of either wildtype or *Usp15* knockout mice. In line with the previous observation, USP15 protein was clearly detectable in MAFs generated from wildtype animals, but was absent in MAFs generated from *Usp15* deletion mutants (see figure 3.16). Hence, deletion of exon eight finally leads to loss of USP15 protein.

MAFs were immortalized by SV40 large T transduction. Two independent each knockout and wildtype derived cell lines were generated. Thus, side effects due to disruption of a certain DNA element, which might distort further analysis could be excluded. In the present study, all experiments were performed with these independently generated MAFs derived from littermates.

4.2.4. USP15 does not reduce the endogenous protein steady state levels of the CRL component RBX1

USP15 has been reported to bind the CSN [189] which is the main regulator of CRLs and it has been reported that USP15 stabilizes components of CRLs [52]. Deletion of CSN subunits in higher eukaryotes impedes embryonic development [182, 100, 161, 87] which might be due to a massive dysregulation of CRLs and their substrates. Knockout mice for cullin1 [167], cullin3 [151], cullin4A [91] and cullin4b [63] support this idea, since each of them results in embryonic lethality. All in all, this suggests that deletion of *Usp15* might result in embryonic lethality. However, homozygous $Usp15^{-/-}$ knockout animals were viable and retarded in growth (see figure 3.15). One component of CRLs that has been reported to be stabilized by USP15 is the RING box protein RBX1 [52]. Now with an in vivo system at hand, it was interesting to evaluate the physiological relevance of the USP15 RBX1 interaction. Therefore, RBX1 protein steady state levels were determined in cells derived from *Usp15* knockout animals and compared to wildtype. Surprisingsly, there was no change of RBX1 protein steady state levels in MAFs derived from two independent either wildtype or knockout animals. However, it cannot be excluded that USP15 deubiquitinates RBX1 or even stabilizes it in vivo affecting the half-life of the protein. Although, this possibility might be unlikely if compared to another in vivo model of USP/E3 ligase interaction, i. e., USP7 and the E3 ligase MDM2. USP7 stabilizes MDM2 as can be seen in $Usp7^{+/-}$ MEFs when protein synthesis is blocked

revealing faster degradation of MDM2 [79] compared to wildtype MEFs. Moreover, MDM2 steady state protein levels are reduced in *Usp7*$^{-/-}$ MEFs [80]. However, the study suggesting USP15 to stabilize RBX1 was performed by overexpression experiments in which USP15 led to slight stabilization of RBX1. The prevalent observation of DUBs stabilizing E3 ligases and the information from the USP15 orthologoue Ubp12p in *S. cerevisiae* stabilizing the substrate specific adapter protein Pop1p [189] and Btb3p [145] supported the notion of USP15 stabilizing RBX1. Therefore, the slight stabilization of overexpressed RBX1 in conjunction with overexpression of USP15 might only be accounted by driving the deubiquitination in a nonphysiological way with excess of enzyme although RBX1 may not be a subtrate under physiological conditions.

However, it cannot be ruled out that USP15 affects stability of other components of CRLs such as substrate receptor proteins or adaptor proteins of CRLs in mice. As mentioned before, Ubp12p stabilizes the substrate specific adapter protein Pop1p [189] and Btb3p [145]. Since *Usp15* knockout animals were viable and survived embryogenesis, there might only be a slight effect on CRL components or only on certain proteins, e. g., substrate receptors or adaptors of CRLs. It would be interesting to determine protein levels of such CRL components.

In conclusion, there is no effect on RBX1 steady state protein levels in *Usp15* knockout MAFs compared to MAFs generated from wildtype animals.

4.2.5. Reexamination of TNF-α signaling

NFκB is a transcription factor important for cell proliferation, immune system development and immune response [50]. NFκB is retained inactive by binding to the inhibitory protein IκBα [50]. Following diverse stimuli, e. g., TNF-α, IκBα is degraded [66] by the proteasome releasing NFκB. Subsequently, NFκB translocates to the nucleus and drives gene expression of target genes. TNF-α induces the degradation of IκBα which reaccumulates after certain time constituting a negative feedback loop [50]. USP15 has been reported to assist in reaccumulation of IκBα post stimulation [148]. To analyze the physiological relevance of this interaction, the effect on IκBα reaccumulation was determined after TNF-α stimulation. Cells derived from knockout and wildtype animals were stimulated with TNF-α, and degradation and reaccumulation of IκBα was monitored in these cells. Neither the kinetics nor the amount of IκBα were changed in *Usp15*$^{-/-}$ MAFs. Over the investigated time course, IκBα was degraded and reaccumulated normally in response to TNF-α (see

figure 3.18). The slight changes in reaccumulation of IκBα reported by Schweitzer et al. [148] were admittedly low and might have been a result from off-target effects induced by the used siRNA against *USP15*.

In conclusion, USP15 does not affect reaccumaltion of the NFκB inhibitor IκBα after TNF-α stimulation under employed experimental conditions (see figure 4.1).

4.2.6. Reexamination of TGF-β signaling

Only recetly, two reports suggested USP15 to be involved in TGF-β signaling [32, 61]. Interestingly, these two reports indicate distinct mechanisms how USP15 enhances TGF-β signaling. Eichhorn et al. [32] reported that USP15 stabilizes TGF-β receptor I (TβRI) promoting oncogenesis through the activation of TGF-β signaling in glioblastoma. Moreover, in their study phosphorylation of the R-SMAD2 is inhibited by USP15 knockdown. To examine the physiological relevance of this observation in vivo, MAFs generated from wildtype or *Usp15*$^{-/-}$ mice were tested for SMAD2 phosphorylation after TGF-β1 stimulation. Interestingly, SMAD2 phosphorylation did neither differ in kinetics nor intensity after TGF-β1 stimulation (see figure 3.19). Eichhorn at al. [32] argued that SMAD7 acts as a scaffold protein stabilizing TβRI through USP15-mediated deubiquitination. Interestingly, the Ub E3 ligase SMURF2 also associates with SMAD7 and ubiquitinates the TβRI [32]. SMAD7 is well established as a key regulator of the negative feedback loop shutting down TGF-β signaling [10]. However, almost at the same time a study reported that MEFs derived from *Smad7*$^{-/-}$ mice displayed higher levels of TβRI protein. If SMAD7 binds USP15 and SMURF2 [32] directing them to the TβRI, then loss of SMAD7 could result in receptor up- or downregulation depending on which interaction is favored in the functional complex, i. e., either ubiquitination or deubiquitination. The observation that loss of SMAD7 results in higher levels of TβRI protein [159] suggests that USP15 plays a minor role in the SMAD7 complex. Higher TβRI protein levels are thought to enhance downstream signaling events such as SMAD2 phosphorylation. Contrariwise, TGF-β-mediated phosphorylation was slightly diminished in *Smad7* deficient cells and expression of TGF-β target genes was not altered in expression compared to wildtype. This suggests that USP15 should not be crucial for target gene expression even if it would affect TβRI stability. However, though loss of USP15 does not affect TGF-β induced SAMD2 phosphorylation it cannot be ruled out that TGF-β signaling is affected by USP15 in certain organs or cell populations.

Inui et al. observed TGF-β1 or BMP-2 signaling is inhibited by knockdown of USP15 [61]. Moreover, TGF-β target genes $p21^{Waf1}$, plasminogen activator inhibitor 1 (PAI1) and cMyc were reduced on protein and transcript level [61]. Also the BMP targets DNA-binding protein inhibitor (ID2) and SMAD7 were reported to be reduced [61]. It can not be excluded that lack of USP15 affects target gene expression. Based on their experiments, they proposed a model in which SMAD3 association with DNA is inhibited by ubiquitination of a Lys residue in a region that is important for DNA binding. USP15 opposes the ubiquitination of SMAD3, so it can assoiate with DNA [61]. Thus, SMAD3 DNA interaction might be affected in cells lacking USP15. *Smad3* knockout animals are viable but die at one to eight weeks [183]. It would be interesting to determine mortality of *Usp15* deficient mice. However, the mortality can differ depending on the genetic background. For instance, mice deficient in *Smad7* die prematurely or are only growth retarded depending on the genetic background [159].

4.2.7. USP15 has most likely no influence on CSN stability

Until recently, USP15 was the only DUB known to bind the CSN [181, 34]. Although some reports discuss the role of CSN acting as a platform or scaffold to bring USP15 to its substrate, its effect on CSN stability has never been assessed. The present study demonstrates that ablation of USP15 expression has no effect on CSN stability as determined by CSN5 and CSN8 steady state levels in MAFs generated from wildtype or $Usp15^{-/-}$ littermates (see figure 3.20). It has been reported that CSN subunits are coordinately expressed. This has been shown by data obtained from siRNA, overexpression [129, 128, 90] and in vivo experiments [87]. For instance, CSN8 knockout in mouse hepatocytes resulted in diminished expression of CSN subunits (CSN3, CSN5, CSN6 and CSN7) [87]. Ablation of USP15 did not affect CSN5 or CSN8 protein levels and due to the coordinated expression of the CSN subunits differential stabilization of any other CSN subunit is unlikely.

Although it is known that USP15 binds to the CSN complex [181, 34], it is still obscure how this interaction is mediated, i. e., either directly or indirectly. The CSN complexes within the cell are not homogenous. There exist also different variants of CSN subunits, e. g., CSN7a and CSN7b. Therefore, USP15 might interact only with a certain population of CSN complexes or even promote formation of certain complex subtypes.

Binding of USP15 to the CSN may fulfill other functions than stabilizing the CSN

complex (see figure 4.1). The CSN complex might regulate specificity of USP15 by acting as a scaffold complex directing USP15 to certain substrates. This notion is supported by the observation that most DUBs seem to be associated with multi-protein complexes [155].

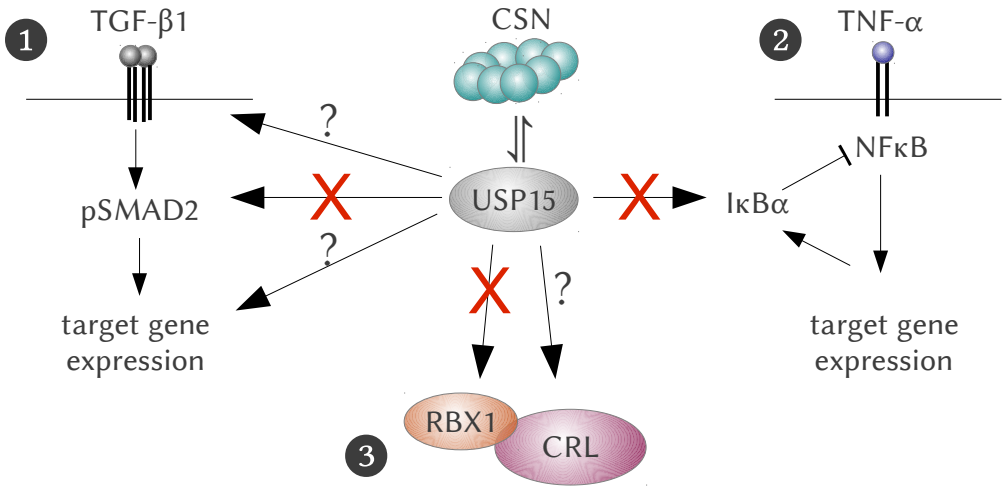

Figure 4.1.: Model for USP15 function in vivo. Role for USP15 in TGF-β1 and TNF-α signaling and its putative interaction with CRLs. USP15 has been shown to associate with the CSN which might act as a platform directing USP15 to certain substrates without affecting its stability. ❶ TGF-β1 binds to its receptor, subsequently leading to SMAD2 phosphorylation and target gene expression. This study demonstrated that USP15 is dispensable for SMAD2 phosphorylation in TGF-β1 stimulated MAFs. Nevertheless, loss of USP15 might affect TβRI stability and/or target gene expression. ❷ TNF-α binds on its receptor leading to degradation of IκBα. Subsequently, NFκB drives target gene transcription including IκBα expression forming a negative feedback loop. This study demonstrates that IκBα reaccumulation is not affected by loss of USP15 in vivo. ❸ RBX1 is a component of CRLs. USP15 did not alter RBX1 steady state protein levels in vivo, but USP15 might affect stability of adaptor proteins or certain substrate receptors.

4.2.8. Outlook

The novel mouse model enables to analyse the consequence of a *Usp15* null allele in various cell types (spatial) or at a certain time point of deleopment (temporal). Since $Usp15^{-/-}$ animals are viable, they can be directly analyzed. To understand the main features of USP15 in vivo, flow cytometric analysis will be carried out to examine the composition certain tissues (e. g., spleen, thymus). It will be analyzed, whether the immune and hematopoetic system develop normally without USP15.

The Wnt pathway has been previously reported to be affected by USP15 [56] as observed by knockdown experiments [56]. USP15 has been suggested to stabilize APC reducing β-catenin levels [56]. We will take advantage of the in vivo mouse

model and investigate the relevance and effect of this observation in *Usp15* deficient MAFs. It will be analyzed, whether *Usp15* MAFs respond normally to Wnt stimulation and if β-catenin is more stabile in these cells.

In this study, MAFs lacking USP15 were not changed in TGF-β1 induced phosphorylation of SMAD2. However, since it has been reported that overexpression of USP15 could stabilize the TGF-β receptor [32], flow cytometric analysis will be carried out to examine the expression level of the TβRI on various cell types. To determine, whether USP15 affects TGF-β or BMP signaling, expression of their target genes will be analyzed (e. g., PAI-1, ID1 [146]). USP15 has been suggested to deubiquitinate SMAD3 which facilitates SMAD3 DNA interaction [61]. If USP15 affects SMAD3 activity, *Usp15*$^{-/-}$ mice should have similar alterations as *Smad3*$^{-/-}$ mice. Both *Smad3*$^{-/-}$ and *Usp15*$^{-/-}$ mice are viable. Noteworthy, *Smad3*$^{-/-}$ mice have a low life expectancy. The mortality of *Usp15*$^{-/-}$ deficiency will be monitored and compared to the mortality of *Smad3*$^{-/-}$ animals. Moreover, neutrophils of *Smad3*$^{-/-}$ mice are defective in chemotaxis stimulated by TGF-β [183]. It will be investigated, whether USP15 deficient animals show similar defects, as one would expect, if USP15 enhances SMAD3 activity in vivo. Another defect of *Smad3*$^{-/-}$ mice that could be tested in *Usp15*$^{-/-}$ mice is the effect of TGF-β stimulation of primary hepatocytes. TGF-β induces apoptosis in primary hepatocytes derived from wildtype but not from *Smad3*$^{-/-}$ animals [65]. Since CD3 activated *Smad3*$^{-/-}$ T-cells fail to TGF-β-mediated inhibition of proliferation [65], it will be interesting to analyze the response of *Usp15*$^{-/-}$ cells to TGF-β stimulation.

There are only a few substrates for USP15 that have been published so far. To identify substrates of USP15, stable isotope labeling by amino acids in cell culture (SILAC) experiments will be performed [122]. This technique is nowadays used quite frequently and is an ideal way to compare the proteome of different cell lines. The labeled proteome of wildtype and *Usp15*$^{-/-}$ cells will be analyzed by mass spectrometry. A procedure to perform such a study already has been discussed [112].

References

[1] Joachim Albers, Jochen Schulze, F. Timo Beil, Matthias Gebauer, Anke Baranowsky, Johannes Keller, Robert P Marshall, Kristofer Wintges, Felix W Friedrich, Matthias Priemel, Arndt F Schilling, Johannes M Rueger, Kerstin Cornils, Boris Fehse, Thomas Streichert, Guido Sauter, Franz Jakob, Karl L Insogna, Barbara Pober, Klaus-Peter Knobeloch, Uta Francke, Michael Amling, and Thorsten Schinke. Control of bone formation by the serpentine receptor frizzled-9. *J Cell Biol*, 192(6):1057–1072, Mar 2011.

[2] Corinne Angelats, Xiao-Wen Wang, Lars S Jermiin, Neal G Copeland, Nancy A Jenkins, and Rohan T Baker. Isolation and characterization of the mouse ubiquitin-specific protease usp15. *Mamm Genome*, 14(1):31–46, Jan 2003.

[3] R. T. Baker, X. W. Wang, E. Woollatt, J. A. White, and G. R. Sutherland. Identification, functional characterization, and chromosomal localization of usp15, a novel human ubiquitin-specific protease related to the unp oncoprotein, and a systematic nomenclature for human ubiquitin-specific proteases. *Genomics*, 59(3):264–274, Aug 1999.

[4] Mario Barro and John T Patton. Rotavirus nonstructural protein 1 subverts innate immune response by inducing degradation of ifn regulatory factor 3. *Proc Natl Acad Sci U S A*, 102(11):4114–4119, Mar 2005.

[5] E. Beitz. Texshade: shading and labeling of multiple sequence alignments using latex2 epsilon. *Bioinformatics*, 16(2):135–139, Feb 2000.

[6] G. R. Bignell, W. Warren, S. Seal, M. Takahashi, E. Rapley, R. Barfoot, H. Green, C. Brown, P. J. Biggs, S. R. Lakhani, C. Jones, J. Hansen, E. Blair, B. Hofmann, R. Siebert, G. Turner, D. G. Evans, C. Schrander-Stumpel, F. A. Beemer, A. van Den Ouweland, D. Halley, B. Delpech, M. G. Cleveland, I. Leigh, J. Leisti, and S. Rasmussen. Identification of the familial cylindromatosis tumour-suppressor gene. *Nat Genet*, 25(2):160–165, Jun 2000.

[7] Ernest C Borden, Ganes C Sen, Gilles Uze, Robert H Silverman, Richard M Ransohoff, Graham R Foster, and George R Stark. Interferons at age 50: past, current and future impact on biomedicine. *Nat Rev Drug Discov*, 6(12):975–990, Dec 2007.

[8] William P Bozza and Zhihao Zhuang. Biochemical characterization of a multidomain deubiquitinating enzyme ubp15 and the regulatory role of its terminal domains. *Biochemistry*, 50(29):6423–6432, Jul 2011.

[9] Anja Bremm, Stefan M V Freund, and David Komander. Lys11-linked ubiquitin chains adopt compact conformations and are preferentially hydrolyzed by the deubiquitinase cezanne. *Nat Struct Mol Biol*, 17(8):939–947, Aug 2010.

[10] Marco A Briones-Orta, Angeles C Tecalco-Cruz, Marcela Sosa-Garrocho, Cassandre Caligaris, and Marina Macías-Silva. Inhibitory smad7: emerging roles in health and disease. *Curr Mol Pharmacol*, 4(2):141–153, Jun 2011.

[11] F. Buchholz, P. O. Angrand, and A. F. Stewart. Improved properties of flp recombinase evolved by cycling mutagenesis. *Nat Biotechnol*, 16(7):657–662, Jul 1998.

[12] Richard Buus, Monica Faronato, Dean E Hammond, Sylvie Urbé, and Michael J Clague. Deubiquitinase activities required for hepatocyte growth factor-induced scattering of epithelial cells. *Curr Biol*, 19(17):1463–1466, Sep 2009.

[13] Ken Cadwell and Laurent Coscoy. Ubiquitination on nonlysine residues by a viral e3 ubiquitin ligase. *Science*, 309(5731):127–130, Jul 2005.

[14] Mary Canning, Chris Boutell, Jane Parkinson, and Roger D Everett. A ring finger ubiquitin ligase is protected from autocatalyzed ubiquitination and degradation by binding to ubiquitin-specific protease usp7. *J Biol Chem*, 279(37):38160–38168, Sep 2004.

[15] Zhongwei Cao, Xiuli Wu, Lily Yen, Colleen Sweeney, and Kermit L Carraway. Neuregulin-induced erbb3 downregulation is mediated by a protein stability cascade involving the e3 ubiquitin ligase nrdp1. *Mol Cell Biol*, 27(6):2180–2188, Mar 2007.

[16] Allan D Capili and Christopher D Lima. Taking it step by step: mechanistic insights from structural studies of ubiquitin/ubiquitin-like protein modification pathways. *Curr Opin Struct Biol*, 17(6):726–735, Dec 2007.

[17] André Catic, Edda Fiebiger, Gregory A Korbel, Daniël Blom, Paul J Galardy, and Hidde L Ploegh. Screen for isg15-crossreactive deubiquitinases. *PLoS One*, 2(7):e679, 2007.

[18] Michael J Clague, Judy M Coulson, and Sylvie Urbé. Cellular functions of the dubs. *J Cell Sci*, 125(Pt 2):277–286, Jan 2012.

[19] Martin A Cohn, Younghoon Kee, Wilhelm Haas, Steven P Gygi, and Alan D D'Andrea. Uaf1 is a subunit of multiple deubiquitinating enzyme complexes. *J Biol Chem*, 284(8):5343–5351, Feb 2009.

[20] Martin A Cohn, Przemyslaw Kowal, Kailin Yang, Wilhelm Haas, Tony T Huang, Steven P Gygi, and Alan D D'Andrea. A uaf1-containing multisubunit protein complex regulates the fanconi anemia pathway. *Mol Cell*, 28(5):786–797, Dec 2007.

[21] Xiu-Li Cong, Miao-Chia Lo, Brian A Reuter, Ming Yan, Jun-Bao Fan, and Dong-Er Zhang. Usp18 promotes conventional cd11b+ dendritic cell development. *J Immunol*, 188(10):4776–4781, May 2012.

[22] Andrea Conidi, Silvia Cazzola, Karen Beets, Kathleen Coddens, Clara Collart, Frederique Cornelis, Luk Cox, Debruyn Joke, Mariya P Dobreva, Ruben Dries, Camila Esguerra, Annick Francis, Abdelilah Ibrahimi, Roel Kroes, Flore Lesage, Elke Maas, Ivan Moya, Paulo N G Pereira, Elke Stappers, Agata Stryjewska, Veronique van den Berghe, Liesbeth Vermeire, Griet Verstappen, Eve Seuntjens, Lieve Umans, An Zwijsen, and Danny Huylebroeck. Few smad proteins and many smad-interacting proteins yield multiple functions and action modes in tgf-beta/bmp signaling in vivo. *Cytokine Growth Factor Rev*, 22(5-6):287–300, 2011.

[23] Gregory A Cope and Raymond J Deshaies. Cop9 signalosome: a multifunctional regulator of scf and other cullin-based ubiquitin ligases. *Cell*, 114(6):663–671, Sep 2003.

[24] Gregory A Cope, Greg S B Suh, L. Aravind, Sylvia E Schwarz, S. Lawrence Zipursky, Eugene V Koonin, and Raymond J Deshaies. Role of predicted metalloprotease motif of jab1/csn5 in cleavage of nedd8 from cul1. *Science*, 298(5593):608–611, Oct 2002.

[25] Eric B Dammer, Chan Hyun Na, Ping Xu, Nicholas T Seyfried, Duc M Duong, Dongmei Cheng, Marla Gearing, Howard Rees, James J Lah, Allan I Levey, John Rush, and Junmin Peng. Polyubiquitin linkage profiles in three models of proteolytic stress suggest the etiology of alzheimer disease. *J Biol Chem*, 286(12):10457–10465, Mar 2011.

[26] Anahita Dastur, Sylvie Beaudenon, Melissa Kelley, Robert M Krug, and Jon M Huibregtse. Herc5, an interferon-induced hect e3 enzyme, is required for conjugation of isg15 in human cells. *J Biol Chem*, 281(7):4334–4338, Feb 2006.

[27] Laurent Daviet and Frédéric Colland. Targeting ubiquitin specific proteases for drug discovery. *Biochimie*, 90(2):270–283, Feb 2008.

[28] Raymond J Deshaies and Claudio A P Joazeiro. Ring domain e3 ubiquitin ligases. *Annu Rev Biochem*, 78:399–434, 2009.

[29] Larissa A Durfee, Nancy Lyon, Kyungwoon Seo, and Jon M Huibregtse. The isg15 conjugation system broadly targets newly synthesized proteins: implications for the antiviral function of isg15. *Mol Cell*, 38(5):722–732, Jun 2010.

[30] G. D. Van Duyne. A structural view of cre-loxp site-specific recombination. *Annu Rev Biophys Biomol Struct*, 30:87–104, 2001.

[31] Mariola J Edelmann and Benedikt M Kessler. Ubiquitin and ubiquitin-like specific proteases targeted by infectious pathogens: Emerging patterns and molecular principles. *Biochim Biophys Acta*, 1782(12):809–816, Dec 2008.

[32] Pieter J A Eichhorn, Laura Rodón, Alba Gonzàlez-Juncà, Annette Dirac, Magüi Gili, Elena Martínez-Sáez, Claudia Aura, Ignasi Barba, Vicente Peg, Aleix Prat, Isabel Cuartas, Jose Jimenez, David García-Dorado, Juan Sahuquillo, Réné Bernards, José Baselga, and Joan Seoane. Usp15 stabilizes tgf-beta receptor i and promotes oncogenesis through the activation of tgf-beta signaling in glioblastoma. *Nat Med*, 18(3):429–435, Mar 2012.

[33] Paul R Elliott, Han Liu, Martyna W Pastok, Günter J Grossmann, Daniel J Rigden, Michael J Clague, Sylvie Urbé, and Igor L Barsukov. Structural variability of the ubiquitin specific protease dusp-ubl double domains. *FEBS Lett*, 585(21):3385–3390, Nov 2011.

[34] Lei Fang, Robyn M Kaake, Vishal R Patel, Yingying Yang, Pierre Baldi, and Lan Huang. Mapping the protein interaction network of the human cop9 signalosome complex using a label-free qtax strategy. *Mol Cell Proteomics*, 11(5):138–147, May 2012.

[35] Daniel Finley. Recognition and processing of ubiquitin-protein conjugates by the proteasome. *Annu Rev Biochem*, 78:477–513, 2009.

[36] Véronique François-Newton, Gabriel Magno de Freitas Almeida, Béatrice Payelle-Brogard, Danièle Monneron, Lydiane Pichard-Garcia, Jacob Piehler, Sandra Pellegrini, and Gilles Uzé. Usp18-based negative feedback control is induced by type i and type iii interferons and specifically inactivates interferon alpha response. *PLoS One*, 6(7):e22200, 2011.

[37] K. A. Furge, Y. W. Zhang, and G. F. Vande Woude. Met receptor tyrosine kinase: enhanced signaling through adapter proteins. *Oncogene*, 19(49):5582–5589, Nov 2000.

[38] Thangiah Geetha, Rajappa S Kenchappa, Marie W Wooten, and Bruce D Carter. Traf6-mediated ubiquitination regulates nuclear translocation of nrif, the p75 receptor interactor. *EMBO J*, 24(22):3859–3868, Nov 2005.

[39] Ruth Geiss-Friedlander and Frauke Melchior. Concepts in sumoylation: a decade on. *Nat Rev Mol Cell Biol*, 8(12):947–956, Dec 2007.

[40] Sankar Ghosh and Matthew S Hayden. New regulators of nf-kappab in inflammation. *Nat Rev Immunol*, 8(11):837–848, Nov 2008.

[41] Nadia V Giannakopoulos, Elena Arutyunova, Caroline Lai, Deborah J Lenschow, Arthur L Haas, and Herbert Whiting Virgin. Isg15 arg151 and the isg15-conjugating enzyme ube1l are important for innate immune control of sindbis virus. *J Virol*, 83(4):1602–1610, Feb 2009.

[42] A. L. Goldberg. Functions of the proteasome: from protein degradation and immune surveillance to cancer therapy. *Biochem Soc Trans*, 35(Pt 1):12–17, Feb 2007.

[43] L. Gong, T. Kamitani, S. Millas, and E. T. Yeh. Identification of a novel isopeptidase with dual specificity for ubiquitin- and nedd8-conjugated proteins. *J Biol Chem*, 275(19):14212–14216, May 2000.

[44] Caroline Grabbe and Ivan Dikic. Functional roles of ubiquitin-like domain (uld) and ubiquitin-binding domain (ubd) containing proteins. *Chem Rev*, 109(4):1481–1494, Apr 2009.

[45] Regina Groisman, Jolanta Polanowska, Isao Kuraoka, Jun ichi Sawada, Masafumi Saijo, Ronny Drapkin, Alexei F Kisselev, Kiyoji Tanaka, and Yoshihiro Nakatani. The ubiquitin ligase activity in the ddb2 and csa complexes is differentially regulated by the cop9 signalosome in response to dna damage. *Cell*, 113(3):357–367, May 2003.

[46] H. Gu, J. D. Marth, P. C. Orban, H. Mossmann, and K. Rajewsky. Deletion of a dna polymerase beta gene segment in t cells using cell type-specific gene targeting. *Science*, 265(5168):103–106, Jul 1994.

[47] A. L. Haas, P. Ahrens, P. M. Bright, and H. Ankel. Interferon induces a 15-kilodalton protein exhibiting marked homology to ubiquitin. *J Biol Chem*, 262(23):11315–11323, Aug 1987.

[48] Hasem Habelhah. Emerging complexity of protein ubiquitination in the nf-kappab pathway. *Genes Cancer*, 1(7):735–747, Jul 2010.

[49] Ronny Hannss and Wolfgang Dubiel. Cop9 signalosome function in the ddr. *FEBS Lett*, 585(18):2845–2852, Sep 2011.

[50] Matthew S Hayden and Sankar Ghosh. Shared principles in nf-kappab signaling. *Cell*, 132(3):344–362, Feb 2008.

[51] A. Hershko and A. Ciechanover. The ubiquitin system. *Annu Rev Biochem*, 67:425–479, 1998.

[52] Bettina K J Hetfeld, Annett Helfrich, Barbara Kapelari, Hartmut Scheel, Kay Hofmann, Adi Guterman, Michael Glickman, Rüdiger Schade, Peter-Michael Kloetzel, and Wolfgang Dubiel. The zinc finger of the csn-associated deubiquitinating enzyme usp15 is essential to rescue the e3 ligase rbx1. *Curr Biol*, 15(13):1217–1221, Jul 2005.

[53] S. Hirotsune, M. W. Fleck, M. J. Gambello, G. J. Bix, A. Chen, G. D. Clark, D. H. Ledbetter, C. J. McBain, and A. Wynshaw-Boris. Graded reduction of pafah1b1 (lis1) activity results in neuronal migration defects and early embryonic lethality. *Nat Genet*, 19(4):333–339, Aug 1998.

[54] Mark Hochstrasser. Origin and function of ubiquitin-like proteins. *Nature*, 458(7237):422–429, Mar 2009.

[55] X. Huang and A. Madan. Cap3: A dna sequence assembly program. *Genome Res*, 9(9):868–877, Sep 1999.

[56] Xiaohua Huang, Corinna Langelotz, Bettina K J Hetfeld-Pechoc, Wolfgang Schwenk, and Wolfgang Dubiel. The cop9 signalosome mediates beta-catenin degradation by deneddylation and blocks adenomatous polyposis coli destruction via usp15. *J Mol Biol*, 391(4):691–702, Aug 2009.

[57] James H Hurley, Evzen Boura, Lars-Anders Carlson, and Bartosz Różycki. Membrane budding. *Cell*, 143(6):875–887, Dec 2010.

[58] Koraljka Husnjak and Ivan Dikic. Ubiquitin-binding proteins: Decoders of ubiquitin-mediated cellular functions. *Annu Rev Biochem*, Apr 2012.

[59] Fumiyo Ikeda and Ivan Dikic. Atypical ubiquitin chains: new molecular signals. 'protein modifications: Beyond the usual suspects' review series. *EMBO Rep*, 9(6):536–542, Jun 2008.

[60] Yasumichi Inoue and Takeshi Imamura. Regulation of tgf-beta family signaling by e3 ubiquitin ligases. *Cancer Sci*, 99(11):2107–2112, Nov 2008.

[61] Masafumi Inui, Andrea Manfrin, Anant Mamidi, Graziano Martello, Leonardo Morsut, Sandra Soligo, Elena Enzo, Stefano Moro, Simona Polo, Sirio Dupont, Michelangelo Cordenonsi, and Stefano Piccolo. Usp15 is a deubiquitylating enzyme for receptor-activated smads. *Nat Cell Biol*, 13(11):1368–1375, Nov 2011.

[62] Yoshitaka Isumi, Tsuyoshi Hirata, Hiroshi Saitoh, Tomoya Miyakawa, Kenji Murakami, Gen Kudoh, Hirofumi Doi, Kohtaro Ishibashi, and Hiroto Nakajima. Transgenic overexpression of usp15 in the heart induces cardiac remodeling in mice. *Biochem Biophys Res Commun*, 405(2):216–221, Feb 2011.

[63] Baichun Jiang, Wei Zhao, Jupeng Yuan, Yanyan Qian, Wenjie Sun, Yongxin Zou, Chenhong Guo, Bingxi Chen, Changshun Shao, and Yaoqin Gong. Lack of cul4b, an e3 ubiquitin ligase component, leads to embryonic lethality and abnormal placental development. *PLoS One*, 7(5):e37070, 2012.

[64] C. Johnston, W. Jiang, T. Chu, and B. Levine. Identification of genes involved in the host response to neurovirulent alphavirus infection. *J Virol*, 75(21):10431–10445, Nov 2001.

[65] Wenjun Ju, Atsushi Ogawa, Joerg Heyer, Dirk Nierhof, Liping Yu, Raju Kucherlapati, David A Shafritz, and Erwin P Böttinger. Deletion of smad2 in mouse liver reveals novel functions in hepatocyte growth and differentiation. *Mol Cell Biol*, 26(2):654–667, Jan 2006.

[66] Naama Kanarek and Yinon Ben-Neriah. Regulation of nf-kappa b by ubiquitination and degradation of the ikappabs. *Immunol Rev*, 246(1):77–94, Mar 2012.

[67] Lars Ketscher, Anja Basters, Marco Prinz, and Klaus-Peter Knobeloch. mherc6 is the essential isg15 e3 ligase in the murine system. *Biochem Biophys Res Commun*, 417(1):135–140, Jan 2012.

[68] Jung Min Kim, Kalindi Parmar, Min Huang, David M Weinstock, Carrie Ann Ruit, Jeffrey L Kutok, and Alan D D'Andrea. Inactivation of murine usp1 results in genomic instability and a fanconi anemia phenotype. *Dev Cell*, 16(2):314–320, Feb 2009.

[69] Keun Il Kim, Oxana A Malakhova, Kasper Hoebe, Ming Yan, Bruce Beutler, and Dong-Er Zhang. Enhanced antibacterial potential in ubp43-deficient mice against salmonella typhimurium infection by up-regulating type i ifn signaling. *J Immunol*, 175(2):847–854, Jul 2005.

[70] Keun Il Kim, Ming Yan, Oxana Malakhova, Jiann-Kae Luo, Mei-Feng Shen, Weiguo Zou, Juan Carlos de la Torre, and Dong-Er Zhang. Ube1l and protein isgylation are not essential for alpha/beta interferon signaling. *Mol Cell Biol*, 26(2):472–479, Jan 2006.

[71] Krit Kitisin, Tapas Saha, Tiffany Blake, Nady Golestaneh, Merlyn Deng, Christine Kim, Yi Tang, Kirti Shetty, Bibhuti Mishra, and Lopa Mishra. Tgf-beta signaling in development. *Sci STKE*, 2007(399):cm1, Aug 2007.

[72] E. Knight, D. Fahey, B. Cordova, M. Hillman, R. Kutny, N. Reich, and D. Blomstrom. A 15-kda interferon-induced protein is derived by cooh-terminal processing of a 17-kda precursor. *J Biol Chem*, 263(10):4520–4522, Apr 1988.

[73] Klaus-Peter Knobeloch. In vivo functions of isgylation. *Subcell Biochem*, 54:215–227, 2010.

[74] Klaus-Peter Knobeloch, Olaf Utermöhlen, Agnes Kisser, Marco Prinz, and Ivan Horak. Reexamination of the role of ubiquitin-like modifier isg15 in the phenotype of ubp43-deficient mice. *Mol Cell Biol*, 25(24):11030–11034, Dec 2005.

[75] David Komander. The emerging complexity of protein ubiquitination. *Biochem Soc Trans*, 37(Pt 5):937–953, Oct 2009.

[76] David Komander. Mechanism, specificity and structure of the deubiquitinases. *Subcell Biochem*, 54:69–87, 2010.

[77] David Komander, Michael J Clague, and Sylvie Urbé. Breaking the chains: structure and function of the deubiquitinases. *Nat Rev Mol Cell Biol*, 10(8):550–563, Aug 2009.

[78] David Komander, Francisca Reyes-Turcu, Julien D F Licchesi, Peter Odenwaelder, Keith D Wilkinson, and David Barford. Molecular discrimination of structurally equivalent lys 63-linked and linear polyubiquitin chains. *EMBO Rep*, 10(5):466–473, May 2009.

[79] N. Kon, Y. Kobayashi, M. Li, C. L. Brooks, T. Ludwig, and W. Gu. Inactivation of hausp in vivo modulates p53 function. *Oncogene*, 29(9):1270–1279, Mar 2010.

[80] N. Kon, J. Zhong, Y. Kobayashi, M. Li, M. Szabolcs, T. Ludwig, P. D. Canoll, and W. Gu. Roles of hausp-mediated p53 regulation in central nervous system development. *Cell Death Differ*, 18(8):1366–1375, Aug 2011.

[81] Zhizhou Kuang, Eun Joo Seo, and Jonathan Leis. Mechanism of inhibition of retrovirus release from cells by interferon-induced gene isg15. *J Virol*, 85(14):7153–7161, Jul 2011.

[82] S. F. Kwok, R. Solano, T. Tsuge, D. A. Chamovitz, J. R. Ecker, M. Matsui, and X. W. Deng. Arabidopsis homologs of a c-jun coactivator are present both in monomeric form and in the cop9 complex, and their abundance is differentially affected by the pleiotropic cop/det/fus mutations. *Plant Cell*, 10(11):1779–1790, Nov 1998.

[83] Ralf Kühn and Raul M Torres. Cre/loxp recombination system and gene targeting. *Methods Mol Biol*, 180:175–204, 2002.

[84] Caroline Lai, Jessica J Struckhoff, Jana Schneider, Luis Martinez-Sobrido, Thorsten Wolff, Adolfo García-Sastre, Dong-Er Zhang, and Deborah J Lenschow. Mice lacking the isg15 e1 enzyme ube1l demonstrate increased susceptibility to both mouse-adapted and non-mouse-adapted influenza b virus infection. *J Virol*, 83(2):1147–1151, Jan 2009.

[85] J. T. Lee and W. Gu. The multiple levels of regulation by p53 ubiquitination. *Cell Death Differ*, 17(1):86–92, Jan 2010.

[86] David S Leggett, John Hanna, Anna Borodovsky, Bernat Crosas, Marion Schmidt, Rohan T Baker, Thomas Walz, Hidde Ploegh, and Daniel Finley. Multiple associated proteins regulate proteasome structure and function. *Mol Cell*, 10(3):495–507, Sep 2002.

[87] D. Lei, F. Li, H. Su, Z. Tian, B. Ye, N. Wei, and X. Wang. Cop9 signalosome subunit 8 is required for postnatal hepatocyte survival and effective proliferation. *Cell Death Differ*, 18(2):259–270, Feb 2011.

[88] Deborah J Lenschow, Nadia V Giannakopoulos, Lacey J Gunn, Christine Johnston, Andy K O'Guin, Robert E Schmidt, Beth Levine, and Herbert W Virgin. Identification of interferon-stimulated gene 15 as an antiviral molecule during sindbis virus infection in vivo. *J Virol*, 79(22):13974–13983, Nov 2005.

[89] Deborah J Lenschow, Caroline Lai, Natalia Frias-Staheli, Nadia V Giannakopoulos, Andrew Lutz, Thorsten Wolff, Anna Osiak, Beth Levine, Robert E Schmidt, Adolfo García-Sastre, David A Leib, Andrew Pekosz, Klaus-Peter Knobeloch, Ivan Horak, and Herbert Whiting Virgin. Ifn-stimulated gene 15 functions as a critical antiviral molecule against influenza, herpes, and sindbis viruses. *Proc Natl Acad Sci U S A*, 104(4):1371–1376, Jan 2007.

[90] Ulrike Leppert, Wolfgang Henke, Xiaohua Huang, Joachim M Müller, and Wolfgang Dubiel. Post-transcriptional fine-tuning of cop9 signalosome subunit biosynthesis is regulated by the c-myc/lin28b/let-7 pathway. *J Mol Biol*, 409(5):710–721, Jun 2011.

[91] Binghui Li, Joseph C Ruiz, and Kristin T Chun. Cul-4a is critical for early embryonic development. *Mol Cell Biol*, 22(14):4997–5005, Jul 2002.

[92] Zaibo Li, Dakun Wang, Edward M Messing, and Guan Wu. Vhl protein-interacting deubiquitinating enzyme 2 deubiquitinates and stabilizes hif-1alpha. *EMBO Rep*, 6(4):373–378, Apr 2005.

[93] Stanley Lipkowitz and Allan M Weissman. Rings of good and evil: Ring finger ubiquitin ligases at the crossroads of tumour suppression and oncogenesis. *Nat Rev Cancer*, 11(9):629–643, Sep 2011.

[94] Cong Liu, Kelly A Powell, Kirsten Mundt, LeJung Wu, Antony M Carr, and Thomas Caspari. Cop9/signalosome subunits and pcu4 regulate ribonucleotide reductase by both checkpoint-dependent and -independent mechanisms. *Genes Dev*, 17(9):1130–1140, May 2003.

[95] L. Q. Liu, R. Ilaria, P. D. Kingsley, A. Iwama, R. A. van Etten, J. Palis, and D. E. Zhang. A novel ubiquitin-specific protease, ubp43, cloned from leukemia fusion protein aml1-eto-expressing mice, functions in hematopoietic cell differentiation. *Mol Cell Biol*, 19(4):3029–3038, Apr 1999.

[96] K. R. Loeb and A. L. Haas. The interferon-inducible 15-kda ubiquitin homolog conjugates to intracellular proteins. *J Biol Chem*, 267(11):7806–7813, Apr 1992.

[97] G. Lu, J. T. Reinert, I. Pitha-Rowe, A. Okumura, M. Kellum, K. P. Knobeloch, B. Hassel, and P. M. Pitha. Isg15 enhances the innate antiviral response by inhibition of irf-3 degradation. *Cell Mol Biol (Noisy-le-grand)*, 52(1):29–41, 2006.

[98] Yu Lu, Olasunkanmi A J Adegoke, Alain Nepveu, Keiichi I Nakayama, Nathalie Bedard, Dongmei Cheng, Junmin Peng, and Simon S Wing. Usp19 deubiquitinating enzyme supports cell proliferation by stabilizing kpc1, a ubiquitin ligase for p27kip1. *Mol Cell Biol*, 29(2):547–558, Jan 2009.

[99] S. Lyapina, G. Cope, A. Shevchenko, G. Serino, T. Tsuge, C. Zhou, D. A. Wolf, N. Wei, A. Shevchenko, and R. J. Deshaies. Promotion of nedd-cul1 conjugate cleavage by cop9 signalosome. *Science*, 292(5520):1382–1385, May 2001.

[100] Karin Lykke-Andersen, Laura Schaefer, Suchithra Menon, Xing-Wang Deng, Jeffrey Boone Miller, and Ning Wei. Disruption of the cop9 signalosome csn2 subunit in mice causes deficient cell proliferation, accumulation of p53 and cyclin e, and early embryonic death. *Mol Cell Biol*, 23(19):6790–6797, Oct 2003.

[101] Zuzanna Makowska, Francois H T Duong, Gaia Trincucci, David F Tough, and Markus H Heim. Interferon-beta and interferon-lambda signaling is not affected by interferon-induced refractoriness to interferon-alpha in vivo. *Hepatology*, 53(4):1154–1163, Apr 2011.

[102] Michael P Malakhov, Oxana A Malakhova, Keun Il Kim, Kenneth J Ritchie, and Dong-Er Zhang. Ubp43 (usp18) specifically removes isg15 from conjugated proteins. *J Biol Chem*, 277(12):9976–9981, Mar 2002.

[103] Oxana Malakhova, Michael Malakhov, Christopher Hetherington, and Dong-Er Zhang. Lipopolysaccharide activates the expression of isg15-specific protease ubp43 via interferon regulatory factor 3. *J Biol Chem*, 277(17):14703–14711, Apr 2002.

[104] Oxana A Malakhova, Keun Il Kim, Jiann-Kae Luo, Weiguo Zou, K. G Suresh Kumar, Serge Y Fuchs, Ke Shuai, and Dong-Er Zhang. Ubp43 is a novel regulator of interferon signaling independent of its isg15 isopeptidase activity. *EMBO J*, 25(11):2358–2367, Jun 2006.

[105] Oxana A Malakhova, Ming Yan, Michael P Malakhov, Youzhong Yuan, Kenneth J Ritchie, Keun Il Kim, Luke F Peterson, Ke Shuai, and Dong-Er Zhang. Protein isgylation modulates the jak-stat signaling pathway. *Genes Dev*, 17(4):455–460, Feb 2003.

[106] Oxana A Malakhova and Dong-Er Zhang. Isg15 inhibits nedd4 ubiquitin e3 activity and enhances the innate antiviral response. *J Biol Chem*, 283(14):8783–8787, Apr 2008.

[107] Lynne E Maquat. Nonsense-mediated mrna decay in mammals. *J Cell Sci*, 118(Pt 9):1773–1776, May 2005.

[108] Fiona M Menzies, Jeannette Huebener, Maurizio Renna, Michael Bonin, Olaf Riess, and David C Rubinsztein. Autophagy induction reduces mutant ataxin-3 levels and toxicity in a mouse model of spinocerebellar ataxia type 3. *Brain*, 133(Pt 1):93–104, Jan 2010.

[109] Erik Meulmeester, Marion Kunze, He Hsuan Hsiao, Henning Urlaub, and Frauke Melchior. Mechanism and consequences for paralog-specific sumoylation of ubiquitin-specific protease 25. *Mol Cell*, 30(5):610–619, Jun 2008.

[110] Hemmo Meyer, Monika Bug, and Sebastian Bremer. Emerging functions of the vcp/p97 aaa-atpase in the ubiquitin system. *Nat Cell Biol*, 14(2):117–123, Feb 2012.

[111] Debdyuti Mukhopadhyay and Howard Riezman. Proteasome-independent functions of ubiquitin in endocytosis and signaling. *Science*, 315(5809):201–205, Jan 2007.

[112] Chan Hyun Na and Junmin Peng. Analysis of ubiquitinated proteome by quantitative mass spectrometry. *Methods Mol Biol*, 893:417–429, 2012.

[113] Andras Nagy, Lynn Mar, and Graham Watts. Creation and use of a cre recombinase transgenic database. *Methods Mol Biol*, 530:365–378, 2009.

[114] Jana Narasimhan, Ming Wang, Zhuji Fu, Jennifer M Klein, Arthur L Haas, and Jung-Ja P Kim. Crystal structure of the interferon-induced ubiquitin-like protein isg15. *J Biol Chem*, 280(29):27356–27365, Jul 2005.

[115] M. J. Nicholl, L. H. Robinson, and C. M. Preston. Activation of cellular interferon-responsive genes after infection of human cells with herpes simplex virus type 1. *J Gen Virol*, 81(Pt 9):2215–2218, Sep 2000.

[116] Sandra Niendorf, Alexander Oksche, Agnes Kisser, Jürgen Löhler, Marco Prinz, Hubert Schorle, Stephan Feller, Marc Lewitzky, Ivan Horak, and Klaus-Peter Knobeloch. Essential role of ubiquitin-specific protease 8 for receptor tyrosine kinase stability and endocytic trafficking in vivo. *Mol Cell Biol*, 27(13):5029–5039, Jul 2007.

[117] Sebastian M B Nijman, Mark P A Luna-Vargas, Arno Velds, Thijn R Brummelkamp, Annette M G Dirac, Titia K Sixma, and René Bernards. A genomic and functional inventory of deubiquitinating enzymes. *Cell*, 123(5):773–786, Dec 2005.

[118] C. Notredame, D. G. Higgins, and J. Heringa. T-coffee: A novel method for fast and accurate multiple sequence alignment. *J Mol Biol*, 302(1):205–217, Sep 2000.

[119] T. A. Nyman, S. Matikainen, T. Sareneva, I. Julkunen, and N. Kalkkinen. Proteome analysis reveals ubiquitin-conjugating enzymes to be a new family of interferon-alpha-regulated genes. *Eur J Biochem*, 267(13):4011–4019, Jul 2000.

[120] Atsushi Okumura, Gengshi Lu, Ian Pitha-Rowe, and Paula M Pitha. Innate antiviral response targets hiv-1 release by the induction of ubiquitin-like protein isg15. *Proc Natl Acad Sci U S A*, 103(5):1440–1445, Jan 2006.

[121] Fumihiko Okumura, Weiguo Zou, and Dong-Er Zhang. Isg15 modification of the eif4e cognate 4ehp enhances cap structure-binding activity of 4ehp. *Genes Dev*, 21(3):255–260, Feb 2007.

[122] Shao-En Ong, Blagoy Blagoev, Irina Kratchmarova, Dan Bach Kristensen, Hanno Steen, Akhilesh Pandey, and Matthias Mann. Stable isotope labeling by amino acids in cell culture, silac, as a simple and accurate approach to expression proteomics. *Mol Cell Proteomics*, 1(5):376–386, May 2002.

[123] Anna Osiak, Olaf Utermöhlen, Sandra Niendorf, Ivan Horak, and Klaus-Peter Knobeloch. Isg15, an interferon-stimulated ubiquitin-like protein, is not essential for stat1 signaling and responses against vesicular stomatitis and lymphocytic choriomeningitis virus. *Mol Cell Biol*, 25(15):6338–6345, Aug 2005.

[124] K. Osoegawa, M. Tateno, P. Y. Woon, E. Frengen, A. G. Mammoser, J. J. Catanese, Y. Hayashizaki, and P. J. de Jong. Bacterial artificial chromosome libraries for mouse sequencing and functional analysis. *Genome Res*, 10(1):116–128, Jan 2000.

[125] V. J. Palombella, O. J. Rando, A. L. Goldberg, and T. Maniatis. The ubiquitin-proteasome pathway is required for processing the nf-kappa b1 precursor protein and the activation of nf-kappa b. *Cell*, 78(5):773–785, Sep 1994.

[126] Martina Panattoni, Francesca Sanvito, Veronica Basso, Claudio Doglioni, Giulia Casorati, Eugenio Montini, Jeffrey R Bender, Anna Mondino, and Ruggero Pardi. Targeted inactivation of the cop9 signalosome impairs multiple stages of t cell development. *J Exp Med*, 205(2):465–477, Feb 2008.

[127] Christiane Pelzer and Marcus Groettrup. Fat10 : Activated by uba6 and functioning in protein degradation. *Subcell Biochem*, 54:238–246, 2010.

[128] Andreas Peth, Christoph Berndt, Wolfgang Henke, and Wolfgang Dubiel. Downregulation of cop9 signalosome subunits differentially affects the csn complex and target protein stability. *BMC Biochem*, 8:27, 2007.

[129] Andreas Peth, Jan Peter Boettcher, and Wolfgang Dubiel. Ubiquitin-dependent proteolysis of the microtubule end-binding protein 1, eb1, is controlled by the cop9 signalosome: possible consequences for microtubule filament stability. *J Mol Biol*, 368(2):550–563, Apr 2007.

[130] C. T. Pham, D. M. MacIvor, B. A. Hug, J. W. Heusel, and T. J. Ley. Long-range disruption of gene expression by a selectable marker cassette. *Proc Natl Acad Sci U S A*, 93(23):13090–13095, Nov 1996.

[131] Cecile M Pickart and Robert E Cohen. Proteasomes and their kin: proteases in the machine age. *Nat Rev Mol Cell Biol*, 5(3):177–187, Mar 2004.

[132] Glenn Randall, Limin Chen, Maryline Panis, Andrew K Fischer, Brett D Lindenbach, Jing Sun, Jenny Heathcote, Charles M Rice, Aled M Edwards, and Ian D McGilvray. Silencing of usp18 potentiates the antiviral activity of interferon against hepatitis c virus infection. *Gastroenterology*, 131(5):1584–1591, Nov 2006.

[133] Francisca E Reyes-Turcu, John R Horton, James E Mullally, Annie Heroux, Xiaodong Cheng, and Keith D Wilkinson. The ubiquitin binding domain znf ubp recognizes the c-terminal diglycine motif of unanchored ubiquitin. *Cell*, 124(6):1197–1208, Mar 2006.

[134] Kenneth J Ritchie, Michael P Malakhov, Christopher J Hetherington, Liming Zhou, Marie-Terese Little, Oxana A Malakhova, Jack C Sipe, Stuart H Orkin, and Dong-Er Zhang. Dysregulation of protein modification by isg15 results in brain cell injury. *Genes Dev*, 16(17):2207–2212, Sep 2002.

[135] S. Rozen and H. Skaletsky. Primer3 on the www for general users and for biologist programmers. *Methods Mol Biol*, 132:365–386, 2000.

[136] Dorothée Ruffieux-Daidié and Olivier Staub. Intracellular ubiquitylation of the epithelial na+ channel controls extracellular proteolytic channel activation via conformational change. *J Biol Chem*, 286(4):2416–2424, Jan 2011.

[137] Anthony J Sadler and Bryan R G Williams. Interferon-inducible antiviral effectors. *Nat Rev Immunol*, 8(7):559–568, Jul 2008.

[138] P. D. Sadowski. Site-specific genetic recombination: hops, flips, and flops. *FASEB J*, 7(9):760–767, Jun 1993.

[139] Anjanabha Saha and Raymond J Deshaies. Multimodal activation of the ubiquitin ligase scf by nedd8 conjugation. *Mol Cell*, 32(1):21–31, Oct 2008.

[140] Kazima Saira, You Zhou, and Clinton Jones. The infected cell protein 0 encoded by bovine herpesvirus 1 (bicp0) induces degradation of interferon response factor 3 and, consequently, inhibits beta interferon promoter activity. *J Virol*, 81(7):3077–3086, Apr 2007.

[141] Magdalena Sarasin-Filipowicz, Xueya Wang, Ming Yan, Francois H T Duong, Valeria Poli, Douglas J Hilton, Dong-Er Zhang, and Markus H Heim. Alpha interferon induces long-lasting refractoriness of jak-stat signaling in the mouse liver through induction of usp18/ubp43. *Mol Cell Biol*, 29(17):4841–4851, Sep 2009.

[142] Antonio Sarikas, Thomas Hartmann, and Zhen-Qiang Pan. The cullin protein family. *Genome Biol*, 12(4):220, 2011.

[143] Hartmut Scheel and Kay Hofmann. Prediction of a common structural scaffold for proteasome lid, cop9-signalosome and eif3 complexes. *BMC Bioinformatics*, 6:71, 2005.

[144] Martin Scheffner and Olivier Staub. Hect e3s and human disease. *BMC Biochem*, 8 Suppl 1:S6, 2007.

[145] Michael W Schmidt, Philip R McQuary, Susan Wee, Kay Hofmann, and Dieter A Wolf. F-box-directed crl complex assembly and regulation by the csn and cand1. *Mol Cell*, 35(5):586–597, Sep 2009.

[146] Bernhard Schmierer and Caroline S Hill. Tgfbeta-smad signal transduction: molecular specificity and functional flexibility. *Nat Rev Mol Cell Biol*, 8(12):970–982, Dec 2007.

[147] C. Schwechheimer and X. W. Deng. Cop9 signalosome revisited: a novel mediator of protein degradation. *Trends Cell Biol*, 11(10):420–426, Oct 2001.

[148] Katrin Schweitzer, Przemyslaw M Bozko, Wolfgang Dubiel, and Michael Naumann. Csn controls nf-kappab by deubiquitinylation of ikappabalpha. *EMBO J*, 26(6):1532–1541, Mar 2007.

[149] M. Seeger, R. Kraft, K. Ferrell, D. Bech-Otschir, R. Dumdey, R. Schade, C. Gordon, M. Naumann, and W. Dubiel. A novel protein complex involved in signal transduction possessing similarities to 26s proteasome subunits. *FASEB J*, 12(6):469–478, Apr 1998.

[150] He-Xin Shi, Kai Yang, Xing Liu, Xin-Yi Liu, Bo Wei, Yu-Fei Shan, Lian-Hui Zhu, and Chen Wang. Positive regulation of interferon regulatory factor 3 activation by herc5 via isg15 modification. *Mol Cell Biol*, 30(10):2424–2436, May 2010.

[151] J. D. Singer, M. Gurian-West, B. Clurman, and J. M. Roberts. Cullin-3 targets cyclin e for ubiquitination and controls s phase in mammalian cells. *Genes Dev*, 13(18):2375–2387, Sep 1999.

[152] Wolfgang Sippl, Vincent Collura, and Frédéric Colland. Ubiquitin-specific proteases as cancer drug targets. *Future Oncol*, 7(5):619–632, May 2011.

[153] O. Smithies, R. G. Gregg, S. S. Boggs, M. A. Koralewski, and R. S. Kucherlapati. Insertion of dna sequences into the human chromosomal beta-globin locus by homologous recombination. *Nature*, 317(6034):230–234, 1985.

[154] Teresa A Soucy, Lawrence R Dick, Peter G Smith, Michael A Milhollen, and James E Brownell. The nedd8 conjugation pathway and its relevance in cancer biology and therapy. *Genes Cancer*, 1(7):708–716, Jul 2010.

[155] Mathew E Sowa, Eric J Bennett, Steven P Gygi, and J. Wade Harper. Defining the human deubiquitinating enzyme interaction landscape. *Cell*, 138(2):389–403, Jul 2009.

[156] Tomoharu Takeuchi, Takayasu Kobayashi, Shinri Tamura, and Hideyoshi Yokosawa. Negative regulation of protein phosphatase 2cbeta by isg15 conjugation. *FEBS Lett*, 580(18):4521–4526, Aug 2006.

[157] J. D. Thompson, D. G. Higgins, and T. J. Gibson. Clustal w: improving the sensitivity of progressive multiple sequence alignment through sequence weighting, position-specific gap penalties and weight matrix choice. *Nucleic Acids Res*, 22(22):4673–4680, Nov 1994.

[158] Sokol V Todi, Brett J Winborn, K. Matthew Scaglione, Jessica R Blount, Sue M Travis, and Henry L Paulson. Ubiquitination directly enhances activity of the deubiquitinating enzyme ataxin-3. *EMBO J*, 28(4):372–382, Feb 2009.

[159] Masayoshi Tojo, Ai Takebe, Satoru Takahashi, Keiji Tanaka, Takeshi Imamura, Kohei Miyazono, and Tomoki Chiba. Smad7-deficient mice show growth retardation with reduced viability. *J Biochem*, 151(6):621–631, Jun 2012.

[160] Kiichiro Tomoda, Yukiko Kubota, Yukinobu Arata, Seiji Mori, Maki Maeda, Toshiaki Tanaka, Minoru Yoshida, Noriko Yoneda-Kato, and Jun ya Kato. The cytoplasmic shuttling and subsequent degradation of p27kip1 mediated by jab1/csn5 and the cop9 signalosome complex. *J Biol Chem*, 277(3):2302–2310, Jan 2002.

[161] Kiichiro Tomoda, Noriko Yoneda-Kato, Akihisa Fukumoto, Shinya Yamanaka, and Jun-Ya Kato. Multiple functions of jab1 are required for early embryonic development and growth potential in mice. *J Biol Chem*, 279(41):43013–43018, Oct 2004.

[162] Raul M. Torres and Ralf Kühn. *Laboratory protocols for conditional gene targeting*. Oxford Uninversity Press (Oxford and New York), 1997.

[163] Eirini Trompouki, Eudoxia Hatzivassiliou, Theodore Tsichritzis, Hannah Farmer, Alan Ashworth, and George Mosialos. Cyld is a deubiquitinating enzyme that negatively regulates nf-kappab activation by tnfr family members. *Nature*, 424(6950):793–796, Aug 2003.

[164] Gijs A Versteeg, Benjamin G Hale, Sander van Boheemen, Thorsten Wolff, Deborah J Lenschow, and Adolfo García-Sastre. Species-specific antagonism of host isgylation by the influenza b virus ns1 protein. *J Virol*, 84(10):5423–5430, May 2010.

[165] Robin M Vos, Jennifer Altreuter, Elizabeth A White, and Peter M Howley. The ubiquitin-specific peptidase usp15 regulates human papillomavirus type 16 e6 protein stability. *J Virol*, 83(17):8885–8892, Sep 2009.

[166] Henning Walczak, Kazuhiro Iwai, and Ivan Dikic. Generation and physiological roles of linear ubiquitin chains. *BMC Biol*, 10:23, 2012.

[167] Y. Wang, S. Penfold, X. Tang, N. Hattori, P. Riley, J. W. Harper, J. C. Cross, and M. Tyers. Deletion of the cul1 gene in mice causes arrest in early embryogenesis and accumulation of cyclin e. *Curr Biol*, 9(20):1191–1194, Oct 1999.

[168] Y. Wang, M. K. Spatz, K. Kannan, H. Hayk, A. Avivi, M. Gorivodsky, M. Pines, A. Yayon, P. Lonai, and D. Givol. A mouse model for achondroplasia produced by targeting fibroblast growth factor receptor 3. *Proc Natl Acad Sci U S A*, 96(8):4455–4460, Apr 1999.

[169] Susan Wee, Rory K Geyer, Takashi Toda, and Dieter A Wolf. Csn facilitates cullin-ring ubiquitin ligase function by counteracting autocatalytic adapter instability. *Nat Cell Biol*, 7(4):387–391, Apr 2005.

[170] N. Wei, D. A. Chamovitz, and X. W. Deng. Arabidopsis cop9 is a component of a novel signaling complex mediating light control of development. *Cell*, 78(1):117–124, Jul 1994.

[171] N. Wei, T. Tsuge, G. Serino, N. Dohmae, K. Takio, M. Matsui, and X. W. Deng. The cop9 complex is conserved between plants and mammals and is related to the 26s proteasome regulatory complex. *Curr Biol*, 8(16):919–922, 1998.

[172] Ning Wei and Xing Wang Deng. The cop9 signalosome. *Annu Rev Cell Dev Biol*, 19:261–286, 2003.

[173] Scott W Werneke, Clementine Schilte, Anjali Rohatgi, Kristen J Monte, Alain Michault, Fernando Arenzana-Seisdedos, Dana L Vanlandingham, Stephen Higgs, Arnaud Fontanet, Matthew L Albert, and Deborah J Lenschow. Isg15 is critical in the control of chikungunya virus infection independent of ube1l mediated conjugation. *PLoS Pathog*, 7(10):e1002322, Oct 2011.

[174] Keith D Wilkinson. Dubs at a glance. *J Cell Sci*, 122(Pt 14):2325–2329, Jul 2009.

[175] Scott M Wilson, Bula Bhattacharyya, Rivka A Rachel, Vincenzo Coppola, Lino Tessarollo, Deborah B Householder, Colin F Fletcher, Richard J Miller, Neal G Copeland, and Nancy A Jenkins. Synaptic defects in ataxia mice result from a mutation in usp14, encoding a ubiquitin-specific protease. *Nat Genet*, 32(3):420–425, Nov 2002.

[176] Dieter A Wolf, Chunshui Zhou, and Susan Wee. The cop9 signalosome: an assembly and maintenance platform for cullin ubiquitin ligases? *Nat Cell Biol*, 5(12):1029–1033, Dec 2003.

[177] Joyce Jing Yi Wong, Yuh Fen Pung, Newman Siu-Kwan Sze, and Keh-Chuang Chin. Herc5 is an ifn-induced hect-type e3 protein ligase that mediates type i ifn-induced isgylation of protein targets. *Proc Natl Acad Sci U S A*, 103(28):10735–10740, Jul 2006.

[178] Katharine H Wrighton, Xia Lin, and Xin-Hua Feng. Phospho-control of tgf-beta superfamily signaling. *Cell Res*, 19(1):8–20, Jan 2009.

[179] Mingli Xu, Masakatsu Takanashi, Kosuke Oikawa, Masami Tanaka, Hirotaka Nishi, Keiichi Isaka, Motoshige Kudo, and Masahiko Kuroda. Usp15 plays an essential role for caspase-3 activation during paclitaxel-induced apoptosis. *Biochem Biophys Res Commun*, 388(2):366–371, Oct 2009.

[180] Ping Xu, Duc M Duong, Nicholas T Seyfried, Dongmei Cheng, Yang Xie, Jessica Robert, John Rush, Mark Hochstrasser, Daniel Finley, and Junmin Peng. Quantitative proteomics reveals the function of unconventional ubiquitin chains in proteasomal degradation. *Cell*, 137(1):133–145, Apr 2009.

[181] Jun ya Kato and Noriko Yoneda-Kato. Mammalian cop9 signalosome. *Genes Cells*, 14(11):1209–1225, Nov 2009.

[182] Jiong Yan, Katherina Walz, Hisashi Nakamura, Sandra Carattini-Rivera, Qi Zhao, Hannes Vogel, Ning Wei, Monica J Justice, Allan Bradley, and James R Lupski. Cop9 signalosome subunit 3 is essential for maintenance of cell proliferation in the mouse embryonic epiblast. *Mol Cell Biol*, 23(19):6798–6808, Oct 2003.

[183] X. Yang, J. J. Letterio, R. J. Lechleider, L. Chen, R. Hayman, H. Gu, A. B. Roberts, and C. Deng. Targeted disruption of smad3 results in impaired mucosal immunity and diminished t cell responsiveness to tgf-beta. *EMBO J*, 18(5):1280–1291, Mar 1999.

[184] Xiaoming Yang, Suchithra Menon, Karin Lykke-Andersen, Tomohiko Tsuge, Di Xiao, Xiping Wang, Roberto J Rodriguez-Suarez, Hui Zhang, and Ning Wei. The cop9 signalosome inhibits p27(kip1) degradation and impedes g1-s phase progression via deneddylation of scf cul1. *Curr Biol*, 12(8):667–672, Apr 2002.

[185] W. Yuan and R. M. Krug. Influenza b virus ns1 protein inhibits conjugation of the interferon (ifn)-induced ubiquitin-like isg15 protein. *EMBO J*, 20(3):362–371, Feb 2001.

[186] Dongxian Zhang and Dong-Er Zhang. Interferon-stimulated gene 15 and the protein isgylation system. *J Interferon Cytokine Res*, 31(1):119–130, Jan 2011.

[187] Yingying Zhang, Xiaowei Zhou, and Peitang Huang. Fanconi anemia and ubiquitination. *J Genet Genomics*, 34(7):573–580, Jul 2007.

[188] Chen Zhao, Sylvie L Beaudenon, Melissa L Kelley, M. Brett Waddell, Weiming Yuan, Brenda A Schulman, Jon M Huibregtse, and Robert M Krug. The ubch8 ubiquitin e2 enzyme is also the e2 enzyme for isg15, an ifn-alpha/beta-induced ubiquitin-like protein. *Proc Natl Acad Sci U S A*, 101(20):7578–7582, May 2004.

[189] Chunshui Zhou, Susan Wee, Edward Rhee, Michael Naumann, Wolfgang Dubiel, and Dieter A Wolf. Fission yeast cop9/signalosome suppresses cullin activity through recruitment of the deubiquitylating enzyme ubp12p. *Mol Cell*, 11(4):927–938, Apr 2003.

[190] Weiguo Zou, Jung-Hwan Kim, Adedayo Handidu, Xiang Li, Keun Il Kim, Ming Yan, Jun Li, and Dong-Er Zhang. Microarray analysis reveals that type i interferon strongly increases the expression of immune-response related genes in ubp43 (usp18) deficient macrophages. *Biochem Biophys Res Commun*, 356(1):193–199, Apr 2007.

[191] Weiguo Zou and Dong-Er Zhang. The interferon-inducible ubiquitin-protein isopeptide ligase (e3) efp also functions as an isg15 e3 ligase. *J Biol Chem*, 281(7):3989–3994, Feb 2006.

A. Appendix

A.1. List of abbreviations

Abbreviation	Description
$\alpha-{}^{32}$P	Radionuclid $^{32}_{15}$P of phosphorus
×g	Multiple of standard gravity g_n (approx. 9.81 m/s^2)
3′	3 prime
5′	5 prime
A. nidulans	*Aspergillus nidulans*
A. thaliana	*Arabisopsis thaliana*
AG	Aktiengesellschaft
aka	Also known as
Ala	Alanine
AMP	Adenosine monophosphate
APC	Adenomatous polyposis coli
APS	Ammonium persulfate
ATP	Adenosine triphosphate
BAC	Bacterial artfificial chromosome
BMP	Bone morphogenic protein
bp	Base pairs
BSA	Bovine serum albumin
bzw.	Beziehungsweise
C61A	Cysteine at amino acid position 61 changed to alanine
CD3/11b	Cluster of differentiation 3/11b
Chl	Chloroform
CHMP5	Charged multivesicular body protein 5
Ci	Curie
CMV	Cytomegalievirus
Co. KG	Compagnie Kommanditgesellschaft
COP9	Constitutive photomorphogenic 9
Corp	Corporation
CP	20 S cylindric core particle
Cre	Cre recombinase (causes recombination)
CRL	Cullin RING Ub ligase
CSN	COP9 signalosome
CYLD	Cylindromatosis gene product
Cys	Cysteine
Cys61	Cysteine at amino acid position 61
dATP	Deoxyadenosine triphosphate
dCTP	Deoxycytidine triphosphate
del	Deleted
DEPC	Diethylpyrocarbonate
dGTP	Deoxyguanosine triphosphate
DMEM	Modified Eagle's medium

DMSO	Dimethylsulfoxide
DNA	Desoxyribonucleic acid
dNTP	Deoxynucleoside triphosphate
dTTP	Deoxythymidine triphosphate
dsDNA	Double stranded desoxyribonucleic acid
DUB	Deubiquitinating enzyme (or reactive towards another UbL)
DUSP	Domain present in Ub-specific proteases
E1	Ub/UbL activating enzyme
E2	Ub/UbL conjugating enzyme
E3	Ub/UbL ligase
E 13.5	Day 13.5 of embryonic development
e. g.	For example, *exempli gratia*
EDTA	Ethylenediamine tetraacetic acid
ES (cells)	Embryonic stem (cells)
ESCRT	Endosmal sorting complex required for transport
etc.	*et cetera*
FAT10	Human leukocyte antigen F adjacent transcript 10
FCS	Fetal calf serum
fl	Floxed (flanked by loxP sites)
FLP, FLPe	Flipase, enhanced flipase
FRT	FLP(e) recognition target
G418	Neomycin, geneticin
Gag	Group-specific antigen
GAPDH	Glycerinaldehyde 3 phosphate dehydrogenase
gDNA	Genomic desoxyribonucleic acid
GmbH	Gesellschaft mit beschränkter Haftung
GSK-3β	Glycogen synthase kinase-3beta
GST	Glutathione S-transferase
GTP	Guanosine triphosphate
h	Hour(s)
HECT	Homologous to E6-AP carboxy terminus domain
HERC5/6	HECT and RLD domain containing E3 ligase 5/6
HGF	Hepatocyte growth factor
HIV	Human immunodeficiency virus
HPV	Human papilloma virus
HSV	Herpes simplex virus
i. e.	That is to say, *id est*
I-SMAD	Inhibitory SMAD
IAA	Isoamylalcohol
Inc.	Incorporation
ICP0	Infected cell polypeptide 0
IFN	Interferon
IFNAR1/2	IFNα receptor 1/2
IKK	IκB kinase

IPS	Impulses per second
IRF-3	IFN regulatory factor-3
IRF-9	IFN regulatory factor-9
ISRE	IFN stimulated response elements
ISG	Interferon stimulated gene
ISG15	Interferon stimulated gene 15
ISGF-3	IFN stimulated gene factor-3
Jab1 (CSN5)	Jun-activation-domain-binding protein 1 (CSN5)
JAK1	Janus kinase 1
K	Lysine
kb	Kilobase pairs
kDa	Kliodalton
KGaA	Kommanditgesellschaft
KPC1	Kip1 ubiquitination-promoting complex 1
LIF	Leukemia inhibitory factor
loxP	Locus of recombination in P1
Ltd.	Limited
Lys	Lysine
M	Molar, mol per liter
M1	Methionine at position 1
MAF	Mouse adult fibroblast
MDM2	Mouse double minute 2
MEF	Mouse embryonic fibroblast
min	Minutes
mRNA	Messenger ribonucleic acid
Mx	Myxovirus (influenza virus) resistance protein
N	Normal
NEAA	Nonessential amino acids
NEDD8	Neuronal precursor expressed developmentally down regulated 8
NFκB	Nuclear factor κ B
neo	Neomycin
neo-fl	Neomycin-floxed
OAS	2′-5′oligo adenylate synthetase
OD_n	Optical density at n nm wavelength
OTU	Ovarian-tumor domain
PAA	Polyacrylamide
PAC	P1 artificial chromosome
PAGE	Polyacrylamide gel electrophoresis
PBS	Phosphate buffered saline
PCR	Polymerase chain reaction
PKR	Protein kinase R
plc.	Public limited company
PMSF	Phenylmethylsulfonylfluorid
poly(A)$_n$	Polyadenylated

poly(I:C)	Polyinosinic-polycytidylic acid
R-SMAD	Regulatory SMAD
RBX1	RING box protein 1
RING	Really interesting new gene
RNA	Ribonucleic acid
RP	19 S regulatory particle
rRNA	Ribosomal RNA
S. pombe	*Schizosaccharomyces pombe*
SART3	Squamous cell carcinoma antigen recognized by T-cells 3
SDS	Sodium dodecyl sulphate
SILAC	Stable isotope labeling by amino acids in cell culture
siRNA	Small interfering ribonucleic acid
SLIM1	Skeletal muscle LIM protein 1
SMURF1/2	SMAD Ub regulatory factor 1/2
ssDNA	Single stranded desoxyribonucleic acid
STAT	Signal transducer and activators of transcription
SUMO	Small ubiquitin-related modifier
SV40	Simian Virus 40
T_a	Annealing temperature
TβR-I	TGF-β receptor I
TCA	Trichloracetic acid
TEMED	(N,N,N',N'-)Tetramethylethylenediamine
TGF-β	Tumor growth factor-β
TNF-α	Tumor necrosis factor-α
TK	Thymidine kinase
TRIS	Tris-(hydroxymethyl)-aminomethane
TSG101	Tumor susceptibility gene 101
TYK2	Janus kinases tyrosine kinase 2
u	Unit
Ub	Ubiquitin
UBE1L	Ub activating enzyme E1 like
UBCH6	Ub conjugating enzyme in human 6
UBD	Ub binding domain
UbL	Ubiquitin-like
UCH	Ub-C-terminal hydrolase
UK	United Kingdom
USA	United States of America
USP	Ubiquitin-specific protease
UV	Ultraviolet
VSP4	Vacuolar protein sorting 4
VSV	Vesicular stomatitis virus
wt	Wildtype
z. B.	Zum Beispiel

A.2. Acknowledgment

Ich möchte mich bei allen bedanken die mich während dieser Arbeit begleitet und ihren Teil zu dieser Arbeit beigetragen haben in dem sie mir halfen oder einfach nur für mich da waren; sei die Begegnung auch noch so kurz gewesen. Insebesondere bedanke ich mich bei:

Wolfgang Dubiel — Ich bedanke mich bei Dir für das Vertrauen in meine Arbeit und dass ich diese Arbeit in Deiner Arbeitsgruppe anfertigen durfte. Ich weiß es zu schätzen, dass Deine Tür für Fragen und Diskussionen immer offen Stand. Ich dank Dir auch für Deine Gelassenheit und Ruhe in schwierigen Situationen. Danke Wolfgang!

Klaus-Peter Knobeloch — Danke Knobi, dass Du mir die Möglichkeit gegeben hast einen Teil dieser Arbeit in Deiner Arbeitsgruppe anzufertigen. Ich bedanke mich auch bei Dir für Deine Ehrlichkeit, Deine Hilfe, Kooperation und Unterstützung innnerhalb und außerhalb des Labors. Ich hab die Zusammenarbeit echt genossen. Ich möchte mich auch dafür bedanken, dass Du (fast) immer zu erreichen warst. Dikussionen mit Dir waren immer sehr inspirierend. Ich danke Dir besonders für die aufbauenden Worte in schwierigen Zeiten und für Deine Kunst der Motivation.

Rupert Mutzel — Danke Rupert für die Selbstverständlichkeit mit der Du damals die Rolle des Zweitgutachters übernommen hast. Ich weiß es sehr zu schätzen und bin mir sicher, dass ich nicht der einzige bin.

Marcus — Für Deine Kompetenz und Hilfe während der Zeit am FMP bin ich Dir unglaublich dankbar. Es ist bewundernswert mit welcher Selbstverständlichkeit und Kompetenz Du immer geholfen hast und vermutlich jetzt anderen hilfst. Danke!

Gesa — Gesa! Danke für das Asyl im FMP und die gemeinsamen radioaktiven Arbeiten! Du hast mir wirklich sehr geholfen. Außerdem tat es immer gut jemanden zu haben der einen versteht.

Ronald Naumann — So Leute wie Dich braucht die Wissenschaft. Grüße an Dich und Deine Prinzessinen!

Simone Wörtge — Die erste Zeit in einem neuen Labor zu arbeiten ist immer sehr anstrengend. Während meines Kurzbesuches in Mainz hätte ich mir keine bessere Einweisung vorstellen können. Das habe ich nicht vergessen.

Tilo — Mensch Tino (das ist kein Schreibfehler!!!), was hätte ich ohne Dich bloß gemacht. Ich dank Dir für die vielen Tipps, die Unterstützung und den Spaß im und außerhalb des Labors! Unsere gemeinsamen Reisen werde ich nicht vergessen! Ich bedanke mich bei Dir auch für das Korrekturlesen dieser Arbeit und die Kom-

mentare zum Manuskript.

AG Dubiel / AG Knobeloch / AG Prinz — Ich bedanke mich bei allen Mitarbeitern für ihre Hilfsbereitschaft.

Manja — Liebe Manja, danke, dass Du immer für mich da warst und Verständnis gezeigt hast. Du hast mich besonders in der schweren Zeit dieser Arbeit begleitet und musstest daher viel Frust ertragen. Danke, dafür und auch für das Korrekturlesen dieser Arbeit.

Nicolas — ich bedanke mich bei Dir und erinnere mich dabei besonders an die die gemeinsame Zeit im Mäusebunker, die Abende nach harter Arbeit und die Diskussionen mit Dir.

Wolfgang Henke — Lieber Wolfgang, Du hast unsere kleine Arbeitsgruppe zu unseren Seminaren wertvoll bereichert. Danke für Deine wertvollen Tipps auch wenn keiner davon seinen Weg in diese Dissertationen gefunden hat.

René — Reneman! Danke für alles, für die Reisen, die Abende und die Gespräche in jeder Lebenslage! Danke, dass Du immer da warst. Wohl war, Architektur und Biologie haben Parallelen.

Erica — Ay Erica, te agradezco muchísimo por motivarme con tu mera existencia y más.

Julia, Silke und den Rest der Clique — Ihr hab alles von Anfang an miterlebt! Ich danke euch, dass ihr immer dabei ward und für die vielen gemeinsamen Abende! Ich hoffe es folgen noch viele weitere gemeinsame Abende!

Martin und Torsten — Hey Jungs, ich brauch Musik zum Leben und bin Euch für jede gemeinsame Probe und jedes Konzert dankbar. Mit Euch zu musizieren hat mir sehr geholfen meinen Kopf wieder freizuspülen, wenn es mal nicht so lief und hat mich zu jeder Zeit aufleben lassen. Ich hoffe IndigoRush wird es noch lange geben – Made for RnR!

Jürgen — Lieber Jürgen, ich dank Dir für Dein Vertrauen und Deine Unterstützung.

Mama — Mama, ich danke Dir für alles! Danke für Deine uneingeschränkte Unterstützung in jeglicher Hinsicht und Dein Vertrauen. Ich hoffe Du bist Stolz auf mich!

A.3. Declaration

I herewith declare that I prepared the presented dissertation myself and without the use of illegitimate aids. I used no other but the indicated sources and accessories. Further, I insure that this dissertation has not before been submitted to any other faculty for examination.

Ronny Hannß, Berlin

A.4. Publications, talks and posters

Publications

COP9 signalosome function in the DDR.
Hannß R, Dubiel W, FEBS Lett. 2011 Apr 16.

Inactivation of the isopeptidase activity of USP18 in vivo enhances ISG15 conjugation and viral resistance but does not affect interferon signaling.
Hannß R *et al.*, Manuscript in preparation

Talks

Genetic approaches to disclose the physiological role of COP9 signalosome mediated deneddylation and USP15 function in vivo.
Hannß R, Knobeloch KP, Dubiel W, DFG SPP1365 2nd annual meeting, Zeuthen, Germany, 2010

COP9 signalosome and USP15 in NFκB activation and promising genetic approaches.
Hannß R, Neuropathology (Marco Prinz), Freiburg, Germany, 2010

Posters

Genetic approaches to disclose the physiological role of COP9 signalosome-mediated deneddylation and USP15 function in vivo.
Hannß R, Knobeloch KP, Dubiel W, ZOMES VI, Safed, Israel, 2010

Interplay of the COP9 signalosome, USP15 and other associated proteins in vivo.
Hannß R, Knobeloch KP, Dubiel W, Trinational Fall Meeting of the Biochemical Societies, Aachen, Germany, 2009

Interplay of the COP9 signalosome, USP15 and other associated proteins in vivo.
Hannß R, Knobeloch KP, Dubiel W, EMBO meeting,Ubiquitin and ubiquitin-like modifiers in health and disease, Riva del Garda, Italy, 2009

Dissection of UBP43 function in vivo.
Hannß R, Knobeloch KP, 9th MDC/FMP PhD Student Retreat, Joachimsthal, Germany, 2007

For reasons of data protection, the CV is not included in the online version.

Der Lebenslauf ist in der Onlineversion aus Gründen des Datenschutzes nicht enthalten.